THE OBSERVED BEHAVIOUR OF PLANETARY SCALE WAVES IN BLOCKING EPISODES.

DAVID JOHN MUIR, B.Sc.

DOCTOR OF PHILOSOPHY.

UNIVERSITY OF EDINBURGH.

1981

This thesis has been composed by the author and reports work carried through entirely by the author. No part of the work has been presented for any other degree or qualification.

I wish to acknowledge the support of the Natural Environment Research Council, through a post graduate research studentship, and of the Department of Meteorology, the University of Edinburgh, in which the work was performed, and, particularly, I wish to acknowledge the supervision of the work by Dr. R.S. Harwood.

ABSTRACT.

The importance of blocking stems from its persistence and from the abnormal weather patterns associated with it. The causes of blocking are, at present, not identified, but there is circumstantial evidence that planetary waves are connected with the phenomenon, viz: the long term mean wave ridges cluster around areas where blocking is most frequent. This work attempts to find a firm connection between blocking and the planetary waves, and to examine some current blocking theories which have planetary waves as an essential element. The study makes use of an objective set of real data covering the period 1/11/76 to 30/4/77 from which the planetary waves are extracted by Fourier analysis along latitude circles.

The search for the effect of blocking on the time evolution of the planetary waves takes the form of a comparison of the time series of amplitude and phase for waves 1 to 8 at 500 mb with the development of concurrent blocking events. The effect of blocking on the kinetic energy of each planetary wave is similarly assessed. The conclusion from this is that no single blocking 'signature' can be identified in the planetary waves - rather a whole range of wave histories is found. Waves 2, 3 and 4, however, are found to be more commonly associated with blocking than are waves 1 and 5 to 8. Further, it is found that wave 4 is associated with long living blocks and that the difference in kinetic energy

between waves when involved in blocking and when not involved is less than 25%.

Three groups of current blocking theories are investigated, viz: (1) where blocks are caused by a superposition of planetary wave ridges; (2) where blocks are caused by non-linear transfers of energy between waves, and (3) where blocks are a manifestation of rotors in planetary waves. Other current theories are also discussed but not dealt with in depth.

The theory that blocks are caused by superposed ridges of planetary waves is studied by comparing the phase positions and amplitudes of the planetary waves with the positions of the blocking anticyclones. It is found that blocks can be described by planetary wave superpositions, the most common being combinations of waves 2, 3 and 4.

The theory that blocks are caused by non-linear wave/wave interactions is investigated by calculating such interactions directly and by comparing them with the simultaneous time evolution of the waves. The conclusion is drawn that this mechanism does play a significant role, but not in all blocks.

The theory that blocking might be a rotor in a planetary wave is examined, but the present theory is found to be too simple to allow accurate comparison with real situations.

CONTENTS.

Chapter 1.

INTRODUCTION.

1.1 Introduction.

Blocking is at present an ill understood phenomenon. It has as yet been studied only in a general way - and mainly on a statistical basis - with a view to uncovering the gross features. Again, though many theories for blocking have been proposed, few studies have looked at real data for verification. This present work advances the study of blocking by addressing these deficiencies. The study is made more particular by the analysis here of many real blocking situations in terms of dynamically significant quantities of the planetary waves, and through the examination, in the light of this analysis, of the implications and predictions of some recent blocking theories in an attempt to decide which are relatable to the real phenomenon.

The results of the study suggest that there is no preferred configuration of planetary waves during blocking. However, the waves, when important, are found to be higher in amplitude and kinetic energy during blocking, and, generally, the total eddy kinetic energy is found to increase. As for the kinetic energy events associated with blocking, the barotropic, horizontal, non-linear interactions between waves do not provide a general explanation. Thus, for a fuller understanding of the wave behaviour during blocking, more study of the energy budgets of the planetary waves is required.

In the rest of the introductory chapter, the phenomenon of blocking is described and the importance of it is set out. Afterwards, the theories that have been proposed for the cause of blocking are discussed. In the later chapters, firstly the data set is described upon which the study is based, then the analysis of the data is outlined, and, finally, the evaluations of three blocking theories are described in depth.

1.2 The Phenomenon of Blocking.

Blocking is the name given to the situation where an anticyclone disrupts the steady progress eastwards of the mid-latitude depressions (The Meteorological Glossary). The anti cyclone excludes depressions from the immediate area thus effectively 'blocking' the normal path of the depressions and the normal, variable weather which they bring. Hence, the name 'blocking anticyclone' or just simply 'blocking.'

Anticyclones, as such, are not uncommon in mid-latitudes but they normally appear as travelling ridges between low pressure centres. Blocking anticyclones are distinguished from these by being larger in area, by being longer lasting and by being slow moving or stationary or even occasionally westwards moving against the normal flow. Subtropical highs are also quasi-stationary and large in area, but they are distinguishable from blocking highs by their being positioned to the south of the depression tracks where they cause no disruption of the flow.

The disruption which blocking anticyclones cause to the flow of depressions can be most easily seen on upper air charts showing the circumpolar mid-latitude jet stream. The 500 mb chart is the chart most commonly chosen for examination since the 500 mb level lies close to the steering level for depressions. The disruption of the depression track is then evident in the disturbed jet stream pattern.

Blocking is best illustrated by an example. Figures 1.1 to 1.4 show a blocking situation and a contrasting normal or zonal situation. Figures 1.1 and 1.2 show 500 mb charts and Figures 1.3 and 1.4 show the corresponding surface charts.

The blocking anticyclone on figure 1.1 is centred at 55° N and west of the Greenwich meridian. Comparing the upper air chart 1.1 for the blocking situation with 1.2 for the normal situation shows the major perturbation of the flow caused by the blocking anticyclone. This takes the form of a deviation of the jet at a point 'A' where it is diverted into a meridional direction with part split off to travel to the south of the block. Associated with the block and the meridional jet are cut off lows to the east and west of the anticyclone at points 'B'. The flow pattern on chart 1.2 is much simpler, with the jet having a purely zonal flow. In contrast to the blocked case, there are no deep cut off lows or large anticyclones.

The systems in the surface charts reflect the jet pattern aloft. On the zonal day (figure 1.4), a normal sequence of depressions is seen occluding over the U.K.

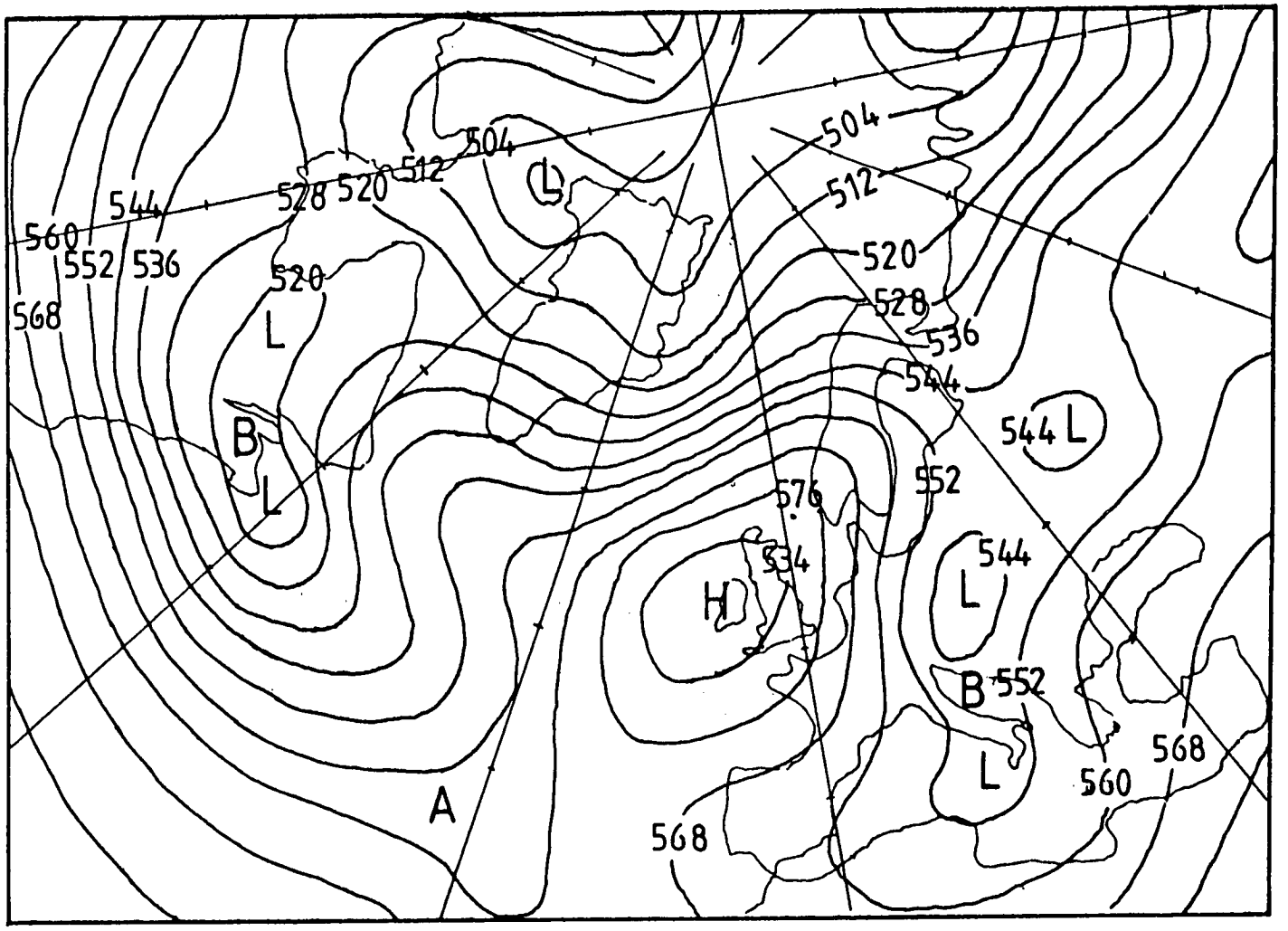

Figure 1.1 20/11/76 500mb. contours in dcm

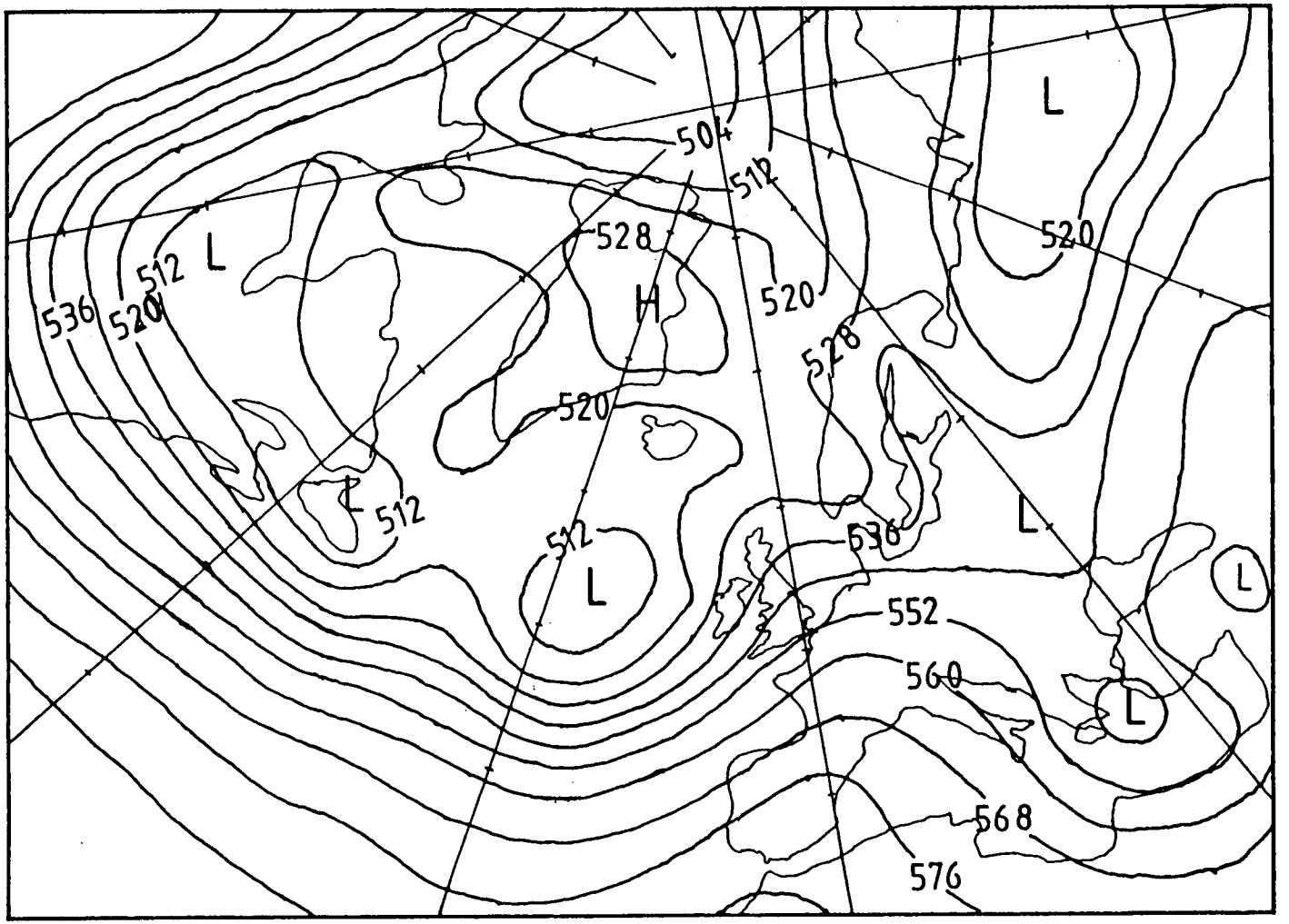

Figure 1.2 5/2/77 500mb. contours in dcm

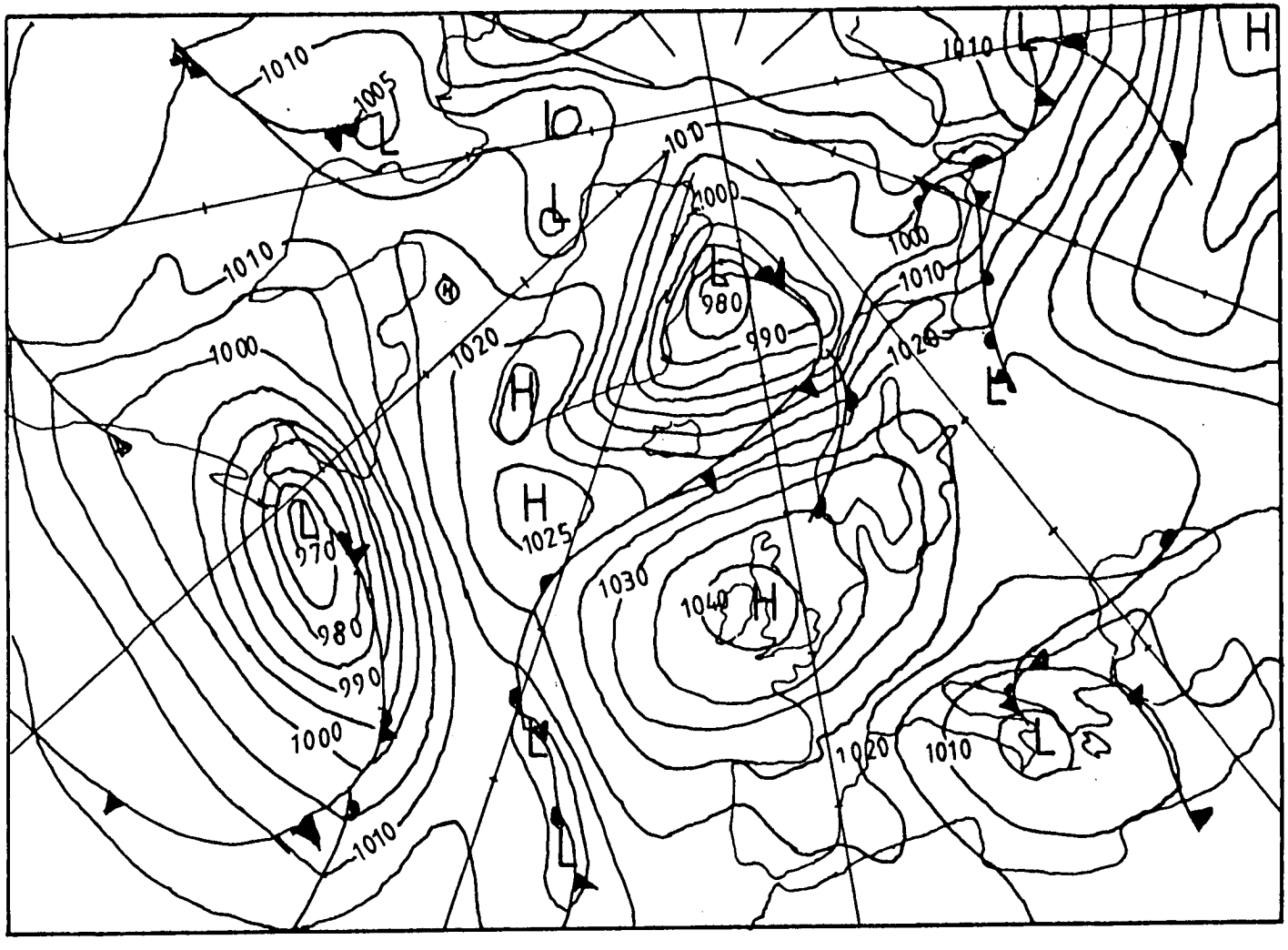

Figure 1.3 20/11/76 surface pressure

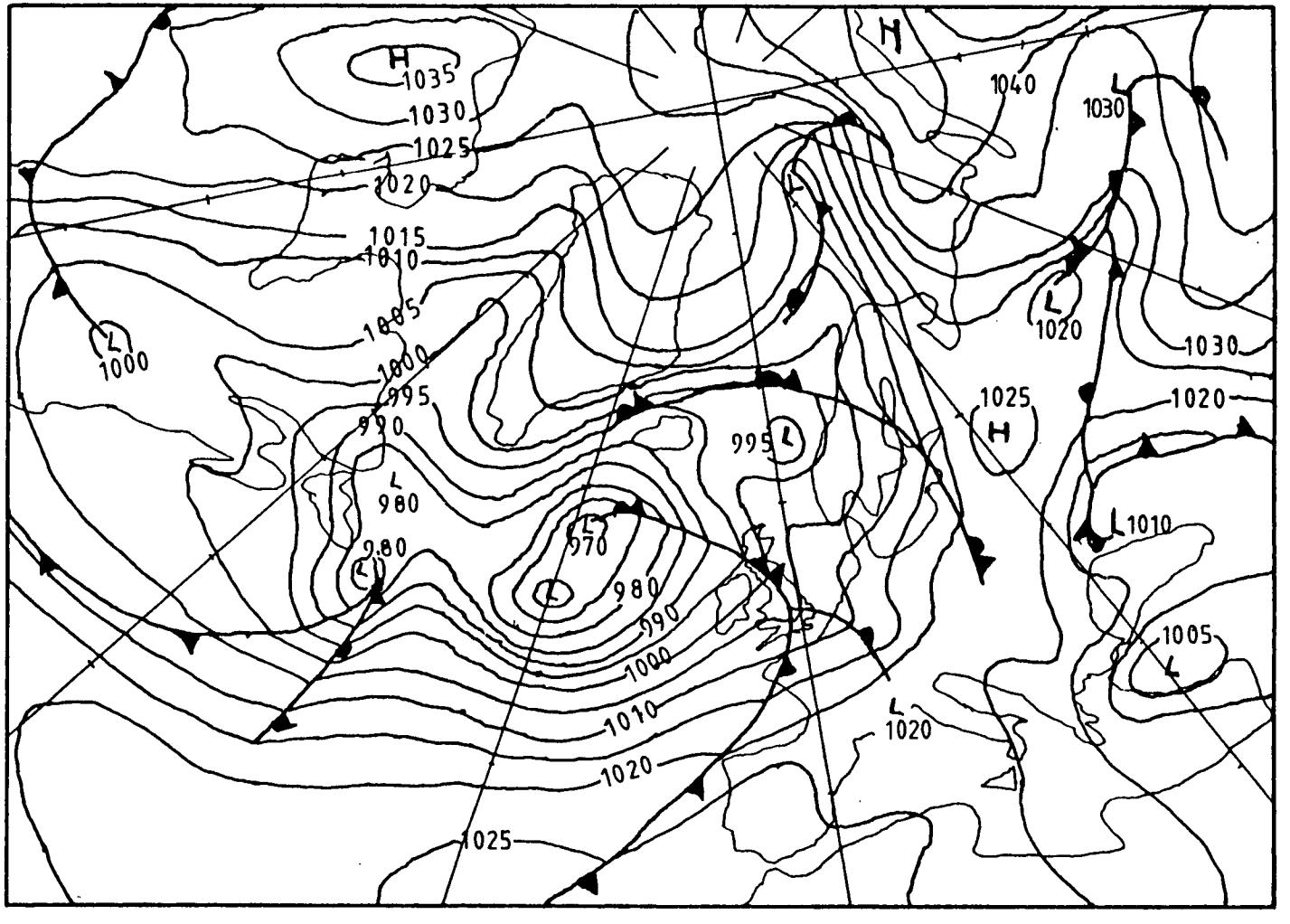

Figure 1.4 5/2/77 surface

with fronts passing into Europe. A young depression is visible over the western Atlantic. The blocked case of figure 1.3 is a complete contrast. Here, a large anticyclone is present beneath the anticyclone aloft and is excluding all fronts from the area of the U.K. Meanwhile, associated with the strong jet and consequent baroclinic zone to the north of the anticyclone, a vigorous depression is passing to the north of Norway. In the western Atlantic a mature and occluded depression is seen under the cut off low. This is to be contrasted with the young depression in the zonal case. Immediately to the west of the surface blocking anticyclone is a weak family of depressions whose fronts are aligned north/south through being prevented from making any progress to the east by the anticyclone.

It can be seen, therefore, that the strongly perturbed jet that occurs in a blocking situation causes a major disruption to the normal progress of depressions. This in turn causes abnormal weather in the area affected involving in some areas an increase in the number of depressions and an absence of depressions in others. Figure 1.5 illustrates this affect. It is taken from Petterssen (1956) and shows the positions of fronts during two contrasting ten day periods. One is a period of zonal flow and the other is a period of 'blocked' flow. The exclusion of fronts from the block is clearly seen.

Not all blocks have the flow pattern of figure 1.1. Indeed, three descriptions are most commonly used to typify blocking flow - ridge or meridional, omega and symmetrical. (See figure 1.6). There is little difference

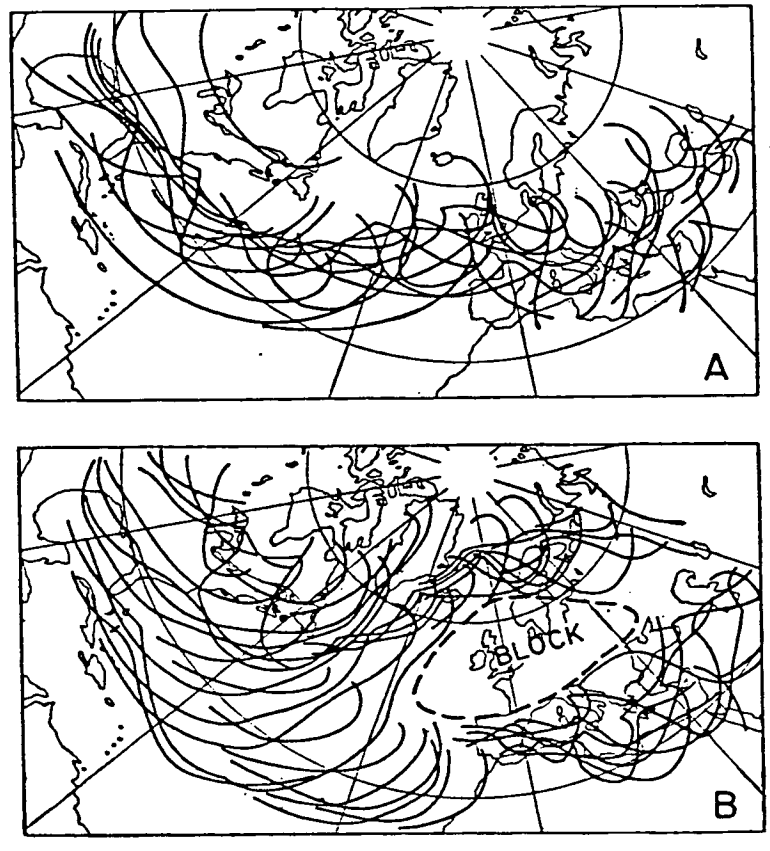

Figure 1.5 Position of fronts during two 10-day periods: A, preceeding the formation; B, following the establishment of a block. From Petterssen.

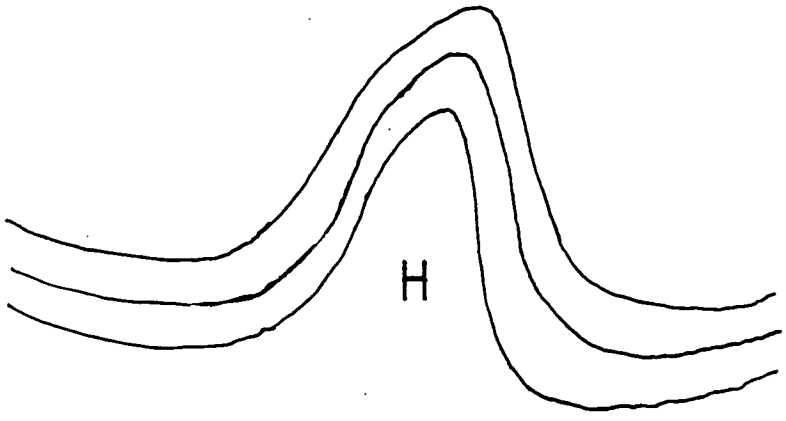

RIDGE TYPE

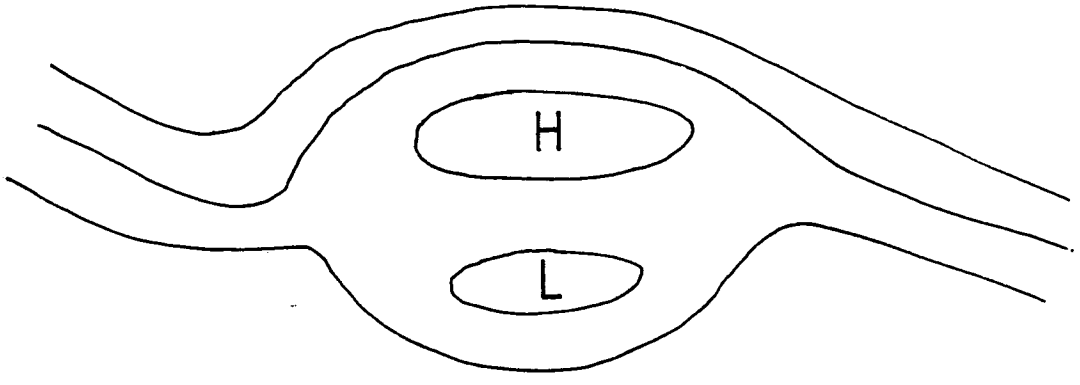

SYMMETRICAL TYPE

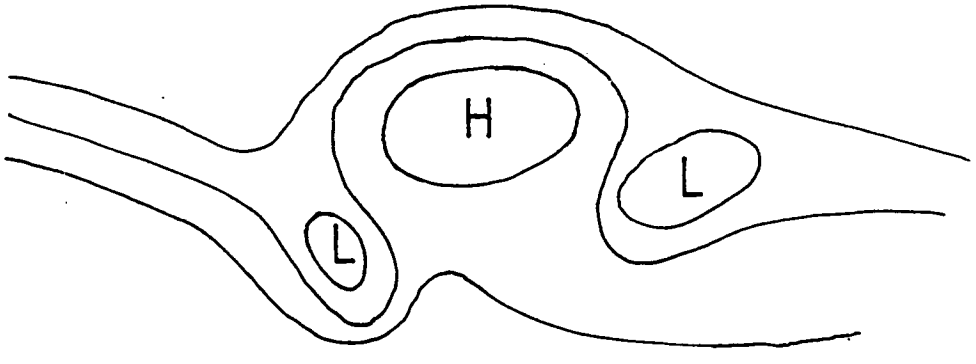

OMEGA TYPE

FIGURE 1.6 Sketches showing the appearance of three common blocking patterns, seen at the 500mb level.

between the omega and symmetrical patterns. Sumner (1954, 1959) recognises only a meridional type, and a diffluent type, which includes both omega and symmetric, whereas Austin (1978) describes all blocks as symmetrical saying that ridge type patterns do not persist but change to symmetrical during the block. In this study all three descriptions will be used. In any block, the flow pattern evolves slowly and might pass through all the three forms.

In all cases the block ends when either the anticyclone diminishes and is overridden by depressions, or moves to such a position that it no longer blocks the normal eastward progress of the depressions.

1.3 The Importance of Blocking.

1.3.1 The Effects of Blocking on the Weather.

The importance of blocking stems from the long life of the system (they have been recorded as lasting for a month (Rex 1950)) coupled with the abnormal weather associated with the disturbance of the depression tracks. As seen from the example of the previous section, the area to the west of a block experiences slow moving depressions with their associated fronts - and a consequent increase in precipitation - while the area under the blocking anticyclone experiences a decrease in precipitation because of the exclusion of fronts from the area by the block. If the anticyclone is cloud free the area can experience an increase in sunshine, which, coupled with decreased precipitation, can cause drought. An example is the summer drought in the U.K. in 1976 (Green 1977, Shaw 1977 and

references). To the east of the anticyclone, the returning south of the jet causes an increase there in the frequency of depressions bringing polar air and causes that area to have a continued spell of cold outbreaks. The long life-time of blocks, meaning that such abnormal weather can persist, leads in severe cases to droughts, floods or heavy snow falls which strongly affect agriculture and commerce. Rex (1950) gives charts which illustrates the altered weather patterns during blocking.

1.3.2 The prediction of blocking.

The predicting of blocking is a problem that only the most recent and complex forecasting models are beginning to solve. Bengtsson (1981) states that, in seven special forecasts carried out by the European Centre for Medium Range Weather Forecasts, the useful predictability ranged from fewer than five days to more than eight. The most successful was a case of blocking. He goes on to describe an exceptionally good forecast, made on the 16th January, 1979, at the onset of a block, which had useful predictability for more than ten days. However, this is only one case of accurate prediction, and this by his most complex model. He found that simpler models with lower resolution did not yield good forecasts because, he suggests, of inadequate representation of interactions between travelling small scale eddies and quasi-stationary systems. What Bengtsson does not discuss is the related problem - not of forecasting the life of a block from its first day, but of forecasting the initiation of a block from days in advance. A knowledge of the dynamics of blocking is

necessary to direct the efforts to improve forecasting models.

1.3.3 The effect of Blocking on climate.

The understanding of blocking is important in the area of climate modelling. Because of the potentially long life of any block and the abnormal weather pattern associated with it, a greater frequency of blocking can affect the seasonal weather and ultimately the climate of a region. The climatologist, therefore, requires to understand how blocking is connected with, and affects, the parameters of climate both locally and globally. Such an understanding can come only through a knowledge of the underlying processes of blocking.

The importance of the study of blocking derives from the local and climatic effects of blocking, whilst the immediacy of the study derives from the poor state of the present knowledge of the processes involved in the phenomenon.

1.4 The Results of Survey Studies of Blocking.

1.4.1 Introduction.

The general facts about blocking come from survey studies. In these, all blocks within a study period are catalogued and distributions of various parameters are then presented. Studies of this type have been published by Sumner (1959), Rex (1950), Treidl, Birch and Sajecki (1981) - hereafter TBS - and others. The most widely known is that of Rex who studied ten years of data.

The most recent study is that of TBS which covers the period 1945 to 1977 and is the longest of its type. It is to this study by TBS that I refer most often in what follows. Each survey differs slightly from the others because each investigator uses his own definition of blocking. This is most apparent in the minimum persistence required: Sumner requires a minimum of three days, whereas Rex requires ten days. These differences are due to the subjective nature of the phenomenon which relies on recognising patterns on daily charts. Despite this, however, the results of the surveys generally agree, showing that, on the whole, blocking can be reliably analysed using only subjective definitions. Blocking definitions are dealt with in more detail in Chapter 2.

The important results from the survey studies concern three attributes of blocking: -

1. The variation of the frequency of blocking with longitude.
2. The variation of the frequency of blocking with season.
3. The distribution of the lifetimes of blocks.

These are discussed in order below.

1.4.2. The Variation of blocking frequency with longitude.

The most important result of the surveys is that blocking occurs at preferred longitudes. Figure 1.7 from TBS shows the frequency of blocking with respect to longitude. The striking conclusion is that blocking occurs most frequently in two areas - 40°E to 40°W comprising the eastern Atlantic and western Europe, and 110°W to 160°W comprising western America and the eastern Pacific.

Following from

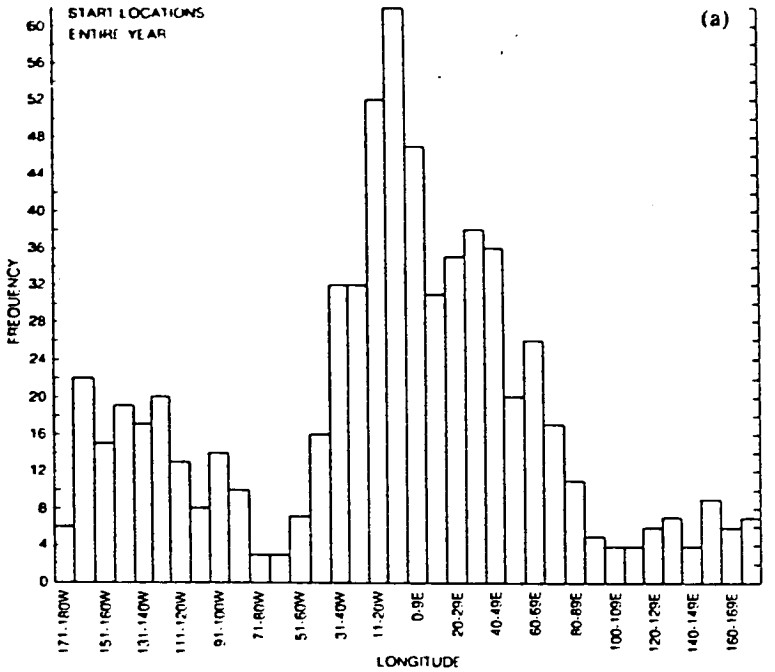

Figure 1.7 From Treidl, Birch and Sajecki: Frequencies of block starts by longitude.

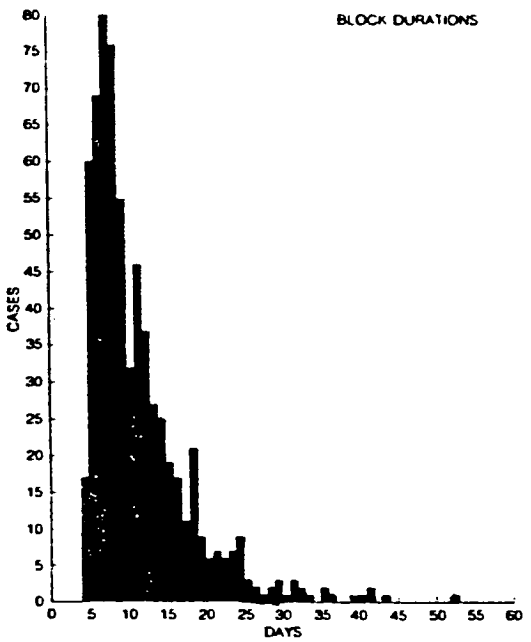

Figure 1.8 From Treidl, Birch and Sajecki: Frequency distribution of block durations, 1954-1977.

this, blocks are usually categorised into European or American types. Also noteworthy is the observation that European blocking is about three times more frequent than American blocking.

1.4.3 The variation of blocking frequency with season.

The frequency of blocking also shows a variation with season. In their study TBS found that blocking was most frequent in the spring season of April, May and June. The seasons were then ranked in the order - Spring, 205 blocks, Winter with 173, Summer with 147 and then Autumn with 139. Also reported by TBS is a slight eastward shift, in the summer months, of the most likely location of blocking.

1.4.4 The duration of blocking.

A distribution of the duration of blocks will depend on the minimum set by definition for the persistence of the features which constitute a block. For instance, Rex has a minimum persistence of ten days and he obtains an average lifetime of 16 days with a mode of 12 days. In contrast, Sumner uses a minimum persistence of 3 days: he obtains a mean lifetime of 14 days and a mode of 7 days. TBS use a minimum persistence of 5 days and find an average lifetime of 12 days and a mode of 8 days in agreement with Sumner. Comparing their results, it appears that Rex set his minimum persistence too high at 10 days since - from TBS - most blocks last only eight. The distribution of lifetimes from TBS is shown in figure 1.8. It is skewed towards the shorter periods. Hence,

the mode lifetime is more representative than the mean. Also evident in figure 1.8 are a few blocks with lifetimes greater than one month. As mentioned in section 1.3, these blocks will have had a profound effect on the climate of that season: the 1976 drought is an example of a very long blocking spell.

Although blocking is referred to often as bringing abnormal weather, it is not in fact a rare phenomenon. The term abnormal must be seen as purely relative; TBS find that, of all the days in the period 1945 - 1977, 55% had a blocking system present somewhere in the northern hemisphere. So, rather than class it as anomalous, it may be more realistic to regard blocking as normal and an uninterrupted zonal flow as abnormal.

1.4.5 Summary of the survey results.

The statistical surveys can be summarised thus -

- Blocking occurs in two preferred areas - between 40°W and 40°E and between 120°W and 170°W - referred to here as European and American Areas respectively.
- Blocking is most frequent in Spring.
- Blocking commonly lasts eight days, but can last for up to a month.
- Blocking affects up to 55% of all days.

1.5 The Connection of Blocking with the Planetary Waves.

1.5.1 Explaining the longitudinal frequency of blocking.

The results described in section 1.4.2 show that blocking has preferred areas of occurrence and indicate that the causes must, in some way, be linked to

geography. Various mechanisms have been suggested to explain this localisation: such as oceanic surface sensible heat flux (White and Clark 1975) and collapsing cold anticyclones (Rex). However, the most objective explanation has been put forward by Austin and involves the planetary waves which are themselves linked to geography.

The planetary waves play an important role in the general circulation, transporting heat and momentum across mid-latitudes, and, for that reason, among others, are being intensively studied. To connect them firmly with blocking, therefore, is an important contribution.

1.5.2 Planetary Waves.

Planetary waves are evident as the sinuous meandering form of the mid-latitude jet stream. When an upper air chart is Fourier analysed into zonal harmonics, a spectrum of component waves is produced. The individual waves in this spectrum are referred to by wavenumber. Conveniently, the wave number equals the number of ridges or troughs of the wave around one latitude circle. Each Fourier analysed wave is described by two parameters - (1) amplitude: the magnitude of the deviation from the mean, and (2) phase: the longitude of the ridge closest to the Greenwich meridion. Different waves in the

spectrum are generated by different mehcanisms. The longest waves 1 to 4 are the planetary waves, so called because they have dimensions of the order of the circumference of the Earth and respond to forcing of the same scale. Waves 6 and higher are called the short waves. They are not global but respond to local effects and result from the Fourier analysis trying to describe depressions. Wave 5 falls somewhere between the two types.

Planetary waves were first described theoretically by Rossby (1950) who showed that conservation of the vertical component of absolute vorticity is the principle of the motion. Since then, studies have shown that the planetary waves are generated by the action of mountain barriers (Charney and Eliassen 1949) and by the action of land-sea temperature contrasts (Smagorinsky 1953) on the jet stream. The waves can propagate both horizontally and vertically (Charney and Drazin 1961) and have been shown to be the cause of the sudden warming phenomenon in the stratosphere (Matsumo 1971, O'Neil & Taylor 1979). Each planetary wave is the resultant of two component waves, one stationary and the other mobile. The stationary components are generated by the forcing which is fixed geographically. Consequently, it is these waves which cause the troughs and ridges on the long term normal charts. The configuration of the phase and amplitude of these waves in the horizontal and vertical depends on the shear of the mean wind and on the exact nature of the thermal cooling aloft (Bates 1977) and varies from week to week as conditions change.

The mobile components of planetary waves are normally generated by the fluctuations in forcing arising from changes in atmospheric conditions, but can be generated by interactions between waves. As their name suggests they are free to move with their phase velocity. See Madden (1979) for a comprehensive discussion.

1.5.3 The circumstantial evidence for a connection between the planetary waves and blocking.

The evidence is presented in this section under four headings each concerned with one of the salient features of blocking as set out in section 1.4.5

1.5.4 Similarities in the longitudes of blocking and the ridges of the stationary waves

The long term mean stationary planetary waves can be found by the Fourier analysis of a long term mean upper air chart. Figure 1.9 contains a plot of the positions in longitude of the ridges of waves 1 to 4 obtained by Fourier analysis from the normal 500 mb charts around 60°N for the four seasons. The plot of blocking frequency versus longitude, taken from TBS, and already appearing as figure 1.7, is repeated at the top of figure 1.9. As pointed out by Austin, the area in which blocking is most frequent corresponds to longitudes where there are close groupings of stationary wave ridges. The blocking area from 100°W to 160°W is one in which the ridges of waves 2, 3 and 4 lie close together, while in the area of greatest blocking frequency, from 40°W to 40°E, the ridges of waves 1 to 4 lie close to each other. In no other longitudes do the mean stationary waves have a closer association. The

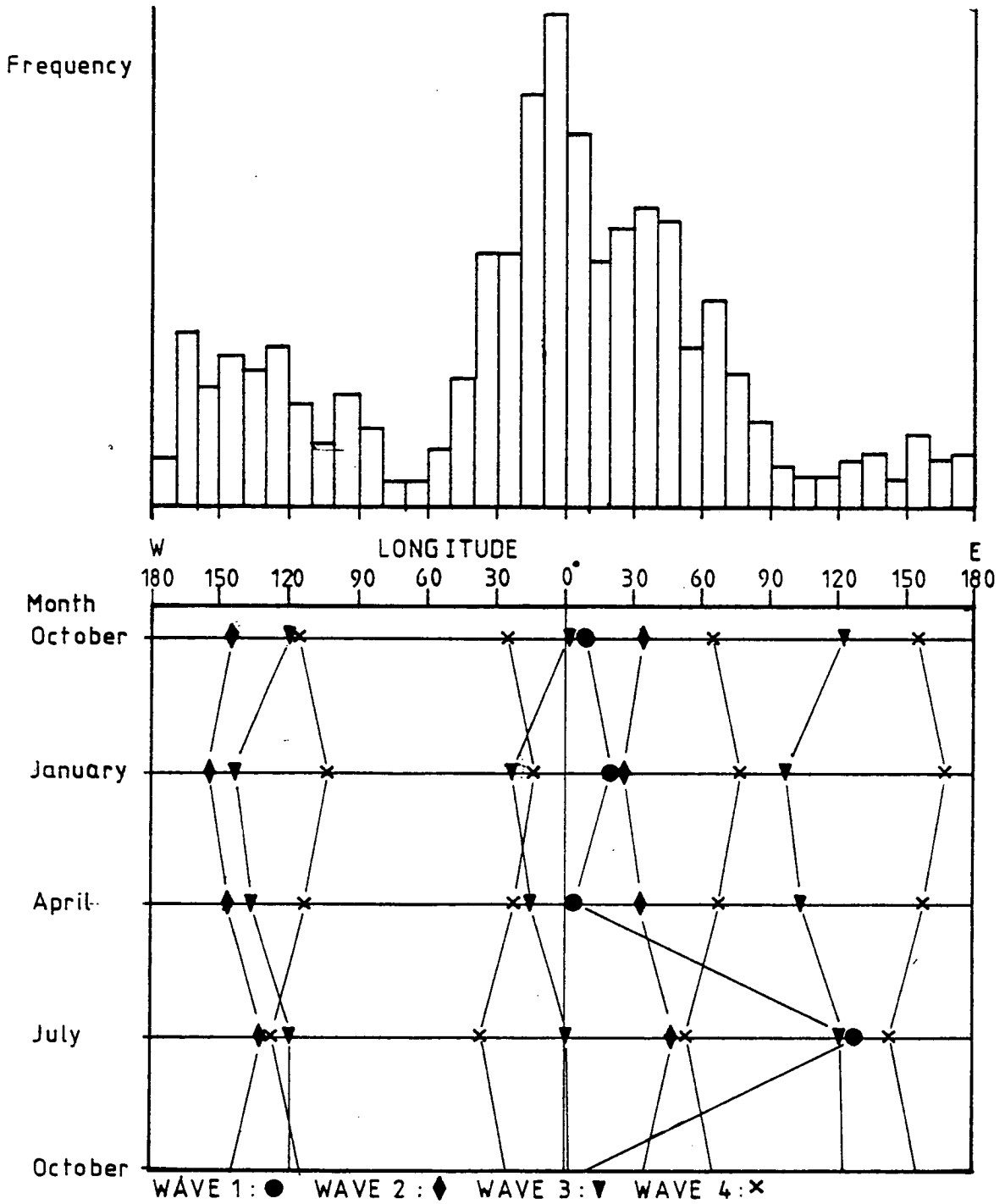

Figure 1.9 The positions of the ridges of waves 1 to 4 at 500 mb. and 60°N from the long term mean charts of Crutcher and Meserve (1970) aligned, for comparison, with figure 1.7.

comclusion is therefore that the longitudinal variation in blocking activity can be explained if blocking is connected with the ridges of stationary planetary waves.

1.5.5 Similarities in seasonal shift and in variations in seasonal activity.

TBS record that in summer the area of peak blocking frequency is shifted slightly east relative to the winter and spring positions. Figure 1.9 shows that in the summer season waves 1 to 3 all move East. Additionally, the survey studies show that blocking is more frequent in winter and spring, and less frequent in summer and autumn, while from figure 1.9 one sees that the wave ridges over the area 40^{o}W to 40^{o}E have their closest approach during the winter and spring months and are spread more widely in the summer. The waves are also generally much weaker during the summer. Again, the conclusion from this is that the seasonal variations of blocking activity can be linked circumstantially to the seasonal changes in the stationary wave pattern.

1.5.6 Similarities in movement.

During their lifetime, blocks are equally likely to progress, remain stationary or retrogress (Sumner). In this they contrast clearly with depressions which are always progressive. Only the long mobile planetary waves are regularly retrogressive. The table below, which is from Madden, shows the observed speed of planetary waves in degrees longitude per day during a winter month and makes the points that wave 4 is slow moving, wave 3 is stationary and waves 2 and 1 are strongly retrogressive.

Observed phase speed of mobile waves for a month of January in degrees longitude per day - from Madden.

Zonal Wavenumber.	1	2	3	4	5	6	7	8
Speed	-22	-13	0	4	7	9	8	7.5

(positive is eastwards)

It can thus be surmised that blocks which retrogress have some connection with waves 1 and 2, whereas blocks which are stationary, or which progress slowly, have connections with waves 3 and 4.

1.5.7 Similarities of Lifetimes.

TBS quote the most probable blocking lifetime as eight days. For comparison, results from a study of time series of the kinetic energy of various waves show that the average lifetime of an energy peak in waves 1 and 3 is ten days (Tsay and Kao 1978). Thus the long waves and blocking have similar timescales.

1.5.8 Summary of section 1.5

In summary, it is found that the planetary waves display the same timescales and similar motions to blocking events. Further, the seasonal and longitudinal variations of blocking can be explained if blocking is associated with the close grouping of the ridges of the stationary planetary waves. This evidence is strongly indicative of planetary wave involvement with blocking.

The next section is devoted to the description of recent theories of blocking, each of which associates planetary waves with blocking in one manner or another.

1.6 Blocking theories utilising planetary waves.

1.6.1 There are theories of blocking which do not involve planetary waves such as those by Rex, and by White and Clark. These propose, respectively, a hydrodynamical jump from supercritical to subcritical flow,and long wavelength baroclinic disturbances forced by high sea surface temperatures. However, the weight of evidence of section 1.5 is in favour of the greater number of theories which embody planetary waves, and only these wave theories are considered in this work.

The various theories are not totally distinct and so are discussed in what follows under headings which describe the aspects of planetary wave behaviour which are supposedly connected with blocking.

1.6.2 Resonance of planetary waves.

Tung and Lindzen (1979) propose a blocking mechanism in which a planetary wave, through becoming resonant, reaches high amplitude. They find that such a resonance can occur when atmospheric conditions are such that the mobile - or free - planetary wave has a zero phase velocity, and thus the natural mode of the atmosphere becomes identical with the forced stationary mode. Resonance in that wavenumber then occurs if the energy of the wave is not dissipated. Tung and Lindzen consider energy dissipations in the form of Eckman pumping and

and Newtonian cooling. They find that damping time scales of four to five days are realistic and yet allow high amplitudes to occur. Wave energy is contained and not radiated away if the energy is not free to propagate vertically but is reflected at some level. The conditions for reflection occur if there is sufficient easterly or strong westerly shear of the mean wind with height in the stratosphere. With this condition in mind, Tung and Lindzen say wave 4 may be the more common blocking wave rather than waves 1, 2 or 3, since the trapping conditions become more sensitive with increasing wavenumber. Thus wave 4 is in general trapped by the wind shears in the lower stratosphere, whereas waves 1 to 3 are not.

Tung and Lindzen's suggestion of wave 4 as the blocking wave fits the circumstantial evidence presented in section 1.5. In the Tung and Lindzen theory, the resonant wave is a mobile wave that has become stationary. Thus, the resonant wave would appear as an enhancement of the long term normal stationary wave and so could explain the geographical variations in blocking frequency.

However, Tung and Lindzen did not consider the energy dissipation via interactions with other wave-numbers which would be present in a real situation. In Chapter 5 it will be seen that such dissipations can have damping times of up to one day only and, in the presence of such strong dissipation, resonance will not occur unless the forcing is increased to compensate.

A search for evidence of this mechanism in real data would mean the investigation of two points, viz:

whether, at the time of each blocking event,

1. the free wave is stationary, and
2. the energy is trapped.

Such an investigation would require solving the vertical structure equations of Tung and Lindzen for actual conditions at the time of blocking. Alternatively, a study of the energy budget might reveal whether the vertical propagation of energy is at a minimum, as it ought to be in this theory when resonance occurs. One possible example of this mechanism is described in Chapter 5. A fully detailed trial of the mechanism was not possible in the limited time available for this study.

1.6.3 Blocking as a metastable state.

Charney and De Vore (1979) have demonstrated through a model that the two components of a simple system consisting of a zonal flow and a single topographically induced planetary wave can interact via the forcing function to produce regular vacillations. The flow predicted by the model alternated between a high zonal index with a low wave amplitude and a low zonal index with a high wave amplitude. In the high amplitude case, the wave was near a resonance state similar to that discussed by Tung and Lindzen. The high and low index flows were metastable. On the strength of their demonstration, the authors suggest that blocking, being an example of low zonal index flow, is a metastable state corresponding to the low index, high wave amplitude flow in the model.

Support for this mechanism comes from a description by Bengtsson of a blocking forecast made by a general circulation model. He says that the highly successful forecast of the life of the block from its day of inception suggests that the block is a quasi stable state. However, how such a mechanism might be verified from real data is unclear. Before real progress might be made in looking for the mechanism in real data, a criterion for state stability must be set up. No hint is available as to what this might be. Alternatively, an analysis of the mean wind/wave forcing and interaction function may be useful. This theory is not investigated in any depth in this study.

1.6.4 Blocking as a rotor in a planetary wave.

Scorer (1979) suggests that blocking is a rotor formed in a high amplitude planetary wave. Rotors are well known in the gravity wave trains which are established when a vertically stratified, stable airstream is disturbed by an obstacle. If the wave amplitude becomes sufficiently large, rotors appear. These are areas of the flow having a closed circulation. Closed circulations of this sort have not been picked out previously in the theoretical description of planetary waves. The normal derivation uses a perturbation technique which limits the amplitude of the wave motion to less than is required for the initiation of rotors. Scorer points out that it is possible to obtain the features of rotors in planetary waves from those for rotors in the extensively studied gravity waves by exploiting a similarity between planetary and gravity waves.

The identification of blocking as a rotor is compatible with both Tung and Lindzen and Charney and DeVore. Both theories have as the block a single wave of large amplitude - just the condition in which rotors form. Indeed Charney and De Vore display flows which have rotors but do not emphasise their importance. Thus Scorer's idea can increase the realism of the results of Tung and Lindzen and of Charney and De Vore by providing a mechanism to produce the closed anticyclonic circulations which are a prominent feature of blocking.

Chapter 6 is devoted to the experimental investigation carried out on examples of rotors in the real data set.

1.6.5 Blocking as a superposition of planetary waves.

The plots in figure 1.9 show that blocking occurs most frequently in those longitudes where the mean planetary wave ridges occur close together. From day to day, the ridges of individual wave numbers are not necessarily to be found in those longitudes: they move into and out of the region with variations in forcing. It can, therefore, happen that the ridge of one planetary wave overlaps the ridge of another forming a strong ridge at that longitude - constructive interference. At other longitudes, the trough of one wave might overlap with the ridge of the other - destructive interference. This is illustrated in figure 1.10. The profiles of a pressure surface along a latitude circle due to the superposition

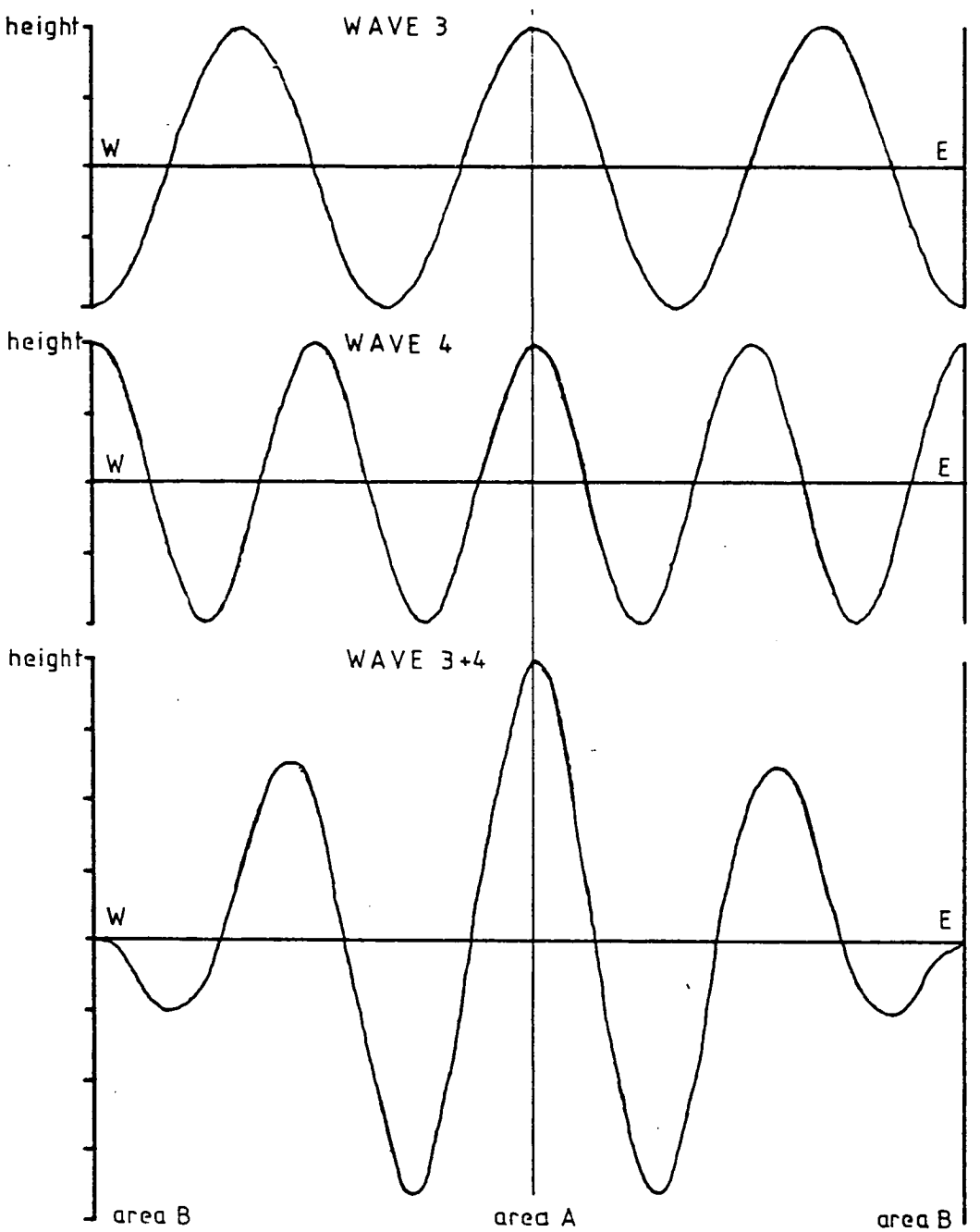

Figure 1.10 Showing how the summation of two waves creates local constructive (area A) and destructive (area B) interference.

of two waves are shown. The waves are in phase in area A and they are out of phase in area B. It is seen that, where the waves interfere constructively, the appearance is that of a local maximum in amplitude.

The theory of blocking as a phenomenon of planetary wave interference assumes that blocks occur where two (or more) planetary waves interfere constructively. On average the waves are at their long term mean positions Therefore, constructive interference between them is most likely to occur at the longitude positions at which ridges of the mean waves are close together. This is exactly the observation and is discussed in section 1.5.

The theory of wave interference as an explanation of blocking is more attractive than those theories which attempt to describe blocking in terms of one wave only, e.g. Tung and Lindzen. If only one wave were involved, blocking would be visible - not as a single anticyclone but as a regular train of ridges equally spaced around a latitude circle, and this regularity is not generally observed. Altogether, single waves of high amplitude cannot be expected fully to explain observed cases of blocking. Other interfering waves must be involved to annul the unwanted extra ridges.

Independently Austin has investigated the same idea using a limited data set. The results showed that blocks in the Atlantic could be explained by an interference of the pairs of waves 1 and 3 or 1 and 2, whereas blocks in American sector could be explained only by a superposition of waves 2 and 3. The short planetary wave, wave 4, Austin found was associated with blocks which

lasted longer.

This theory is investigated more fully in the next section and the verification of it, carried out on an extensive data set as part of this work, is given in detail in Chapter 3.

1.6.6 Blocking as a consequence of interaction between stationary and mobile planetary waves.

Egger (1978) uses the results of a numerical model to extend an interference mechanism for blocking. He suggests that a slow moving mobile planetary wave interacts with other stationary waves in such a way as to gain energy from the stationary waves, and that blocking occurs when the amplified mobile wave interferes with the stationary wave in the manner of section 1.6.5. There is thus a direct link between sections 1.6.5 and 1.6.6. Egger's theory is attractive because it provides a dynamical connection between the planetary waves which are interfering, the link being the transports of energy between the stationary and the mobile waves which are a consequence of the non-linearity of the governing equations.

The theory of Charney and De Vore also deals with interactions, but, in that case, the interactions are between the mean flow and the stationary waves and are by way of the topographic forcing function.

Egger's mechanism is equivocal with respect to Tung and Lindzen's theory because wave-wave interactions via the non-linearities can result in either a gain or a

loss to any interacting wave. If a resonance situation arises, the sign of the interactions will determine whether they increase the amplification or the damping.

Egger's theory is investigated closely as part of this study in chapter 5, where the non-linear interactions between the waves are calculated directly.

1.7 The Present Study.

The present study is an investigation of the veracity of some recent blocking theories involving the planetary waves when applied to a real data set. The logical first step is to analyse the relationship in real data between blocking and planetary waves without regard to theory. This is done early in Chapter 3, where the blocks from a winter and spring season are each compared with the planetary waves of the same period. The data set from which the blocks and the waves are taken is described in Chapter 2. Later, in Chapter 3, the idea of blocking being an interference between two or more planetary waves is dealt with fully.

Results from a similar independent analysis were published by Austin as this study was in progress. However, Austin's analysis is much simpler than the one presented here in a number of respects. Firstly, there is the difference in the number and type of blocks analysed. Austin analyses only seven, chosen to represent typical occurrences, while this study analyses all eighteen available from the six month period covered by the objective data set, and not chosen for their appearance. Secondly,

the present study covers the planetary waves at all the important latitudes whereas Austin's is limited to two latitudes. That this study is larger and more detailed than Austin's is of particular note as, with the known large variability of the atmosphere from period to period, it is important to analyse as many blocks as fully as possible.

Chapter 4 examines the behaviour of the kinetic energy of each wave during blocking. This is done to provide a link between the analysis of Chapter 3 and the wave-wave interaction diagnostics of Chapter 5. Additionally, some statements in the literature regarding the time evolution of the kinetic energy are examined.

Chapter 5 attempts to investigate Egger's mechanism for blocking. It is logical to study this since it is closely similar to the interference mechanism examined in Chapter 3. In order to uncover the mechanism, the wave-wave interactions are evaluated and, since these are fluxes of energy, their effect is compared to the analysed kinetic energy from Chapter 4.

Lastly, in Chapter 6, Scorer's theory is examined in a simple way. This theory is of interest because many theories assume blocking to be caused by a high amplitude wave, and rotors are a feature of high amplitude waves. A simple theory for rotors in Rossby waves is worked out following Scorer's suggestions, and the objective data set is searched for evidence of rotors.

Chapter 2. THE DATA SET.

2.1 Introduction.

A comparison of blocking with the variations of the planetary waves requires both a catalogue of blocking events and a record of the planetary waves covering the same period. At the outset of this study an objective data set covering the period 1/11/76 to 30/4/77 was made available by the Meteorological Office, and, from this, the planetary waves were calculated. For comparison, a detailed descriptive catalogue of the blocking events was compiled, as a second part of this study, for the same period as the objective data set. The blocking catalogue and its compilation are described in section 2.2 below, and the description of the data set follows in section 2.3.

2.2 The Blocking Catalogue.

2.2.1 A Blocking definition.

To compile a catalogue of blocking one requires a definition of blocking. Such a definition describes those attributes which the 500 mb flow must have if the flow is to be considered blocked. The 500 mb flow is chosen almost exclusively by investigators because 500 mb represents the steering level for depressions, and hence a block is most visible at this level. The most important effect of blocking is that it disturbs the normal flow of depressions. Therfore, all the requirements of a definition are to ensure that only disturbed patterns of the flow are considered.

2.2.2 The minimum persistence of blocks.

The first part of any definition is the minimum lifetime of a block. Rex required his blocks to persist for ten days, whereas Sumner required only three days. At ten days, the definition will only pick out strongly disturbed flow patterns, whereas, at three days, the definition scarcely distinguishes blocking highs from slow moving transient ridges. Recent definitions from Austin and TBS, and the definition in this study, compromise requiring a persistence of five days. This is long enough to avoid the inclusion of any transient ridge yet short enough to include all blocking situations.

2.2.3 The definition of the minimum intensity of a block.

Longevity of an anticyclone is not enough to define a block. The sub-tropical anticyclone persists for months but it is not a block. The difference lies in the position of the anticyclone; for a blocking high, this must lie across the normal track of the depressions - a requirement not fulfilled by the subtropical high. To ensure the proper positioning of the high, Rex requires that the jet be split into equal parts to north and south of the block. In practice, this is an unsatisfactory requirement because it excludes ridge shaped blocks which do not split the jet. Also, the strength of any southern jet is difficult to assess by eye from the charts because of the reduced contour gradients in lower latitudes consequent upon the decreased Coriolis parameter.

In this study I require that, on the 500 mb charts, the flow be of one of the recognised patterns - ridge, omega or symmetrical - and that the anticyclone, both at 500 mb and at the surface, must encroach substantially on the normal path of the jet and on the normal depression tracks. Sumner has a similar requirement. TBS require that both surface and 500 mb anticyclones have a closed isopleth, but this is too dependent on the particular contour analysis.

The beginning and ending days of a blocking episode are determined from the observed growth or decay of the anticyclone, or from the time of exclusion or penetration of depressions into the blocked area, or both. There is a degree of variability in this determination but any variations do not amount to more than a day either way in the block's lifetime. Variability of this sort cannot be avoided when such subjective assessments are made. The size of the variation would have little effect on the later analysis of the planetary waves in this study.

2.2.4 Summary of the blocking definition used.

In summary, the blocking definition used in this study is: for an anticyclonic system to be considered a block it must

1 Last for five days at least,

2 Be of one of the three patterns - ridge, omega or symmetric, and

3 Interrupt the jet and affect the normal progress of depressions.

2.2.5 The Blocking catalogue.

The catalogue of blocks for the period 1/11/76 to 30/4/77 was compiled from the daily 500 mb and surface hemisphere charts taken from the European Meteorological Bulletin using the definition outlined in the previous section. From the charts, a detailed description of each block was made. These appear in appendix 1. The date of each block, along with my reference number for it, appears in table 2.1. Eighteen blocks were found within nine periods, some of which consisted of more than one block running sequentially or, less frequently, simultaneously. Thirteen blocks were found in the Atlantic/European sector and five in the Pacific/American sector. There were two cases of blocking in both sectors at the same time.

2.3 The Objective Data Set.

The objective data set from which the planetary wave data was calculated was obtained from the Meteorological Office where it had been collected for their own research purposes and comprises objectively analysed heights on all synoptic pressure levels in the northern hemisphere for each day of the period 1/11/76 to 30/4/77. It is the same data set as was used and described by O'Neill and Taylor (1979). However, only the 500 mb level is used in this study. The data, as supplied, is gridded on a polar stereographic array of 3209 points and covers from 15°N to the pole. The calculations of zonal harmonic waves and interactions

(necessary for chapters 3, 4 and 5) require, for convenience, the data to be in the form of a latitude/longitude grid. Therefore, before use, the 500 mb data is converted by simple interpolation into a regular latitude/longitude grid of 16 x 32 points - giving 5^{o} resolution in latitude and 11^{o} resolution in longitude. This is regarded as sufficiently fine for the present study where the maximum zonal wavenumber to be dealt with is 8, which, at a minimum, requires a resolution of 22^{o} in longitude.

2.4 Postscript.

This chapter has discussed and put forward the definition of blocking used in the production of the detailed blocking catalogue which appears in appendix 1. An objective data set for the same period was also described from which, in chapter 3, planetary wave data is calculated and then compared with the blocking events from the catalogue. The objective data set is again used in Chapters 4 and 5 when wave kinetic energy and wave-wave interactions are calculated - again for comparison with the blocking events from the catalogue.

Table 2.1.

Blocks occurring in the period 1/11/76 to 30/4/77.

Reference No.	Starting date.	Finishing date.	Duration in days.	Typical longitude of anticyclone.
E1	Pre.11/76	5/11/76		20°E
A1	10/11/76	15/11/76	6	120°W
E2	19/11/76	26/11/76	8	20°W
A2	26/11/76	1/12/76	6	135°W
E3	11/12/76	20/12/76	10	0°E
E4	22/12/76	30/12/76	9	30°W
E4A	27/12/76	31/12/76	5	75°E
E4B	31/12/76	7/1/77	8	40°E
E5	7/1/77	14/1/77	8	40°W
A3	4/1/77	16/1/77	13	135°W
E5A	13/1/77	19/1/77	7	30°E
A4	23/1/77	30/1/77	8	130°W
E6	22/2/77	2/3/77	9	20°W
E7	11/3/77	20/3/77	10	40°E
E8	21/3/77	26/3/77	6	20°W
A5	30/3/77	7/4/77	9	135°W
E9	2/4/77	9/4/77	8	30°W
E10	11/4/77	16/4/77	6	55°E
E11	21/4/77	29/4/77	9	70°E

Chapter 3. THE ANALYSIS OF BLOCKING INTO ZONAL HARMONIC COMPONENTS AND A COMPARISON WITH THE RESULTS OF AUSTIN'S WORK.

3.1 Introduction and Austin's results.

3.1.1 Introduction.

In this chapter, I analyse subjectively the amplitude and phase behaviour of individual planetary waves in a search for any relationship between them and blocking. In this I extend Austin's study. Analysis of the eighteen blocks in the study period supports Austin's conclusion about American blocking, but reveals that her conclusions about European blocking must be modified to take more account of waves higher than wavenumber 3.

3.1.2 Austin's results and conclusions.

Austin postulated that blocking occurred when the crests of two planetary waves coincided: the reinforcement of one crest by another creates the central anticyclone of a block. To test this, Austin chose to analyse seven blocking events covering all three possibilities: two cases of European/Atlantic blocking, three cases of American/Pacific blocking and one case of blocking in both areas simultaneously. The seven were chosen as good examples of their type.

The planetary waves were found by Fourier analysis of the height of the 500mb surface around two latitudes, viz. 60^{o}N and 40^{o}N and the time series of amplitude and phase were used to correlate the wave activity with the blocking.

Austin concluded that: -

(a) Atlantic blocking was due to a superposition upon wave 1 of either wave 2 or wave 3.

(b) Pacific blocking was due to a superposition of waves 2 and 3, but only if wave 1 were weak.

(c) Longer living blocks were maintained by a strong wave 4.

(d) The waves which created blocks had amplitudes higher than average.

(e) The waves which created blocks had phases close to the phases of the long term normal waves.

3.1.3 The limitations of Austin's analysis.

Austin's analysis was limited to seven blocks only. The large variability of the atmosphere makes it desirable to analyse as large a sample of events as possible. Thus the present study is more satisfactory in analysing eighteen blocks - thirteen European and five American. Austin analyses three and four respectively. In this study there are two double blocks whereas Austin analyses only one.

Austin's analysis is also limited in that she considered just two latitude bands. An analysis limited to two latitudes shows only structures large in meridional extent, and an increase in the latitudinal resolution is therefore desirable. Also, if blocks can indeed be related to specific wave superpositions, any theoretical attempt at explanation will require a knowledge of the meridional wavenumber as well as the normal longitudinal wave number. Illustrating this point is Egger's choice of a meridional wave of number 2 for his blocking wave.

To quote from his paper - 'Blocking situations are characterised by a high pressure cell to the north with an adjoining low to its south. Hence a wave with meridional wavenumber 2 should be a member of the block'. The geometry of Egger's beta plane model means that his meridional wave 2 corresponds only roughly to wave 2 on the hemisphere. However, the 5^{o}latitudinal resolution in this present study is able to judge the correctness of Egger's decision by enabling the meridional structure to be seen. Also, the plots obtained with this higher resolution show much structure, especially in high latitudes, which a simpler two latitude analysis would have missed, and illustrate the limitations of Austin's study.

3.2 The calculation of the time series of amplitude and phase.

3.2.1 The calculation of amplitude and phase.

The data set covers each day for the period November, 1976 to April, 1977 inclusive and extends latitudinally from 15^{o}N to the pole. As described in chapter 2 the 500mb heights are used exclusvely but are first put into the form of a latitude/longitude grid. For this chapter's analysis the planetary waves are found by Fourier analysing the grid along the sixteen latitudes to obtain the amplitudes and phases of the height waves. The analysis is cut short at wavenumber 8. The wavelength of wave 8 is 45^{o} in longitude and this is shorter than the size of most blocks. The results show the calculation of higher waves to be unnecessary. The analysis in this chapter also includes examination of the

zonal mean wind. This was calculated geostrophically using the zonal mean height at each of the sixteen latitudes of the grid and simple first order derivatives with latitude.

3.2.2 Presentation of the Results.

The time series of zonal mean wind and of amplitude for each wave are obtained as a two dimensional chart, see figures 3.1 to 3.10. The time axis extends from 1st November, 1976 to 30th April, 1977, and the latitude axis from 15°N to 85°N. The values of amplitude and zonal mean wind for each day and latitude are given as contours. The phases of the waves are also presented. In this study, the phase is defined as the longitude of the maximum of the wave closest to the Greenwich Meridian. Because the phase angle is discontinuous at 180° the phases cannot be displayed as contours, as the amplitudes are, nor as fully. Instead, the phases at only two latitudes are illustrated, although the phases at all latitudes are used in the analysis, and these are presented as longitude/time sections. Figures 3.11 to 3.14 show the phases at latitude 60°N and latitude 45°N. Latitude 60°N is chosen because blocking anticyclones are commonly centred on this latitude, and 45°N is chosen because this is the latitude of the leading and trailing cut off lows. The longitude/time sections for waves 1 to 4 show the longitudinal position of every ridge. For waves 5 to 8, this would be too confusing. Instead, the height profile due to these waves, reconstructed from the Fourier coefficients, is plotted daily.

3.3 The Analysis of the amplitude and phase data.

The amplitude and phase data are related to the blocking events by subjective analysis. The essential part of a block is considered to be the anticyclone. Hence, waves are considered important if they have phases which place their ridges over the position of the blocking anticyclone and, the greater the amplitude of the wave, the more important it is considered to be. If the wave amplitude peaks during the block, this is also considered to be further evidence connecting the wave with the block. A detailed wave history of each block is therefore compiled by comparing the amplitude and phase of each wave with the contemporaneous position, movement and intensity of the blocking anticyclone.

The histories of the eighteen blocks are set out in appendix 2. At the end of each there is a short description of the structure of the zonal wind over that block with, finally, a note of the waves considered important for that block.

An objective analysis of the data would provide a more concrete assessment of the importance of each wave to blocking. However such an analysis would require objective criteria for 'importance'. Only by first identifying the relationships between planetary waves and blocking can one hope to formulate such realistic objective criteria. This study seeks to bring out through a subjective analysis any connection between the waves and blocking which might be used in the future on an objective basis.

3.4 Analysis of the European blocks.

3.4.1 Introduction.

Austin's principal conclusion concerning European blocking is that these blocks are due to the superposition of the ridges of either waves 1 and 3 or waves 1 and 2. In this study, there are ten cases of Atlantic blocking, ranging in lifetime from five to ten days with which we can test Austin's conclusions, and, in fact, only three blocks in this study are caused by these combinations. They are E3, E8 and E4B.

3.4.2 European blocks conforming to Austin's descriptions.

Blocks E3 and E8 both have high latitude anti-cyclones and, in both cases, waves 1 and 2 have amplitude maxima in the band 60° - 70°N. In high latitudes, E3, which lasted ten days, is caused by a superposition of waves 1 and 2, but, in mid-latitudes, the ridging is caused by wave 4. E8, which lasts only six days, is initiated by wave 3 and subsequently maintained by a strong combination of waves 1 and 2.

Block E4B is due to a very high amplitude of wave 1 at 50°N. This has the effect of displacing the main jet stream north of its normal position. The jet is not strongly meridional as in E3 and E8. Wave 2 is strong during E4B but to the north of wave 1, and is associated with the main blocking ridge which retrogressed throughout the life of this block. The large longitudinal extent of E4B is due to the block's being caused by the very long

wavelength of waves 1 and 2 at unusually low latitudes where waves 3 and 4 are more to be expected. However, at this time waves 3 and 4 are passing through a weak period.

It is my observation that blocks often decay when the high latitude anticyclone moves off either to the east or the west causing the blocking ridge to appear to swing or 'flop over'. Afterwards the ridge either subsides south or breaks in the middle with the high latitude anticyclone continuing to move away. E8 is an example of the latter sequence though either E4 or E5 is better. The explanation appears to lie in the greater prominance of mobile waves in high latitudes than in mid and low latitudes where stationary waves dominate. This can be seen by comparing figures 3.11 and 3.12. The northern anticyclones of blocks, being caused by the planetary waves, will therefore display mobility.

3.4.3 European blocks not conforming to Austin's descriptions.

The remaining seven European blocks do not bear out Austin's conclusion. A combination of waves 1 and 2 or 1 and 3 is not entirely responsible. The combinations involved are - waves 1,4,3 (bis), 3,4,2; 3,4,5,6; 1,3,4,6; 2,4 and 2,3. Certain of the blocks are similar in some aspects but essentially each has a unique history.

E2 and E6 are similar. They are both caused by waves 1, 3 and 4. They are centred over the same longitude of 20°W. They last about the same time, and they are both of the ridge type. However, block E2 occurs during a period of strong amplitudes, with wave 4 especially strong, whereas

E6 occurs during a period of generally low amplitudes with only wave 1 strong. E2 starts with a wave 1 in coincidence with a strong wave 4. However, in mid-period the wave 1 weakens as a wave 3 amplifies to take its place. Wave 4, the main blocking wave, lasts throughout the block.

In contrast E6 starts when wave 1 amplifies strongly. Waves 4 and 3, the other blocking waves, are in phase with wave 1 but are not much above average amplitudes. The greatest difference between E6 and E2 is the contribution made to E6 by wave 6. On the synoptic charts, the blocking zone appears as a large area of slack gradients across which a sharp slow moving ridge progresses. This ridge is the wave 6 feature.

The other European block in which wave 6 plays an important part is E5A. The blocking area in E5A is created by waves 3 and 4, but waves 5 and 6 together cause the slow eastward moving ridge in mid-latitudes. Whenever they occur during blocking, waves 5 and 6 are progressive. At the time of E5A, an unusual stratospheric warming is taking place with the zonal wind reversal reaching to the surface and, at 500 mb, as far south as 55°N (O'Neill and Taylor). E5A and E6 therefore occur in very different circumstances.

Blocks E4A and E10 can be grouped together because they are positioned farther east than the others in this study. E10 occurs at 55°E and E4A at 75°E. Both are formed on the eastern ridge of a strong wave 3 in latitudes around 60°N. Both appear when a previous block farther west is decaying. In both, wave 2 plays an important part. In

E4A, wave 2 amplifies at first in reinforcement of wave 3 but later ends the block by moving swiftly west out of coincidence with wave 3. In E10, wave 2 amplifies in coincidence with wave 3. Since both waves 2 and 3 are progressive, the block progresses throughout its life. E10 ends when wave 3 decays and the anticyclone moves off east with wave 2. Both blocks appear in the first ridge downstream from an Atlantic block. E4A occurs simultaneously with its parent Atlantic block, E4, whereas E10 occurs after an unusually strong wave 4 block, E9. When waves have phases differing significantly from their normal, they are usually mobile. In E10, waves 3 and 2 depart significantly from their normal phases, hence the mobility of the block.

The remaining three blocks of this group are E5, E7 and E11. E7 and E11 are similar because they feature waves 2, 3 and 4 and occur east of 0°, E7 is at 40°E and E11 at 70°E. E7 occurs as waves 2 and 4 come into phase with each other. Wave 3 is also in phase but is weak. E11 occurs as wave 3 amplifies in phase with a strong wave 2 though it subsequently decays. In both blocks neither wave 3 nor wave 4 is strong. E5, however, is quite dissimilar. It occurs in mid-Atlantic at 40°W and is caused by a very strong wave 3 which produces an extensive ridge from low to high latitudes. It decays in an unusual way with the northern tip of the ridge at 70°N moving swiftly west and passing to the north of a very large cut off low over North America. The explanation is that wave 2 takes over from wave 3 in high latitudes when

wave 3 collapses at the end of the period. As wave 2 is moving swiftly west, the anticyclone also moves west.

3.4.4 Summary of the analysis of European blocks.

The longwave combinations which cause the purely European blocks in this study are -

1,2,3 1,2,4 1,3,4 2,3,4 1,2
2,3 3,4

Although not all possible combinations of waves 1 to 4 have been found, from the variety that has it seems only reasonable to infer that European blocking can be caused by any combination of waves 1 to 4. The table below shows the number of times that each wave is prominent in the eleven blocks described in section 3.4.3.

Wave number	1	2	3	4
Number of times cited as important	5	8	8	6

It is seen that waves 1 to 4 are almost equally often prominent with waves 2 and 3 marginally more often. Waves 5 and 6 are only occasionally cited as important. This is less restrictive than Austin's conclusion where only waves 1 and 2 or 1 and 3 are held responsible. If this were true, then wave 1 should be the most common wave. This is not found in the present results where wave 1 is the least common of the long waves.

3.5 Analysis of the American blocks.

3.5.1 The wave behaviour in each of the three cases.

In this study there are three examples of Pacific blocking - A1, A2 and A4 all of which have as their basis a superposition of waves 2 and 3. They can be described in two groups because A1 includes wave 4 in its make up whereas A2 and A4 include waves 5 and 6 and are each followed by a 'grey' period.

Block A1 is relatively simple. It is caused by an amplification of wave 3 as it and wave 4 move into coincidence with wave 2. During the period a pronounced double jet is evident. The block finishes when wave 2 falls in amplitude, the waves move away from coincidence, and the double jet breaks down.

Like A1, blocks A2 and A4 arise from a superposition and amplification of waves 2 and 3 but, in contrast, wave 4 is not involved, while waves 5 and 6 cause a slow moving ridge which progresses through the blocking zone. Both blocks finish when waves 5 and 6 fall to normal amplitudes, even though, in both cases, the main blocking waves 2 and 3 are still strong and cause the jet to remain disturbed for over another six days. In A4, a small but short lived ridge occurs during this 'grey' period but was too short lived to be catalogued as a block. A2 and A4 differ in their profiles of zonal mean wind. In A2 a double jet is formed early but breaks down during the block only to reappear during the following 'grey' period. A4 has no double jet, having easterly winds in mid and high

latitudes. During its 'grey' period a jet is formed at 85°N with easterlies to the south matching exactly the 'mini' blocking event mentioned above.

3.5.2 The special role of waves 5 and 6 in blocks A2 and A4.

It appears that the ridge in the region of 50°N to 60°N formed by the short waves 5 and 6 determines the durations of the blocks A2 and A4. The region 50° to 60°N lies on the northern side of the jet stream and across the normal track of depressions, and any strong ridge in this critical area stops the progression of depressions. In A2 and A4 this critical ridge is caused by waves 5 and 6. So, when they become weak, the ridging across the jet weakens, allowing depressions to pass and ends the block.

3.5.3 Comparison with Austin's conclusion.

From the results it is clear that Austin is correct is describing American blocking as a wave 2 and 3 superposition, with those waves having near normal phases. Also wave 1 is never involved, but wave 4 is of importance on some occasions. In addition, it is seen that waves 5 and 6, when they appear and reach high amplitudes during the block, can play a decisive part in determining the duration of the block. They create ridges across the sensitive area of the mid-latitude jet where the depression track lies.

3.6 Analysis of the double blocks.

3.6.1 Analysis of the two examples.

Twice in this study blocks occur at a European and an American location simultaneously. Each is a unique event. In A3/E5 wave 3 achieves its highest amplitudes, while in A5/E9 wave 4 achieves its highest. Both blocks are caused by a superposition of waves 3 and 4 with European and American ridges at 30°W and 135°W respectively. The longitude difference of 100° lies between the wavelength of wave 3 and the wavelength of wave 4. For both events the phases of waves 3 and 4 match more closely over the European ridge. The superposition over the American area is not so precise and the blocking ridge takes up a middle position. Both double blocks happen in periods when waves 1 and 2 are unusually low, thus allowing waves 3 and 4 to become more intense.

3.6.2 Comparison with Austin's findings.

The two blocks are quite unlike those described by Austin which were caused by waves 2, 3 and 1. This highlights the variety of possible blocking wave combinations which make it impossible to reach any general conclusion from such a small set of examples.

3.6.3 Another type of double block - double European.

Before concluding the section on double blocking it is worth noting that there is another double block in the study period. It consists of E4 and E4A which have been dealt with earlier as individual blocks in the section on

European blocking. In this double block, E4 is at 30°W and E4A is at 80°E, a difference in longitude of 110° which is close to the wavelength of wave 3. It is caused by a strong wave 3 and so is similar to the conventional double block A3/E5. Otherwise, this double block is atypical. In the conventional double block the American ridge is upstream of the European ridge, whereas, in this case, the second ridge is downstream of the European.

3.6.4 Summary of the results of the analysis of double blocking.

The waves causing double blocking in this study in the American and European areas are numbers 3 and 4. They have high amplitudes. They coincide more closely over the Atlantic block, while the American block lies mid-way between the wave 3 and wave 4 ridges. Double blocks, again caused by a high amplitude wave 3, can occur with a parent block in the European area and a secondary block formed on the next ridge down stream. The conclusion is that wave 3 is the most important wave for double blocking, as concluded by Austin, but it must be reinforced. Wave 4 is the most suitable wave to reinforce wave 3 because it fits the set longitudinal gap between the American and European sectors.

In what follows, the members of double blocks are treated independently as European or American blocks, except where otherwise noted.

3.7 Presentation and discussion of results concerning all of the blocks.

3.7.1 The phase behaviour of waves during blocking.

Austin says that blocking happens when the participating waves have near normal phases. This must be so if the theory of blocks occurring as superpositions of planetary waves is to explain the longitudinal frequency of blocking. From the phase plots of waves 1 to 4 around 60°N it is found that in 50% of all cases the average position of every important wave during blocking is displaced less than one tenth of a wavelength from the normal position, and in 70% of all cases the displacement is less than two fifths of a wavelength. The present results therefore agree with Austin's conclusion: blocking waves are near normal in phase.

3.7.2 The role of wave 4 in long lived blocks.

Austin concludes that wave 4 is significant in longer living blocks, and this conclusion can be checked with the present analysis. Of the seven longest living blocks, six include wave 4, whereas of the six shortest living blocks only two include wave 4. If the statement is recast, and one suggests that the participation of wave 4 is an indicator of longer living blocks, it follows that the average lifetime of blocks with wave 4 is greater than that of blocks without. For all of the blocks studied, the average lifetime of the twelve blocks which include wave 4 is 8.8 days, and of the six which do not is 6.7 days. The difference between these two means is statistically

significant at the 5% level. Hence, Austin's conclusion is substantially correct: wave 4 is connected with longer living blocks.

3.7.3 Short wave-long wave interactions.

Slow eastward moving ridges, together with upstream and downstream cut off lows are caused by waves 5 and 6. In four cases - A2, A4, E6, E5A - these waves interfere constructively with the long waves, and, at the same time, achieve large amplitudes. It is these unusually large amplitudes, coupled with the observed slow moving ridges created by these waves which progress across the larger scale blocking zone, that leads one to speculate on the role of these short waves in the blocking process. I suggest that some form of interaction between the planetary waves and the shorter waves may be taking place, causing the short waves to become slower moving than normal and higher in amplitude. One possibility is that the large slack area of meridional height gradient at the block which is created by the long wave superposition is affecting waves 5 and 6. The high amplitudes may be achieved, either by direct energy conversion from the long waves, or from optimised growth factors - such as thermal gradients, etc. - produced as a secondary consequence of the planetary wave superposition.

The importance of waves 5 and 6 is discussed further in chapters 5 and 6.

3.7.4 The role of the zonal mean wind.

Austin suggests that the zonal mean wind decreases during blocking. To examine this, figure 3.15 is presented. It shows the time series of a zonal index composed of the average zonal wind between 45° and 60°N, the data being taken from the values for figure 3.10. This latitude band is chosen because it is here that blocking is expected to have most effect.

The zonal index has been studied previously because it shows periodic behaviour such as is to be seen in figure 3.15. Studies have shown (Petterssen) that zonal type flow is persistent when the index is high, and that meridional flow is persistent when it is low. The cycle is also connected with periodic kinetic energy exchange between the mean flow and the eddies (Reiter 1969). The blocking theory of Charney and DeVore suggests that blocking will occur on a low zonal index when wave amplitudes are high.

The present series can be examined through a superposed epoch analysis performed using the first day of blocking as the key day. The result for all eighteen blocks is shown in figure 3.16. Also plotted is the mean index for the whole period. The error bars plotted on each point represent the standard error expected from an eighteen point mean taken from the data whose standard deviation is 3.9 ms^{-1}.

The figure shows that the zonal index during blocking is lower than average and tends to decrease with time. However, the deviations from the average are small,

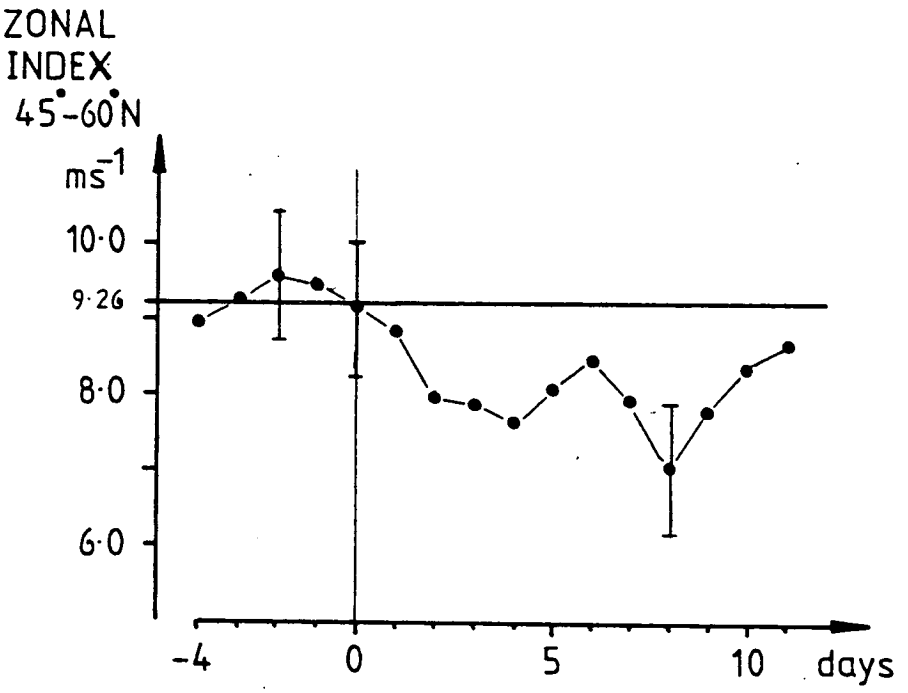

Figure 3.16 Superposed epoch analysis of the zonal index using the initial day of blocking as the key day. The mean zonal index of 9.26 ms^{-1} is marked by a line.

few being significant even at the 10% level. The figure supports both Austin's and Charney and DeVore's ideas though the evidence is not strong enough to be conclusive.

Also important is the structure of the zonal mean wind with latitude. It might be expected that, because blocks cause high-latitude jets, a high latitude westerly jet would be apparent in the zonal mean wind during blocking. From the blocks in this study double jet structures are found to be equally as common as other patterns - ten blocks with and eight blocks without. Although blocks undoubtedly do produce high latitude jets locally, they are not always apparent in the zonal mean.

Double jets appear to be slightly connected with the occurrence of wave 4, and to be present in shorter lived blocks. Of the ten blocks with a double jet, only five include wave 4, whereas of the eight without a double jet, seven include wave 4. The average lifetime of blocks with a double jet is 7.4 days, and, without, is 8.9 days, though the difference is only statistically significant at the 15% level. Hence, blocks with no double jet appear to be slightly longer living and to have a wave 4 present, but more data are necessary to make the connection more evident.

3.7.5 The relative importance of each wave.

This study has described eighteen blocks in terms of planetary waves and has shown that every block has as its basis a combination of waves with wavenumbers between 1 and 4. The table below shows the number of times that each wavenumber is involved in a description of blocking.

The waves are those cited as important for each block in appendix 2.

Wave number	Number of times cited		
	European	American	All blocks
1	5	0	5
2	8	4	12
3	10	5	15
4	8	4	12
5	1	2	3
6	2	1	3

From this table it is evident that, overall, wave 3 is most commonly involved, with waves 2 and 4 equal second, and wave 1 least common of the long wave group. When the frequencies are looked at with reference to blocking locality, it is clear that waves 2, 3 and 4 are nearly equally common in both European and American blocking, but wave 1 is only present in European blocks. These findings closely correspond to the suggestions put forward in section 1.6.5. There it is suggested that if blocking were connected to the long term stationary waves then the variations in blocking frequency with longitude could be explained. The hypothesis leads one to expect European blocking to be made up from waves 1 to 4 and to expect American blocking to be made up from waves 2 to 4 only. This is what is found.

3.7.6 Preferred wave combinations for blocking.

One objective of this study is to decide whether there is any particular combination or configuration of waves that might serve as an identifier of blocking - a blocking signature. No one such configuration or combination of waves is found but three combinations occur more often than the others. The table below lists the observed combinations and the number of blocks they describe.

Wave combinations	Number of blocks European	American	total
1,2,3	1		1
1,2,4	1		1
1,3,4	2		2
1,2	1		1
2,3,4	1	3	4
2,4	1		1
2,3	3	1	4
3,4	3	1	4

Clearly combinations with waves 3 and 4 and 2 are most common. For European blocking the preferred combinations are 2,3 and 3,4: for American blocking the 2,3,4 combination appears most commonly. Many combinations appear, however, especially in European blocking which suggests that all possible combinations may occur of which only some are found in this study. In the case of

American blocking, wave 1 is never involved so there are fewer wave combinations available.

If blocking occurs on the chance superposition of two or more planetary waves, there are 11 combinations of waves 1,2,3 and 4 which could cause European blocking, but only 4 combinations of waves 2, 3 and 4 which could cause American blocking. The ratio 11:4 will be the ratio of European to American blocking if all combinations are equally probable. The observed ratio in this study is 13:5. The ratio from Treidl, Birch and Sajecki is approximately 3:1. Both of these are close to the ratio 11:4. This strongly suggests that the frequency of blocking occurrence is dependent on the number of possible wave configurations. This is connected with the fact that waves are near normal in phase during blocking. The normal phasing ensuring that there is a ridge of each of waves 1 to 4 close to 0^{o} longitude and that there is a ridge for waves 2 to 4 near $130^{o}W$. Waves which are near normal interact and superimpose in the European and American sectors because of the clustering there of their normal ridges. Superpositions of near normal planetary waves can therefore explain the observed frequency and spatial distribution of blocking.

3.8 Summary of the results and of the comparison with Austin's results.

Austin concluded that American blocks could be explained as a superposition of waves 2 and 3 in the absence of wave 1. The present study agrees with this conclusion, but it does not agree with Austin's conclusion about European and double blocking. The analysis of European blocking - which contains five times as many blocks as Austin's - finds waves 1 to 4 almost equally important, the preferred combinations being 2,3; 3,4 and 1,3,4 whereas Austin found only waves 1 to 3 important with preferred combinations of 1,2 and 1,3. This difference in the perceived importance of wave 4 is also evident in the cases of double blocking: in this study waves 4 and 3 make up the blocks whereas in Austin's a combination of waves 1, 2 and 3 were responsible.

Austin concluded that wave 4 maintained long-lived blocks, and the present results support this. This last point together with the general importance of the part played by wave 4 lead one to assert that wave 4 is the most important long wave for blocking. The next in importance is wave 3 which even has a numerical superiority over wave 4 - it is considered important in fifteen out of the eighteen cases of blocking. Wave 3 makes an excellent partner to wave 4 because its normal ridges lie at both of the longitudes of most frequent blocking and in close proximity to wave 4's ridges. Wave 2, numerically equally important to wave 4, has its normal ridge well placed over the

American area but a little east of the European blocking area.

The present results also agree with Austin in showing the close association between blocking, the waves which produce it, and the long term stationary waves, i.e. the results show that, during blocking, the waves are near their long term normal positions. Thus there is established a connection between blocking and the long term mean waves. Therefore, through the connection between the long term mean waves and the long term mean climate there exists a connection between blocking and climate: change the positions of the long term stationary waves - say by changing the structure of the forcing - then the position of blocking will change and the long term climatic chart will change.

Austin suggests that the zonal wind decreases during blocks. The present analysis of the zonal wind agrees with this conclusion albeit with reservations about the statistical significance of the result. What Austin could not have known, for it requires a fine latitudinal resolution, is that high latitude jets are not favoured during blocking but are only equally as probable as no such jet being present. Additionally a zonal wind not having a high-latitude jet is correlated with longer-living blocks. This result, like that of wave 4's connection to longevity, can only be explained speculatively. Since a double jet structure is associated with shorter blocks it is also associated with a lack of wave 4, implying that a high

latitude jet is a poor producer of wave 4. Two explanations can be put forward. First the high latitude jet might lie over topography unsuited to the forcing of wave 4, or, second, extra wave 4 forced by the high-latitude jet might interfere destructively with the normally forced wave thereby reducing the amplitude.

The final point of disparity between the present results and Austin's is in the occasional importance of waves 5 and 6. On four occasions wave 5 and/or 6 was influential during blocking, reaching, for them, high amplitudes. This is seen as evidence of coupling between the long waves and the short waves. Waves 5 and 6 are normally considered to be due to the Fourier analysis of depressions. Hence, this involvement of waves 5 and 6 during blocking can be seen as a coupling between the long waves and the depressions. But this is just what a block is supposed to be; an interaction between the depressions and a stationary anticyclone. So it is possible that the actual mechanism whereby the block is affecting the depressions is in evidence in these four events. Further study is required to clarify this mechanism.

3.9 Conclusions.

An analysis of eighteen blocking situations has been carried through using the technique of zonal harmonic analysis to calculate the amplitudes and phases of the planetary wave components. The conclusions to be drawn from the analysis are: -

(a) European blocks are based upon combinations of waves 1 to 4.

(b) American blocks are based upon combinations of waves 2 to 4.

(c) The favoured combinations of waves are 2,3; 3,4 and 1,3,4 for Eurpean blocks and 2,3,4 for American blocks.

(d) The long waves are near their normal phases during blocking.

(e) The most common wave has wavenumber 3.

(f) Blocks which have along life are associated with wavenumber 4.

(g) The zonal mean wind appears to be lower than average and to decrease during blocking.

(h) A double jet structure in the zonal mean wind is connected with blocks of shorter duration.

(i) The ratio of American to European blocking is close to the ratio of the number of combinations of waves 1 to 4 available in each sector.

(j) Waves 5 and 6 are occasionally important: it is suggested that this is evidence of interaction between the long waves and the baroclinic waves.

Chapter 4 THE EFFECT OF BLOCKING ON THE ZONAL HARMONIC COMPONENTS OF KINETIC ENERGY.

4.1 Introduction.

Chapter 3 has shown that the amplitude and the phase of zonal harmonic waves are useful parameters in describing blocks. An explanation of the time evolution of these parameters is necessary if a fuller understanding of the blocking mechanism is to be approached. This requires diagnostic relations derived from first principles which can describe the time rate of change of amplitude and phase in each wave. These, unfortunately, are not available because the exact specification of the forcing of each wave is not known. Theoretical study (Bates 1977) shows that the structure of the waves is highly sensitive to the structure of the forcing and dissipation functions. Therefore, it is necessary to follow an alternative route by studying parameters for which the diagnostic relations are known and relating them to blocking. In this chapter the kinetic energy in each wavenumber is chosen as the parameter for study. There are four reasons for the choice, viz:-

(a) The kinetic energy expressed in zonal harmonics is closely related to the amplitude and phase of the wave and therefore the findings of chapter 3 are relevant.

(b) Equations for the time rate of change of kinetic energy expressed in zonal Fourier harmonics are available in the literature (Saltzman 1970).

(c) There are, in the literature, a few statements about the behaviour of the zonal mean kinetic

(c) energy and the total eddy kinetic energy during blocking, which can be examined as part of a fuller study.

(d) The important features of kinetic energy behaviour during blocking can be compared with predictions made by some theories of blocking. In chapter 5, the kinetic energy events which are identified in this chapter are matched to diagnostics and used to assessthe applicability of Egger's model.

4.2 The formulation of the kinetic energy.

The formulation used in this study is taken from Saltzman (1970) and is chosen because it expresses the kinetic energy in zonal harmonics. It also makes use of Fourier components of the geopotential height field and, as is important, through kinetic energy being a function of volume, it can be applied to any latitude band and pressure thickness. The expression for energy is then directly relatable to and calculable from the amplitudes and phases of the height field discussed in chapter 3. The energy is taken as geostrophic. The formulation is: -

$$K(n)=\int_{\phi}\int_{p}\int_{0}^{2\pi}(|U(n)|^2+|V(n)|^2)\,d\lambda\, a\cos\phi\, d\phi\frac{dp}{g}$$

$$K(0)=\int_{\phi}\int_{p}\int_{0}^{2\pi}\frac{\bar{U}^2}{2}\,d\lambda\, a\cos\phi\, d\phi\,\frac{dp}{g}$$

where $K(n)$ is the energy in wavenumber n integrated between the limits of latitude and pressure.

$K(0)$ ditto for the zonal wind, wave 0.

ϕ is latitude.

p is pressure.

a is the radius of the earth. g is the gravitational acceleration.

$\bar{U}$ is the zonal mean wind.

$U(n)$, $V(n)$ are the complex Fourier coefficients of zonal and meridional velocity respectively, where

$$U(n) = \frac{-g}{fa}\frac{\partial A(n)}{\partial \phi} \qquad V(n) = \frac{gni\,A(n)}{fa\cos\phi}$$

$A(n)$ is the complex Fourier coefficient of geopotential height.

The complex Fourier series is defined, if f is any suitable function, as $F(n)$ where

$$f(\lambda) = \sum_{n=-\infty}^{n=+\infty} F(n)\, e^{-in\lambda}$$

4.3 The similarity between a kinetic energy analysis and the analysis in chapter 3.

As can be seen in section 4.2, the kinetic energy is closely allied to the distribution in latitude of the amplitude and the phase of the height waves. The kinetic energy is a measure of the intensity of each wave, and an analysis of the energy-time series is the simpler because there is only one value for each wavenumber each day. The results of the two analyses can be expected to be similar except that the kinetic energy puts greater emphasis on the higher wavenumbers, such as 5 and 6, than does the amplitude analysis. This is not unwelcome. In chapter 3 the amplitudes were analysed in an attempt to specify patterns of the height field during blocking. Generally the more meridional the flow the more conspicuous the block. Now, for the same amplitude high wavenumbers cause, locally, a more meridional flow than do low wavenumbers. The amplitude analysis does not bring this out. Indeed, since the amplitudes decrease rapidly with wavenumber, the higher waves are easily overlooked. The bias in the kinetic energy analysis tends to compensate for this. On the negative side, the kinetic energy, being an integration over an area on a sphere, places more emphasis on the lower latitudes. However, the extent to which blocking affects the kinetic energy shows just how important blocking is on the large scale.

4.4 Previous conclusions about the behaviour of the kinetic energy.

4.4.1 The conclusion of Lejenas.

Lejenas (1977) summarises the observational results of Miyokoda and of Winston in an idealised diagram. This shows the time evolutions of zonal kinetic energy (ZKE) and of total eddy kinetic energy (TEKE) with respect to the day of initiation of a block. Figure 4.1 is reproduced from his diagram. The figure suggests that the ZKE is at a minimum on the day of initiation and that it climbs, to peak six days afterwards. The TEKE displays the same behaviour. It peaks at the same time as the ZKE but has its minimum four days before the block is initiated.

This summary is based on observational studies of only two blocks. Later, in this chapter, the behaviours of the energy in the eighteen blocks in the study period are matched to Lejenas' suggestions. It is found that, although there are many cases where the ZKE and TEKE follow Lejenas' pattern, only for the TEKE is it more common than other patterns.

4.4.2 The conclusions of Everson and Davis.

Everson and Davis (1970), on the basis of a model study, and examination of a short time series, suggest that blocking is initiated on local minima of total hemispherical kinetic energy. This agrees with Lejenas. In figure 4.1 both the ZKE and TEKE are low, implying a minimum in total kinetic energy (TKE). This suggestion is

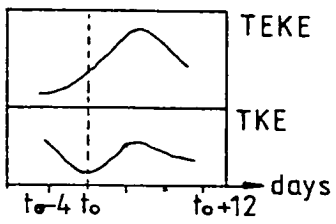

Figure 4.1 Idealized picture of energy changes during a blocking situation. Day $t = t_o$ is the onset of blocking. From Lejenas.

investigated later by examining the time series of TKE. It is found that in eleven of the eighteen blocks, a local minimum is present at initiation.

4.4.3 The behaviour of the wave amplitudes.

Austin states that the amplitudes of waves involved in blocking are higher than normal. This could have been considered in chapter 3, but the important amplitudes of any wave do not always occur at one latitude and thus a simple investigation using one latitude only would not be satisfactory. Using the kinetic energy overcomes the difficulty because all latitudes are included. If Austin is correct, the important waves in each block have greater than normal kinetic energies. This possibility is examined in section 4.8.4.

4.4.4 Using the energy series to examine blocking theories.

A few theories of blocking are described in chapter 1. Here, it is possible to put these theories to a test using the energy series. For instance, Scorer's theory suggests that the blocking wave is high in amplitude during blocking. This must be manifest as high kinetic energy, probably coming to a peak during the block. Also, Charney and DeVore's theorem explains blocking as part of a vacillation cycle with one wave interacting with the zonal mean wind such that the two oscillate in amplitude but out of phase with each other. This must be visible on the energy series as a peak in ZKE followed by a peak in wave energy in a regular sequence.

In Egger's model, the blocking wave gains energy from the other waves by interaction, and it might therefore be expected to peak in energy during blocking, although this is not entirely apparent in Egger's results. What is important for Egger's model is that any changes in wave energy that do occur must be due to interaction between waves. This possibility is examined in detail in chapter 5. For the investigation, however, it is necessary to prepare a list of the important energy changes which take place.

4.5 The calculation of the energy/time series.

The kinetic energy for each wavenumber is calculated using the relations presented in section 4.2 The data for the calculations are the same as are used in the amplitude and phase analysis. There are therefore sixteen points at which Fourier coefficients of height are available from 15°N to 90°N. The zonal component of velocity is found by using the first order gradients of height with latitude. The zonal components therefore relate to latitudes midway between the meridional components. They are brought together by interpolating extra values of each set of components at points mid way between the originals. The technique of fitting cubic splines is used for the interpolation because it gives the 'smoothest' curve passing through all the data points. Thus the calculation has 31 latitude points available. The latitude bounds of the integration are 20°N and 80°N. This covers all important latitudes while avoiding computational difficulty at the pole. Only the 500 mb

height coefficients are used, so that the integration with respect to pressure is not performed. The results are normalised to give kinetic energy per unit area using the area of the earth between 20° and 80°N. The resulting kinetic energy behaviour is presented for each of waves 0 to 8 in figures 4.2 to 4.10 as a time series covering the period of the data, 1/11/76 to 30/4/77.

In addition to the single wave series, the TKE and TEKE are required. They are found by summing over the waves 0 to 8 and 1 to 8 respectively.

4.6 The analysis.

The analysis consists of two parts: (1) the description of the events in the individual wave energy series, and (2) the investigation of the behaviour of the TKE, TEKE and ZKE. The full results of part 1 of the analysis are presented in appendix 3.

The individual wave energy events have to be identified for comparison with the descriptions from the analyses in chapter 3 and as a basis for the investigation in chapter 5. For this reason, the events in each wave energy series are ranked according to their individuality and 'fit' to the block in which they occur, i.e. if the event, such as a peak, fits the blocking dates well, then it is assumed to be related and important to that block. This is referred to later as ranking by 'subjective importance'. Additionally, for comparison with the foregoing, the events are ranked according to their energy magnitude.

The behaviours of the TKE, TEKE and ZKE are

analysed in two ways. From section 4.4.1, one recalls the suggestion that the TEKE has a minimum four days before blocking starts and peaks six days later. Accordingly, for each block, the behaviour of the TEKE is examined for two features, a minimum a few days before initiation, and a maximum a few days after. The ZKE and TKE are examined similarly. Thus the number of blocks which appear to fit Lejenas' pattern is found. The results of this are discussed in sections 4.8.5, 6 and 7. Additionally superposed epoch analyses are performed on the ZKE, the TEKE and the TKE series using the initial day of blocking as the key day. These are also presented and described in sections 4.8.5, 6 and 7.

4.7 The results: discussion of individual blocks.

4.7.1 The classification of the kinetic energy events.

Important kinetic energy events occur in association with every block except one, and, for the purpose of describing their major features more simply, the events are grouped into four types, viz: -

(a) Events which are clearly related to the block by fitting in well with the period of blocking.

(b) Events which carry over, i.e. which are of major importance for a period longer than the duration of the block and which may span more than one block.

(c) Events in which no wave series shows any significant feature over the period of a block.

(d) Events which suggest coupling between waves.

The classifications are not exclusive. Events of more than one type can occur in any one block, and one event may be a good example of several types. Each type is now taken in turn and the better examples of the type are described.

4.7.2 Energy events which match the blocking period well.

These are mostly energy peaks, but there are a few examples of the opposite kind, namely, energy minima. The foremost example of the latter occurs during block E10. Before E10, waves 4 and 6 are unusually high. Both fall abruptly on the initiation of the block, pass through a minimum during the block, and recover their original amplitudes by the end. Such behaviour is important in that it allows less energetic wavenumbers to become prominent, as in E10, when a peak in wave 5 is prominent.

Similar circumstances in A2 give the best and most striking example of an energy peak fitting a block. A2, as mentioned in chapter 3, has two phases, the first being a blocking period and the second being a 'grey' almost blocked period. During the blocking period, waves 3 and 4 pass through minima, and waves 5 and 6 rise to high energy peaks. The dates of amplification and decay of wave 5 match exactly the blocking dates. In the subsequent 'grey' period, waves 3 and 4 come to maxima. Thus the kinetic energy fits the observations well and there is close agreement between this analysis and the amplitude and phase analysis. The block is caused by a strong amplification of waves 5 and 6 as waves 3 and 4

decay. The 'grey' period is separate and is caused by the long waves.

Another American block A4 is closely similar to A2 with waves 5 and 7 specific to the block and waves 2 and 4 centred on the 'grey' period. Further blocks with distinctive energy peaks are the Atlantic block E5A and the double blocks E5/A3 and E9/A5. It may not be coincidence that the two double blocks of the study occur when wave 3 and wave 4 reach the highest energies recorded for them in the series. Wave 4 (along with an unusually high wave 6) peaks during E9/A5, and wave 3 peaks during both E5/A3 and E5A.

The peaks described above are the most prominent occurring, but there is at least one peak in most blocks. Not all of them, however, fit closely within the blocking period. The amplification can occur for a time before or the decay endure for a time after blocking. This is more evident in the long waves which show longer timescales in their pulsations than do waves 5 to 8. Good examples of such long wave behaviour can be seen in wave 2 in A2 and wave 4 in E2.

4.7.3 Energy events which span more than one block.

Those events which span more than one block occur mostly in the weeks containing E4, E4B, E5, E5A, which is a time of continuous blocking. There are three 'carry-over' events. The first begins during E4. Spanning the end of E4 and the beginning of E4B, there is a unique peak in

zonal mean kinetic energy. Simultaneously there is a wave 2 maximum in energy. The second starts in E4B. During E4B there is a collapse of the peaks of wave 0 and 2 and there arises the most powerful wave 1 peak of this study, peaking on the day of the changeover from E4B to E5 before falling during E5 to normal levels. The third 'carryover' event is in wave 4 and begins in E5. Throughout E5, wave 4 amplifies. It continues high into E5A and finally falls at the end of E5A. This examination of the 'carryover' events in this sequence shows that even important and energetic events are difficult to connect with particular blocks. Consequently the occurrance of a block is difficult to infer from the kinetic energy history alone.

There are two important events that start in a blocking period and then outlast it. They occur in the latter halves of E6 and E8. In E8 wave 2 amplifies very strongly until two days after the end of the block, when it collapses. In E6, the event is a simultaneous amplification of waves 3 and 4. Starting in mid-block, the energy rises to a sharp peak two days after the block has finished. This event is also described in section 4.7.5 since there is strong evidence of coupling with the zonal mean wind.

4.7.4 Blocks where there are no energy features of any significance.

During E7 there are no events which are readily associable with the period. Waves 5 and 6 show short lived peaks on the first day and in mid period. As for the long waves, 2 and 4 show little variation, while 1 and 3 only

show amplification on the last day. This block appears to have little effect on the kinetic energy. Blocks can vary from strongly affecting the kinetic energy to having little affect.

4.7.5 Energy events which may be evidence of coupling between waves.

There are five major examples to be described, each showing a different aspect of possible interaction.

In E2 a moderate wave 1 decays sharply and simultaneously with a sharp amplification of wave 3. This happens in the presence of a strong wave 4.

In E10 waves 4 and 6 fall simultaneously through a minimum from being very high. In the minimum, a strong wave 5 appears.

In E4 a peak in TEKE decays simultaneously with an amplification of wave 0. This amplification of wave 0 is unique in the series. The energy gained by wave 0 equals that lost by the TEKE.

In E5 a cascade is evident. E5 starts on a very high peak of wave 1. As this peak in wave 1 decays, a strong peak rises in wave 3. As the peak in wave 3 decays a strong peak rises in wave 5.

In E6 a sharp decrease of the zonal mean wind signals a sharp amplification of waves 6 and 7 and a slower but very strong amplification of waves 3 and 4. On the breakdown of waves 3 and 4, waves 6 and 7 again peak strongly.

4.7.6 Evidence to support Egger's model.

Egger constructed his model to investigate the premise that a blocking wave has a high amplitude and stationary phase through interacting with other waves. Distinguishing waves of high amplitude during blocking implies that they will have a peak in energy during the block. The events described in the previous sections show that peaking is common during blocking. So, there are many events in this study that could be Egger in type, i.e. created by wave/wave interaction. Chapter 5 investigates the possibility by comparing the energy changes in the catalogued events with calculated wave/wave interactions.

4.7.7 Evidence for vacillation - Charney and DeVore's model.

Charney and De Vore's model of vacillation implies that the kinetic energy of both wave 0 and the interacting wave should undergo regular, but out of phase pulsations. They imply that blocking occurs on the peak of the cycle when the wave has highest energy.

There are two distinct events in this study possibly showing interaction between wave 0 and others. One occurs during E4, when a TEKE peak immediately precedes a wave 0 peak, the TEKE peak being caused by a simultaneous peaking of waves 1,3,4 and 5. The other is during E6, when a sharp drop in wave 0 kinetic energy is simultaneous with a sharp amplification of waves 3 and 4. Both events are indicative of interaction between the zonal wind and the waves. Both events occur in

association with blocks, the peaks in waves 3 and 4 in E6 occurring immediately after the end of E6.

In these two real cases, the interaction is between a number of waves and the zonal mean - not purely an interaction between a single wave and the zonal mean. Also, both cases are singular, i.e. they are not part of a regular train of events. To this extent, these events are not similar to the simple model. More investigation of the actual interactions in the real events is required, as is a generalisation of the model to cover situations with many waves.

4.8 The results: general.

4.8.1 The relative importance of wave 1 to 8.

To show how the waves are ordered in importance, various tables are assembled from the data in appendix 3.

First, the table following shows the number of times that each wavenumber is considered significant enough to be included in the description and in the importance ranking:

Wave number	0	1	2	3	4	5	6	7	8
Number of times cited	3	7	9	8	9	7	9	2	1

The most commonly cited are wavenumbers 2, 4 and 6, but all waves from 1 to 6 are comparably common.

Second, the next table shows the number of times each wave number is ranked, 1st, 2nd, 3rd etc. in order of subjective importance.

		Wave number								
		0	1	2	3	4	5	6	7	8
Rank	1st	2		3	2	3	4	1		
	2nd	1	2	2	4	2		3		
	3rd		2	3		1	3	2	2	
	4th		2	1	2	2		2		
	5th		1							1

The waves 2, 4 and 5 are equally often considered most important for blocking while the waves 3 and 6 are most commonly considered to rank second in importance.

Thirdly, the table below shows the number of times each wavenumber is ranked, 1st, 2nd and 3rd etc. when they are ordered for each block in descending values of energy.

		Wave number								
		0	1	2	3	4	5	6	7	8
Rank	1st	2		5	3	3	2			
	2nd	1	2	2	4	2	1	2		
	3rd		4	2	1	2	2	1	1	
	4th		1			1	2	4	1	
	5th					1		2		1

This gives a slightly different picture, wave 2 being the most powerful and commonly cited wave. Waves 3 and 4 are the next most common and powerful. Wave 1, being low in kinetic energy, is not often cited, coming generally third in energy importance.

4.8.2 Summary of the results of section 4.8.1.

From the tables, one can conclude that the most important waves, in the sense that they are most commonly cited as subjectively important, and the most energetic during blocking, are numbers 2 and 4. Waves 3 and 5 share second place. Wave 3 is generally more energetic than 5, but 5 displays behaviour more closely related to individual blocks and so ranks more highly in subjective importance.

4.8.3 Comparison with the results of the amplitude and phase analysis.

The table below shows the waves mentioned in the energy analysis together with those from the amplitude and phase analysis. It can be seen that there is both agreement and disagreement between them.

As predicted earlier the energy analysis finds waves 5, 6 and 7 important more often than the amplitude analysis does. An examination of the events shows that this is so for three reasons.

(a) The kinetic energy has no phase information and hence cannot distinguish slow moving ridges from swiftly moving depressions.

(b) The kinetic energy is biased to low latitudes where the higher number waves are more prominent. The amplitude analysis tends to look more to higher latitudes.

(c) The expression for the kinetic energy contains the wavenumber explicitly and this compensates for the small amplitudes of the higher waves.

Block	Wavenumbers KE analysis	Amplitude and phase analysis	Comments.
A1	2,3,5,6	2,3,4	Waves 5 and 6 constitute a mobile Pacific trough. Wave 4 only peaks in mid-latitudes.
E2	4,3,1	4,1,3	No difference.
A2	5,6,1,3,4	5,6,2,3	Wave 1 has its peak too low in latitude while Wave 4 has an amplitude minimum during this block. Wave 2 peaks in higher latitudes.
E3	4,2	1,2,4	Wave 1 peaks in high latitudes.
E4	3,2	3,2	
E4B	6,2,1,8	2,1	Waves 6 and 8 constitute a trough in western Atlantic.
E5/A3	3,1,4,5	3,4	Wave 5 is present in low latitudes as is wave 1.
E5A	3,4,1,5	3,4,5,6	Wave 6 is not high in amplitude; its phase is important. Wave 1 lies to the west of the blocking ridge.
A4	5,2,4,6	2,3,5,4	Wave 3 energy is high but falls continuously showing no distinguishing behaviour.

Comparing wave events: kinetic energy analysis versus amplitude and phase analysis.

Block	Wavenumbers KE analysis	Amplitude and phase analysis	Comments.
E6	1,2,4,6,7	1,3,4,6	Wave 2 peaks in amplitude in lower latitudes. Wave 3 is not high in amplitude; phase is important. Wave 7 is part of a progressive trough in the Atlantic.
E7	5,3,6	2,4	Waves 2,4 peak in high latitudes; phase is also important. Wave 3 peaks south of the block and is out of phase. Waves 5 and 6 are a depression in the Atlantic.
E8	2,6,7	1,2,3	Waves 6 and 7 are mobile waves in the American sector. Waves 1 and 3 peak in amplitude in high latitudes.
A5/E9	4,6,7,2	4,3,2	Waves 6 and 7 peak in amplitude in lower latitudes. Wave 3 peaks in amplitude in higher latitudes.
E10	5,4,6,3,1	3,2	Waves 1,4,5 peak in amplitude too far south of the block. Wave 6 shows a minimum in amplitude during the block. Wave 2 peaks in high latitudes.
E11	2	2,4,3	Waves 4 and 3 peak in high latitudes.

Comparing wave events contd.

For waves 1 to 4, the differences arise from the same affects. Most commonly, the difference is due to the amplitude and phase analysis distinguishing between latitudes, concentrating on higher latitudes.

These effects were all predicted in section 4.3. For the kinetic energy analysis to be closer to the amplitude and phase analysis, it would be necessary to reduce the area of the integration to concentrate on higher latitudes.

4.8.4 Do blocking waves have higher than average kinetic energy?

It is suggested in section 4.4.3 that the kinetic energy series be used to examine Austin's statement that the waves involved in blocking have amplitudes higher than normal. If the waves are higher in amplitude, they must also be higher in kinetic energy. This suggestion may be tested by examining the average kinetic energy in each wave during each block, the test being whether the average energy during blocking is higher than the general average. To eliminate any seasonal trends in the kinetic energy of individual waves, the general average for the month may be subtracted from the averages during blocking. If the important waves during blocking are higher in amplitude than normal, then the mean of the difference for each wave between the kinetic energy during blocking and the monthly mean kinetic energy should be significantly greater than zero.

In this work, the suggestion is tested in the above way for each wave separately. The data necessary for the

test is tabulated below. First, there is a listing of the $\langle$ average kinetic energy of each wave during each block. Then there follows a listing of the average energy of each wave over each month. The waves expected to be higher in energy are those judged important in each block. These can be identified from either the energy analysis itself - appendix 3, or from the amplitude analysis - appendix 2.

If the important waves in each block are taken to be those lying in the first or second rank of importance in appendix 3, then the test is whether the energy analysis finds more peaking than dipping behaviour. The most common waves are examined viz. wavenumbers 2,3,4 and 6, and the results are as follows: -

Wavenumber	Mean difference between monthly mean and block mean.	Number of blocks in the test.
2	43.4 $Jm^{-2}mb^{-1}$	5
3	21.2	6
4	58.6	5
6	71.6	4

All the waves show positive mean differences showing that the important waves during blocking tend to be above average. Only wave 3 using a simple t test does not differ significantly from zero at the 10% level.

A closer investigation of Austin's statement is performed if the important waves for each block are taken from the amplitude and phase analysis - appendix 2. This asks whether the waves chosen on the basis of amplitude and phase have higher energies during blocking. If they have

AVERAGE KINETIC ENERGY IN EACH WAVE FOR EACH BLOCK AND EACH MONTH. UNITS J*M**-2*MB**-1

BLOCK	WAVE 0	WAVE 1	WAVE 2	WAVE 3	WAVE 4	WAVE 5	WAVE 6	WAVE 7	WAVE 8
A1	0.105E 04	0.143E 03	0.257E 03	0.141E 03	0.143E 03	0.954E 02	0.139E 03	0.631E 02	0.517E 02
E2	0.973E 03	0.169E 03	0.132E 03	0.196E 03	0.254E 03	0.124E 03	0.771E 02	0.613E 02	0.653E 02
A2	0.104E 04	0.235E 03	0.156E 03	0.249E 03	0.125E 03	0.249E 03	0.236E 03	0.107E 03	0.647E 02
E3	0.128E 04	0.197E 03	0.302E 03	0.157E 03	0.239E 03	0.934E 02	0.104E 03	0.114E 03	0.898E 02
E4	0.136E 04	0.165E 03	0.255E 03	0.268E 03	0.177E 03	0.125E 03	0.980E 02	0.103E 03	0.102E 03
E4A	0.150E 04	0.152E 03	0.316E 03	0.272E 03	0.196E 03	0.158E 03	0.122E 03	0.986E 02	0.846E 02
EAB	0.145E 04	0.274E 03	0.276E 03	0.228E 03	0.933E 02	0.804E 02	0.166E 03	0.847E 02	0.803E 02
E5	0.145E 04	0.236E 03	0.178E 03	0.340E 03	0.204E 03	0.150E 03	0.125E 03	0.900E 02	0.706E 02
A3	0.145E 04	0.257E 03	0.180E 03	0.294E 03	0.173E 03	0.135E 03	0.127E 03	0.103E 03	0.783E 02
E5A	0.156E 04	0.206E 03	0.148E 03	0.323E 03	0.245E 03	0.151E 03	0.108E 03	0.117E 03	0.844E 02
A4	0.148E 04	0.138E 03	0.251E 03	0.258E 03	0.135E 03	0.202E 03	0.131E 03	0.126E 03	0.626E 02
E6	0.137E 04	0.195E 03	0.216E 03	0.148E 03	0.141E 03	0.166E 03	0.146E 03	0.142E 03	0.126E 03
E7	0.976E 03	0.808E 02	0.201E 03	0.181E 03	0.152E 03	0.145E 03	0.941E 02	0.125E 03	0.882E 02
E8	0.962E 03	0.158E 03	0.275E 03	0.116E 03	0.114E 03	0.752E 02	0.191E 03	0.211E 03	0.732E 02
A5	0.788E 03	0.863E 02	0.169E 03	0.119E 03	0.235E 03	0.116E 03	0.271E 03	0.171E 03	0.953E 02
E9	0.779E 03	0.111E 03	0.170E 03	0.115E 03	0.310E 03	0.128E 03	0.273E 03	0.165E 03	0.646E 02
E10	0.726E 03	0.136E 03	0.101E 03	0.167E 03	0.202E 03	0.179E 03	0.112E 03	0.117E 03	0.902E 02
E11	0.606E 03	0.154E 03	0.215E 03	0.771E 02	0.128E 03	0.853E 02	0.150E 03	0.918E 02	0.748E 02
NOV	0.976E 03	0.155E 03	0.170E 03	0.148E 03	0.167E 03	0.155E 03	0.116E 03	0.791E 02	0.756E 02
DEC	0.126E 04	0.191E 03	0.269E 03	0.226E 03	0.200E 03	0.110E 03	0.975E 02	0.129E 03	0.892E 02
JAN	0.148E 04	0.201E 03	0.215E 03	0.299E 03	0.160E 03	0.149E 03	0.130E 03	0.105E 03	0.733E 02
FEB	0.144E 04	0.192E 03	0.269E 03	0.195E 03	0.166E 03	0.139E 03	0.128E 03	0.105E 03	0.720E 02
MAR	0.101E 04	0.117E 03	0.197E 03	0.199E 03	0.151E 03	0.128E 03	0.146E 03	0.159E 03	0.917E 02
APR	0.692E 03	0.129E 03	0.158E 03	0.115E 03	0.215E 03	0.122E 03	0.188E 03	0.130E 03	0.779E 02

higher energies then they must have higher than normal amplitudes. For this test only waves 2,3 and 4 were used. The results are: -

Wavenumber	Mean difference between monthly mean and block mean.	Number of blocks in the test.
2	25.7 $Jm^{-2}mb^{-1}$	12
3	8.01	15
4	19.0	12

Again the waves all show a higher average energy during the blocks in which they are judged important, but no mean difference is significantly greater than 0 at the 10% level.

To highlight the difference between cases where a wave is important to a block and cases where it is not, the average deviation for cases where the waves are not important to the block is shown below. (Importance is taken from the amplitude analysis).

Wavenumber	Mean difference between monthly mean and block mean.	Number of blocks in the test.
2	-36.3 $Jm^{-2}mb^{-1}$	6
3	-52.67	3
4	-30.9	6

If the two distributions, with the wave being important, and with the wave not important, are tested for dissimilarity using a test, then they all show significance greater than 10%.

These results, therefore, do support Austin's statement that blocking waves have higher than normal

amplitudes. The last paragraph has especially shown that analysing blocks using amplitude and phase differentiates between high and low energy waves. The difference between 'important' and 'not important' wave energies is about 60 $Jm^{-2}mb^{-1}$. This is roughly 25% of the average energy of these waves.

4.8.5 The behaviour of the TEKE.

Lejenas suggests that the TEKE rises from a minimum four days before the first day of blocking to peak six days into the block. A subjective analysis of figure 4.11 finds eleven blocks (A1, A2, E4, E4A, E4B, A3, E5A, A4, E8, A5, E9) which follow a pattern of minimum before and maximum after block initiation. Of the seven blocks which depart from this pattern, four show a maximum before initiation and a minimum after, and three show a minimum before initiation but no significant maximum after. This analysis therefore shows that Lejenas' pattern is not universal but it does appear to be more common.

The results of performing a superposed epoch analysis on the series of figure 4.11 is given in figure 4.13. The key day is taken as the first day of blocking - called day zero in the figure. Figure 4.12 shows three analyses - one performed on all blocks, one for the eleven blocks showing the Lejenas pattern and one for the seven blocks deviating from the pattern. The error bars are the expected standard deviation of the mean of a sample of 18 points, or 11 or 7 as appropriate, taken from the population represented by the whole series of figure 4.10.

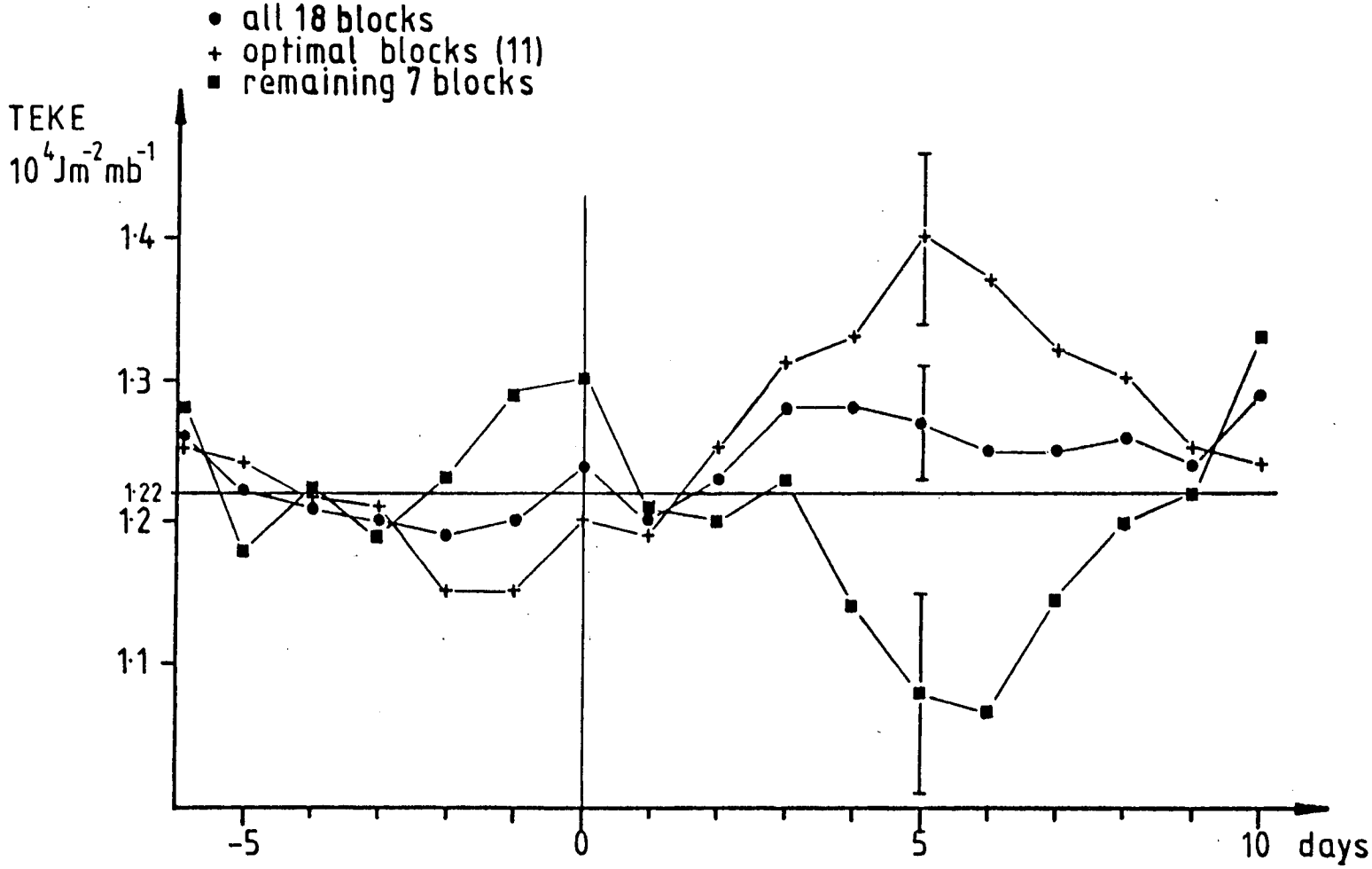

Figure 4.13 Superposed epoch analysis of the TEKE using the initial day of blocking as the key day. The mean TEKE is marked by a line.

The mean TEKE of the whole series is marked as a reference line.

The curve for the eleven optimal blocks shows the pattern as suggested by Lejenas distinctly. The minimum before blocking occurs at -1.5 days, i.e. slightly later than Lejenas' minimum: the maximum occurs at 5 days, slightly earlier than the 6 days that Lejenas suggests.

The curve for the seven blocks which deviate from the Lejenas pattern shows almost opposite behaviour except that there is a slight minimum before initiation at -3 days.

The curve for all blocks shows the dominance of the Lejenas patterned blocks. The curve has a minimum at -2 days and a maximum at 4 days.

The Lejenas pattern of behaviour is more generally observed than is the opposite, but in both cases the maximum deviations from average occur $5\frac{1}{2}$ days after initiation. Blocking, therefore, appears to cause distinct changes in TEKE, either increasing it or decreasing it, but increasing is more common. For either type of behaviour the TEKE shows a minimum some two or three days before blocking.

4.8.6 The Behaviour of the ZKE.

Lejenas suggests that the zonal kinetic energy is at a minimum on the initial day of blocking and that it rises to a peak roughly six days later. A subjective analysis of the time series of figure 4.2 finds nine blocks (E2, A2, E4, E5, A3, A4, E8, A5, E9) whose ZKE behaviour matches Lejenas' pattern. Of the other nine blocks, six show the opposite pattern of behaviour, i.e. peak at

initiation and come to a minimum during the block (A1,E4B, E6, E7, E10, E11), while the remaining three have ZKE peaks during the block but no minimum at initiation (E3, E4A, E5A).

Various superposed epoch analyses performed using the time series of ZKE yield the results presented in figure 4.14. The key day is again the initial day of blocking.

The curve for the nine optimal blocks shows a close correspondence to the Lejenas pattern; a minimum on the initial day, and a maximum thereafter. The maximum is however a little later than Lejenas suggests, at nine days. The curve for the nine blocks which depart from the Lejenas pattern shows entirely opposite behaviour. Thus the curve for all blocks shows no significant change during blocking. Hence the Lejenas pattern for the ZKE, though it does occur, is not favoured and is not dominant as in the TEKE.

A systematic effect having a bearing on Lejenas' suggestions is illustrated in figure 4.14 with two curves - one for the 11 blocks before January 31st and the other for the 7 blocks after January 31st. One shows a rising ZKE and the other a falling ZKE. This is due to the seasonal cycle visible in the ZKE. This trend is apparently maintained during blocking. Thus, during the winter, the normal increase in ZKE will favour patterns which show greater ZKE at the close than at initiation, and during the spring,when the ZKE is normally decreasing,patterns like Lejenas' will not be favoured. In this study, of the

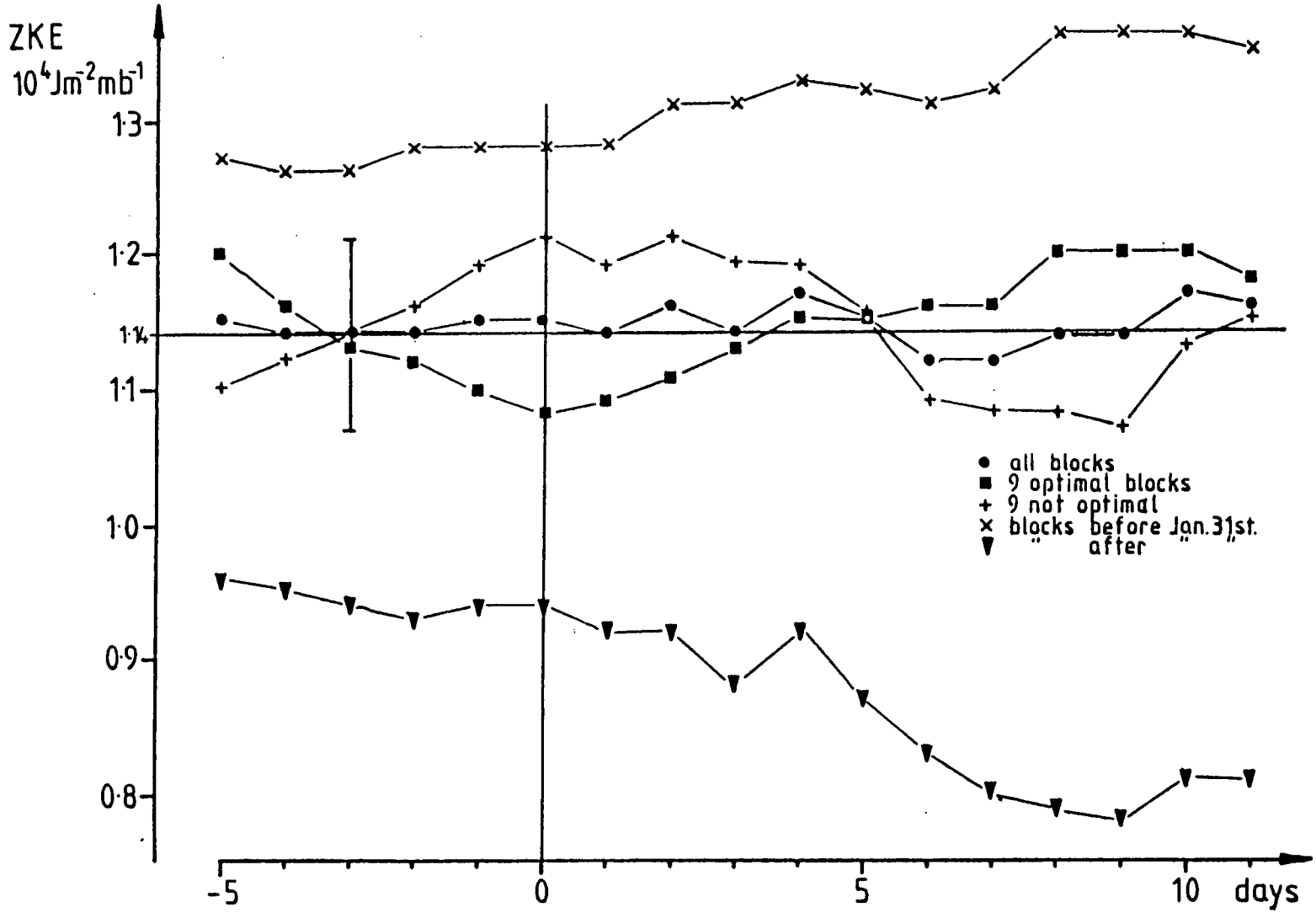

Figure 4.14 Superposed epoch analysis of the ZKE using the initial day of blocking as the key day. The error bar represents the standard error of a mean of eighteen points.

eleven blocks before January 31st, six are of the Lejenas pattern, three show a maximum but no minimum, and only two blocks show a maximum at initiation. After January 31st, there are only three blocks of the Lejenas pattern, but four blocks of opposite type.

Lejenas' suggestions are based on two observational studies, one for a December and one for a January, i.e. both during a period of increasing ZKE. The present results suggest that the time of year from which the results are drawn is an important factor.

One further point can be made from these analyses. The ZKE is very strongly affected by the subtropical jet because of the speed and low latitude of the jet. Yet the ZKE follows its normal seasonal trend during blocking. From this it can be surmised that the sub-tropical jet is little affected by blocking.

4.8.7 The behaviour of the TKE.

Everson and Davis suggest that blocking is initiated on local minima of total hemispherical kinetic energy. A subjective analysis of the TKE series of figure 4.12 concludes that in 11 out of the 18 blocks there is a local minimum near the day of initiation.

Figure 4.15 shows a superposed epoch analysis of the TKE. The curve for the eleven optimal cases and the curve for all blocks both show a minimum about two days before block initiation. The seven blocks which do not conform show peaking on the initial day instead.

On balance the Everson and Davis' behaviour

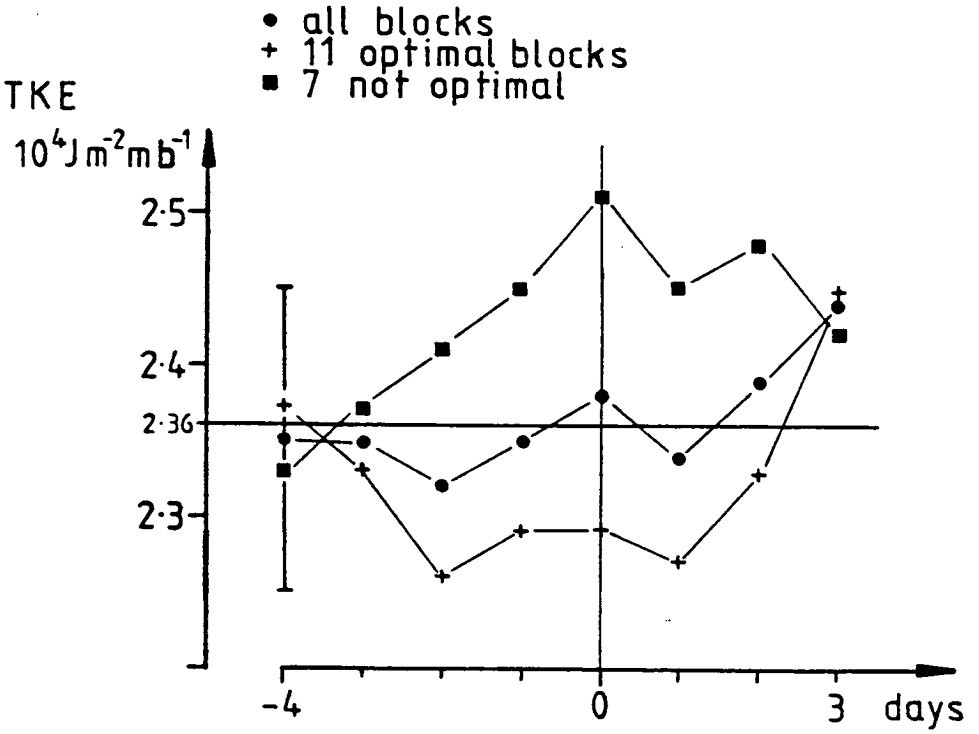

Figure 4.15 Superposed epoch analysis of TKE using the initial day of blocking as the key day. The mean TKE is indicated by a line. The error bar represents the expected standard deviation of an 18 point mean taken from the whole TKE series.

appears to dominate but the minimum is a little earlier than they suggest coming 2 days before blocking. However, the significance of the result is in question because none of the points depart from the average by more than the expected error of an 18 point mean. An analysis of a greater number of blocks is required if a significant result is to be obtained.

4.9 Discussion of results.

This chapter investigates the time evolution of the kinetic energy of zonal harmonic waves with respect to blocking. Choosing a parameter like the kinetic energy is advantageous because diagnostic relations for its generation and decay are available and well understood. In chapter 5 some diagnostics for the kinetic energy during blocking are examined.

4.9.1 The energy events - section 4.7.

In section 4.7 individual blocks were categorised into various classes according to their energy events. A whole variety of histories is presented and again, as was concluded in chapter 3, no particular pattern, or clear blocking signature, is evident. However, it is apparent that the association of blocking with wave energy can vary in magnitude from blocks being associated with large changes in energy to blocks having little effect on the energy. Hence, blocking can occasionally be important on a hemispherical scale, at least as far as kinetic energy is concerned. It is possible that a larger sample of blocks might show some blocking patterns, but it is clear,

considering the variability in the energy behaviour, that the sample available for this study is too small.

4.9.2 The energy analysis - section 4.8.

Section 4.8 looks at the general trends in the pattern of energy behaviour during blocking. The energy analysis appears to agree broadly with the amplitude and phase analysis. The most important blocking waves are waves 2 and 4 followed by waves 3,5 and6 in that order. The differences between the amplitude and phase analysis and the kinetic energy analysis arise because the kinetic energy,being the result of an integration over an area, is biased towards events in low latitudes. This could be combated by limiting the integration to north of 45^{o}N say. The energy would then more closely apply to the sensitive area for blocking but at the cost of its generality on a hemispherical scale.

The time behaviour of the energies of individual waves shows that each tends to be higher in energy when involved in blocking than when not involved. The excess is about 25% of the average energy of waves 2, 3 and 4. This difference is not great which accounts for the difficulty in trying to specify conditions of blocking.

Related to the above, is the pattern of the TEKE. This is shown to pass through a minimum roughly three days before blocking and to peak 5 days later. The TEKE thus shows also that in total the waves are higher in energy during blocking.

The results from studying the behaviour of the

ZKE show that it tends simply to follow its seasonal pattern despite blocking. Thus any statement referring to the behaviour of the zonal wind must also refer to the time of year of the observations. On occasion the ZKE does exhibit the pattern suggested by Lejenas, but this is only equally as common as other patterns of behaviour. The implication of Charney and DeVore's model is that the peak in ZKE should be synchronised with a minimum in the TEKE. The observations therefore do not in general accord with the model. There are however particular events which might: these must be left to a later study.

4.10 Conclusions.

The investigations of this chapter show that -

(a) Blocking is associated with variable degrees of change in the kinetic energy of waves 0 to 8, i.e. the changes for individual waves are observed to vary from none to very strong. It must be noted that this is on a large scale - nearly hemispherical.

(b) Waves 2 and 4 are the most important waves connected with blocking in this analysis.

(c) Waves 2, 3 and 4, when important during blocking, are higher in energy by approximately 25% than when they are not important.

(d) The TEKE tends to pass through a minimum 3 days before blocking and a peak 5 days after the start.

(e) The ZKE has a minimum on the first day of blocking and a peak on the eighth day, but the opposite pattern is

equally common. Overall, the ZKE tends to follow the seasonal trend.

(f) Blocks are initiated on local minima of total hemispherical kinetic energy.

Chapter 5. THE IMPORTANCE OF BAROTROPIC, NON-LINEAR, WAVE-WAVE INTERACTIONS.

5.1 Introduction.

In this chapter horizontal, barotropic, non-linear wave-wave interactions are studied. Egger's success in describing blocking with his simple model suggests that these interactions are controlling the time evolution of the waves. Because his model is restricted to waves 1, 2 and 3 only, while the atmosphere has many degrees of freedom, Egger's results cannot necessarily be taken as an accurate representation of reality. A study of real data is required to see if a mechanism corresponding to Egger's is indeed operating. To this end, the non-linear interactions are calculated directly from the data and compared with the time evolution of each wave energy.

Egger's postulate and numerical experiments are summarised in section 5.2 (some related work by Tsay and Kao being outlined in 5.3). My main data sequence is examined for events conforming to Egger's type in sections 5.5 - 5.7 and the results are discussed in sections 5.8 and 9.

5.2 The possible role of non-linear interactions during blocking: Egger's model.

5.2.1. Egger's postulate.

Egger used a numerical model to examine whether blocking might be explained by interactions between stationary planetary waves and free planetary waves. Egger postulates that blocking occurs when a free wave interacts

with topographically forced stationary waves. The free wave becomes slow moving, grows as a result of the interaction, and combines with the stationary waves to cause blocking.

5.2.2 Egger's model.

Theory states that the simplest set of waves that can interact is a set of three chosen such that the sum of the wavenumbers of two equals that of the third (Longuet-Higgins and Gill 1967). In Egger's model, the three waves are nunbers 1, 2 and 3. Waves 1 and 3 are orographically forced and wave 2 is free to be generated and amplified by the interactions.

The model is formulated on a beta plane, and calculations of streamfunction are truncated above wave number 3.

5.2.3 Egger's experiments.

Egger describes three main experiments made with his model: -

(a) Barotropic (1): The model has a single pressure level and an imposed zonal wind. Waves 1 and 3 are forced by a suitable orographic boundary condition. Wave 2 is expected to grow by interaction with waves 1 and 3. In order that the interaction be optimal, the strength of the zonal wind is chosen so that the phase speed of wave 2 is zero. The waves are not allowed to interact with the zonal mean wind.

(b) Barotropic (2): As in (1) except that the waves are allowed to interact with the zonal mean wind.

(c) Baroclinic: A two level baroclinic system is

constructed having the same bottom boundary as experiments 1 and 2.

In each case, as a control, the model was run a second time with no bottom boundary forcing.

5.2.4 Egger's results.

Blocking is defined by Egger as a system showing a distinct splitting of the jet which persists for at least five model days. In all three experiments realistic blocking patterns of this description are evident. Figure 5.1 is reproduced from Egger's paper. It shows stream-function patterns for various significant days from the second experiment. Model blocks are present on charts (a), (c) and (d). The same block is present in both charts (c) and (d) at x = 6. This is the main block of the experiment. It lasts a simulated ten days and produces a pronounced double jet in the zonal wind. Realistic mobility of troughs associated with the block is also exhibited. When the same experiments are done with no stationary forcing of waves 1 and 3, Egger finds that blocking does not occur.

5.2.5 Egger's conclusions.

Egger concludes that geographically fixed forcing is a necessary requirement for blocking and that non-linear wave wave interactions cause blocks. He points out, however, that effects of friction, diabatic heating, higher waves and spherical geometry are not present in the model. Hence, his mechanism of blocking may, in the real atmosphere, be entirely set aside by effects due to these other processes.

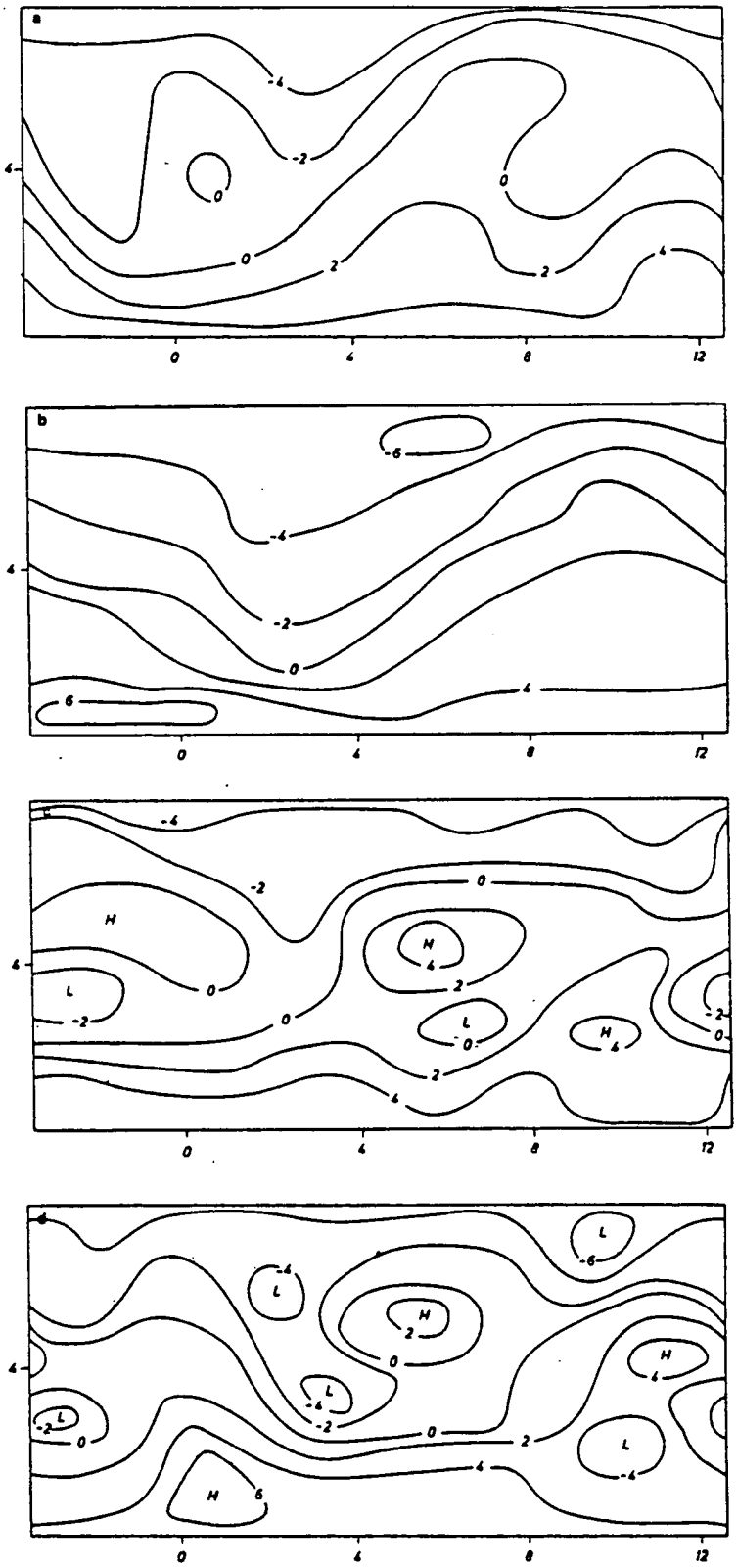

Figure 5.1 Streamfunction at days 10 (a), 17 (b), 27 (c) and 32 (d) of Egger's second experiment.

5.3 Related work by Tsay and Kao.

Evidence that Egger's mechanism might occur in the real atmosphere comes from a study by Tsay and Kao, who used data for a winter season to investigate the energetics of time oscillations in the kinetic energy of waves 1 to 8. They calculated the non-linear and other interactions directly and compared them with the actual changes in kinetic energy. They were able to show that non-linear interactions do indeed play a large part in the energy cycles of waves 1 to 8. Moreover, they found that waves 1 and 3 were more closely controlled by the non-linear interactions than were waves 4 to 8. For waves 4 to 8 baroclinic conversions from available potential energy to wave kinetic energy were significant. Wave 2 was found to differ from the others. It always lost energy via the non-linear interactions and gained energy via baroclinic conversions. Thus, if blocks are connected with peaks in kinetic energy, then Tsay and Kao's results show that Egger's choice of wave 2 as a blocking wave is unfortunate for in reality it differs in energetics from waves 1 and 3.

5.4 The method used in looking for evidence of Egger's mechanism in real data.

The rest of this chapter is devoted to seeking evidence that Egger's mechanism is operating in real blocking situations. Egger's model has wave 2 controlled by interactions with waves 1 and 3. In the real situation there are many more waves, and,in particular, wave 2 is not always the most important. It even appears to differ slightly in its energy cycle from the other waves. For

this reason the mechanism is generalised to include any wave number. In this study Egger's mechanism is said to operate if any wavenumber which takes an important role in blocking is controlled by wave wave interactions.

Egger's third experiment is the most complex, being baroclinic, yet it does not achieve greater realism than the first two. The first two experiments are barotropic and within a single level. Thus, of the many possible non-linear interactions that exist to match Egger's limitations, only those which are barotropic and act horizontally are studied here. The formulation for these interactions comes from Saltzman (1970), and is detailed in section 5.5. The interactions appear as conversions of kinetic energy between waves. To find examples of Egger's mechanism, therefore, it is necessary to compare calculated interactions with changes in kinetic energy. If the mechanism is operative the two should match.

Chapter 4 contains details of the kinetic energy history of each wave arranged in order of individuality to each block. In this chapter the non-linear interactions are quantified and then compared with the kinetic energy changes. To be significant, Egger's mechanism must explain the behaviour of the waves identified in the chapter 4 analysis as most important.

5.5 The calculation of the time series of non-linear interactions.

5.5.1 Expressions for the non-linear interactions.

Non-linear interaction terms arise when the rate of change of zonally integrated kinetic energy is expressed in Fourier harmonics. Formulations for the non-linear interactions were given by Saltzman, who developed the equations in zonal harmonics, giving his equations the advantage of being adaptable to any latitude band. Later reformulations were made by Tomatsu (1976) and Tsay and Kao. The success of Egger's single level barotropic model leads one to examine only barotropic interactions operating in the horizontal. Hence, interactions due to vertical velocities or thermal effects are not calculated and only geostrophic velocities are used. The relevant expressions from Saltzman (1970) are: -

The rate of change of zonal kinetic energy.

$$\frac{\partial K(0)}{\partial t} = \int_p \int_\phi \left(\sum_{n=1}^{\infty} M(n) + \text{other terms} \right) 2\pi \frac{a^2}{g} \cos\phi \, d\phi \, dp$$

a is the radius of the earth.

g is the acceleration due to gravity.

ϕ is latitude.

p is pressure.

'other terms' are those due to mean meridional vertical and thermal motions.

$$M(n) = MB(n) + M_1(n)$$

$M(n)$ is the conversion of energy into the zonal mean from wave number n .

$$M_1(n) = \left(U(n)V(-n) + U(-n)V(n) \right) \frac{\cos\phi}{a} \frac{\partial}{\partial\phi} \left(\frac{\bar{U}}{\cos\phi} \right)$$

$$MB(n) = -\frac{1}{a\cos\phi} \frac{\partial}{\partial\phi} \left(\bar{U} \cos\phi \left(U(n)V(-n) + U(-n)V(n) \right) \right)$$

$MB(n)$ when integrated, represents a boundary flux due to the interaction between wave n and wave 0. It is not present in Saltzman's formulations because his integration is over the whole sphere, in which case $MB(n) = 0$. This study is over a limited latitude band hence $MB(n)$ must be present.

$U(n), V(n)$ are complex Fourier coefficients of zonal and meridional velocity. See chapter 4, section 4.2

The rate of change of kinetic energy of wave number n .

$$\frac{\partial K(n)}{\partial t} = \int_p \int_\phi (-M_1(n) + L(n) + \text{other terms}) 2\pi \frac{a^2}{g} \cos\phi \, d\phi \, dp$$

$M_1(n)$ is the interaction with the zonal mean.

'Other terms' are due to conversions from potential energy and via vertical motions.

$$L(n) = \sum_{\substack{m=-\infty \\ m \neq 0}}^{m=+\infty} \Big[\frac{in}{a\cos\phi} \big(U(m)[U(-n)U(n-m) - U(n)U(-n-m)] + V(m)[V(-n)U(n-m) - U(n)U(-n-m)] \big)$$

$$+ \frac{1}{a\cos\phi} \Big(U(-n) \frac{\partial}{\partial\phi} (U(m)V(n-m)\cos\phi) + U(n) \frac{\partial}{\partial\phi} (U(m)V(-n-m)\cos\phi)$$

$$+ V(-n) \frac{\partial}{\partial\phi} (V(m)V(n-m)\cos\phi) + V(n) \frac{\partial}{\partial\phi} (V(m)V(-n-m)\cos\phi) \Big)$$

$$- \frac{\tan\phi}{a} \big(V(m)[U(-n)U(n-m) + U(n)U(-n-m)] - U(m)[V(-n)U(n-m) + V(n)U(-n-m)] \big) \Big]$$

$L(n)$ is the term describing the non-linear interactions between waves. It is a flux of energy into wavenumber n from all other waves. Each $L(n)$ is a summation over all possible triads of waves. A triad is a group of three waves such that their wavenumbers, n_1, n_2, n_3 satisfy $n_1 \pm n_2 \pm n_3 = 0$.

5.5.2 The calculation of the interactions: general.

The general form of the calculation is as follows: -

The principal wave number 'n' is chosen.

Each individual triad into that wavenumber is now dealt with separately. Here the individual triads are described by the notation n(r,s) where r and s are the two wavenumbers involved in energy exchange with wavenumber n. The velocity components at each latitude are then calculated from the geopotential height components. Next, the three main terms in L(n) are formed, integrated with respect to latitude, and summed to find the contribution from the individual triad.

All triad contributions into the wavenumber n are then summed to form the non-linear interaction total, NLIT, value for the day of the data. This is the total contribution to the kinetic energy change in wavenumber n through interactions with all other waves.

The geopotential height data are the same Fourier coefficients as are used in chapters 3 and 4. The interactions are therefore for the 500mb surface, and waves 0 to 8 only.

The latitudinal bounds of the integration are the same as chapter 4, viz: $20^{\circ}N$ and $80^{\circ}N$. This is chosen to cover all areas of interest yet avoid difficulty at the pole.

The NLIT values are normalised using the area of

the earth between the limits of the integration. The NLIT values for the study period are plotted as time series.

5.5.3 The calculation: detail.

The Fourier coefficients of height are positioned at 16 latitude points from 15°N to 90°N. Since the interactions are described in velocities, these height coefficients are turned into velocity coefficients before entering the main calculation. There are four velocity coefficients, 2u and 2v. To improve the accuracy of the integration, and to align the v components with the u components (which appear between data latitudes, since they are derived using first order derivatives with latitude) new point values are interpolated mid-way between the originals. Hence the input to the main calculation has 31 latitude points. The interpolation routine uses the technique of fitting cubic splines which ensures that the fitted curve is the smoothest possible that passes through all data points.

The interactions are calculated for each individual triad. The expressions for the interactions require derivatives of products involving tangents, cosines and velocity products, and these are all carried through analytically to their simplest forms before the calculation. The derivatives of the velocity products are evaluated from the curve fitted by the cubic spline technique through all the latitude values for the product. Here, using the cubic spline ensures the continuity of

first and second derivatives.

The integration with latitude is carried out for the large terms in L(n) and M(n) separately. Finally, the sum of the terms is formed and normalised to obtain the value for the triad. The individual triad contributions to the wave being investigated are then added to obtain the NLIT value for that wave and that day.

5.5.4 The calculation: accuracy.

The velocity components vary with latitude in a rapid and complicated way and it is necessary to check that there is sufficient latitudinal resolution in the data. This is done by going back to the original data for the one day, 1/11/76, and calculating a new latitude grid with double the resolution of the old, i.e. with 31 points in latitude. This new set is then put through the same routines as is the old. The triad contributions to wave 8 with this new data are examined in particular. They are shown in the table below with the 16 point values for comparison. Wave 8 is chosen because some terms in the interaction are proportional to wavenumber, and also the highest waves are most sensitive to changes in the data. The first day of November is chosen because it is a day of weak interactions in wave 8 and should be a more testing day.

Table comparing the strengths of various triads into wave 8, calculated using 16 point and 31 point data for 1/11/76.

	Triad		10^{-3} Wm^{-2} mb^{-1}		
Resolution	4,4	3,5	2,6	1,7	0,8
16 point	.290	.347	.019	-.103	-.448
31 point	.372	.372	-.007	-.085	-.432

The two resolutions agree well showing that the data with higher resolution does not contain significantly more important information.

The graph below, figure 5.2, shows the latitudinal variation of the terms of triad 8(7,1) before integration. This is presented to show how well the two resolutions match in their latitudinal structure. The sets of results agree closely. Most importantly the lower resolution results show the same general latitudinal structure as the higher showing again that the lower resolution is sufficiently good to cope with the observed latitudinal variations.

5.5.5 Presentation of the results.

The time series of the NLIT are presented in figures 5.3 to 5.11. They are placed below the kinetic energy series of the relevant wavenumber for easy comparison.

The NLIT plotted for each wave is the sum of the L(n) for the contributing triads less $M_1(n)$. For wave 0, it is the sum of all the M(n) which is plotted. Positive values represent a gain in energy by the wave.

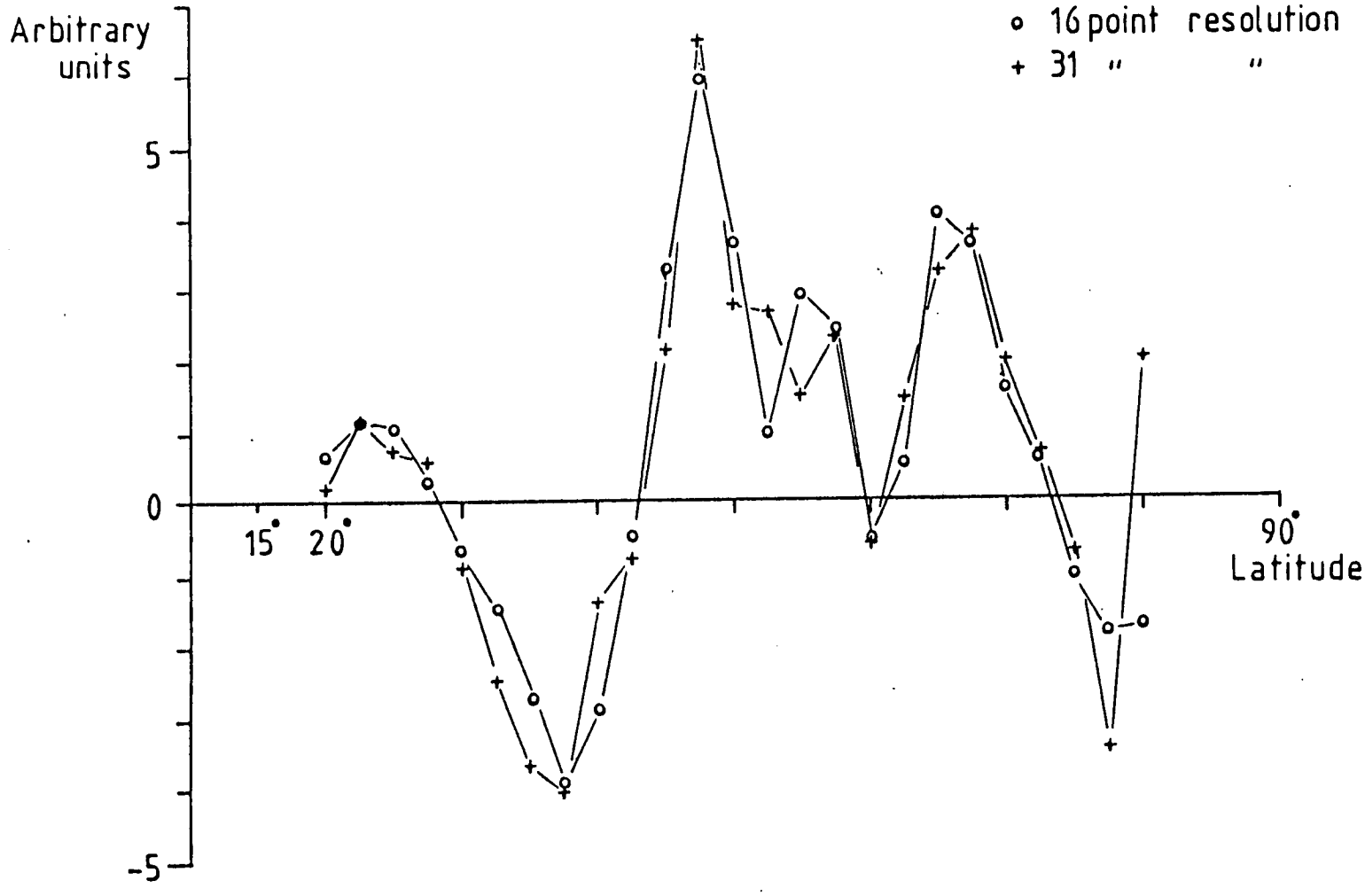

FIGURE 5.2 LATITUDE DISTRIBUTION OF TRIAD. 8(7,1) BEFORE INTEGRATION

The vertical scales in these figures have been chosen for the convenience of display. To compare the kinetic energy changes with NLIT's, 1 unit on the NLIT plots represent a change of 1.24 units per day on the kinetic energy plots, assuming that the NLIT stays constant for the day.

5.5.6 The large variations observed in the NLIT series.

The NLIT series show large day to day variations and frequent sign changes. The appearance suggests that the values include a large component of noise possibly deriving from the original data or generated by unexpected instability in the calculations. Alternatively the twenty four hour interval may not be short enough to detail the variations accurately. However, although the plots show frequent peaks, many of these consist of two or more data points and the major peaks are simultaneous with major kinetic energy changes. Both facts suggests that the variations are real.

Similar, but much shorter, time plots of the barotropic interactions showing similar daily variations are presented by Murakami (1965) and Perry (1967). Reiter (1967) in his review shows results of the interaction between the zonal mean wind and the waves. He quotes the standard deviation of the interaction of the mean wind with wave 4 as 1.9×10^{17} ergs/second/mb and the mean as 0.1×10^{17} ergs/second/mb. The standard deviation being much greater than the mean implies a large variation from

day to day, and frequent changes of sign. Murakami only displays 3 day mean values, yet his plots, presented in figure 5.12, show sign changes and variations similar to these in the present NLIT plots. For comparison with Murakami, and an assessment of the strength of one day variations, a filtered version of wave 4's NLIT is presented in figure 5.13. The filter is a three day unitary filter which reduces one day variations to zero. The filtered series and Murakami's show similar variations which suggests that the variation present in the NLIT plots is normal.

Further evidence that the NLIT series are not random comes from the autocorrelation coefficient for one day lag. For wave 4, this has a value of 0.3 and is significantly greater than the zero expected if the series were indeed random at the 0.1% level.

Thus it is concluded that the series do show a proportion of day to day noise. Allowances for this are made in the analysis which follows which is performed on unfiltered series. In comparing the NLIT fluxes with the kinetic energy changes, the NLIT values are averaged over the period of the change: since this usually means averaging over at least two days, it takes some account of any noise in the NLIT.

5.6 The analysis of the time series.

The analysis is performed to match the observed kinetic energy changes with the NLIT fluxes. For this purpose the fluxes are assumed constant for the day they represent. The important kinetic energy changes during the

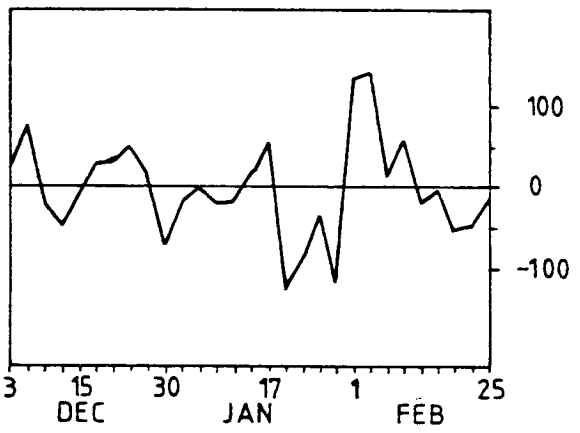

Figure 5.12 Time plot of L from Murakami for waves 1 and 2 together showing the interaction with waves 3 to 10 as three day means. The area of integration is bounded by 50 and 100 mb and 25°N and 70°N. Units are 10^{18} ergs/sec.

blocks are detailed in appendix 3. Both amplifications and decays are analysed. If the NLIT flux implies a kinetic energy change greater than or equal to the observed change, it is taken to be the cause of the change.

The results of this analysis are contained in appendix 4. These are presented in detail for each event in each block in the order of the importance attached to the event in appendix 3.

5.7 The results described and categorised.

5.7.1 Detecting Egger's mechanism.

In this study we accept as fitting Egger's mechanism any wave that amplifies by interacting with other waves and that causes a block. Certain recognisable features provide satisfactory evidence for such behaviour in the present data. Thus it is sufficient for a wave to amplify or to come to a peak in energy during the block, for that wave to form a crucial part of the block, and for the changes in kinetic energy of that wave to be explained by the NLIT.

5.7.2 Partitioning the results according to the degree of agreement between the NLIT and the kinetic energy events.

The kinetic energy events from appendix 3 can be put into three categories viz:-

(a) Completely consistent: the NLIT is consistent with the observed kinetic energy changes.

(b) Partly consistent: the NLIT is consistent with only the amplification or the decay of the event.

(c) not consistent: the NLIT is not consistent with any part of the event: the fluxes are too low or of the wrong sign.

The number of occurrences in each class is tabled below against the subjective importance ranking of the event in the kinetic energy analysis.

Importance	Wholly consistent	Partly consistent	Not consistent
1st	7	5	3
2nd	5	4	5
3rd	3	4	6
4th	1	3	5
5th	1	1	2

Only the events ranked first have a bias in favour of consistency showing that in these events the non-linear interactions play a most important role. The events of lesser importance are not strongly controlled by the non-linear interactions.

Egger's mechanism is strongly supported by this evidence, but it is shown presently that not all of the events of first importance fit Egger's mechanism properly.

5.7.3 Blocks for which the most important energy events can be explained by the NLIT.

The seven blocks during which the first ranked waves are completely explained viz:- E3, E4, E4B, E5, E6, E8 and E11 are examined in detail in this section.

Block E3.

This block fits Egger's pattern in so far as its major wave, wave 4, amplifies and decays under the control

of the non-linear fluxes. Wave 2 is present but is of secondary importance. It does not fit an Egger model because its kinetic energy changes are not consistent with the NLIT. This contrast between wave 4 and wave 2 serves to show that the non-linear interactions are not a complete description of this block.

Block E4.

The principal energy event during this block can be explained by the NLIT, yet E4 is not a block of Egger's type. The important events are an amplification of wave 0 and wave 2 after a period of decline from a peak in the TEKE. The decay of the TEKE peak and the amplification of wave 0 are explained by the NLIT, the fluxes showing that the waves involved in the TEKE peak lose strongly via the non-linear interactions. The energy appears to go into wave 0. Wave 2 amplifies simultaneously with wave 0 but this is not explained by the NLIT and it is likely that wave 2 gains energy from the increased forcing due to the accelerated zonal wind. E4 is thus not an example of the Egger mechanism.

Block E4B.

This block is mentioned in the chapter on kinetic energy as characterised by energy events which overlap its boundaries. It inherits, from E4, peaks in wave 0 and wave 2, and it leaves, for E5, a strong peak in wave 1. Wave 6 is the most important wave during E4B and its energy change is described by the NLIT. The energy in wave 6 is built up from wave 0 when that wave decays. This is surmised because

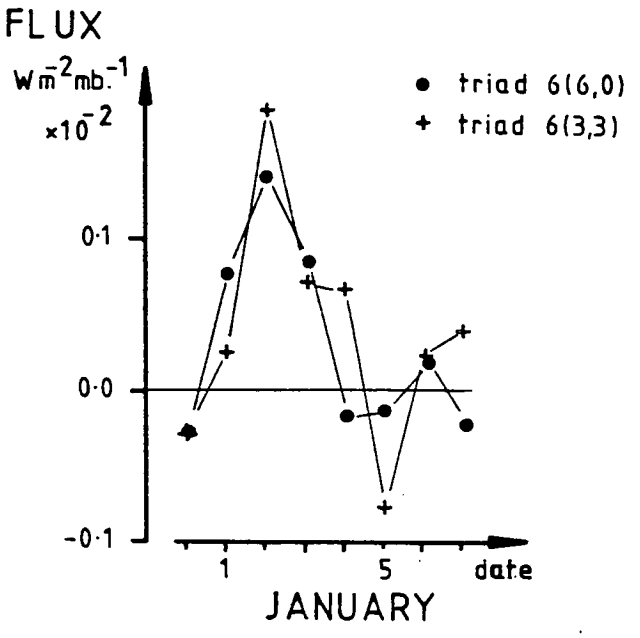

Figure 5.14 Time evolution of the energy fluxes in triads 6(6,0) and 6(3,3) during E4B.

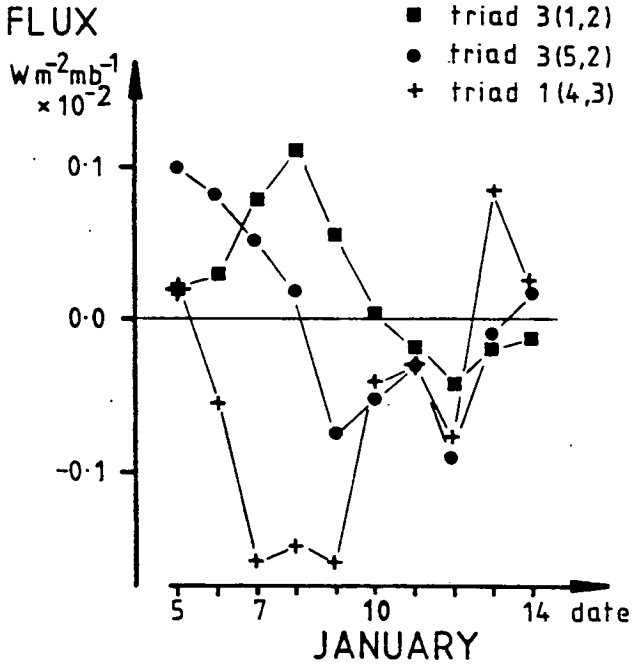

Figure 5.15 Time evolution of the energy fluxes in triads 3(1,2), 3(5,2) and 1(3,4) during E5.

the NLIT gains during wave 6's amplification come mostly from triads 6(6,0) and 6(3,3). The course of these during E4B is shown in figure 5.14. What are not consistent with the NLITs are the decay of wave 2 and the amplification of wave 1. It must be assumed that these are due to changes in the orographic forcing or in the vertical structure. E4B does seem to fit a block of Egger's type with its main wave forced by the non-linear interactions. Its energy supply, however, comes not from forced stationary waves but from a slightly different source - a store of energy in an energy peak of another wavenumber, the energy being transferred from this store via the non-linear interactions.

Block E5.

During E5, waves 1, 3 and 5 peak in succession. The highest, and most important, event is the peak in wave 3, and both the amplification and the decay are consistent with but not as great as the changes implied by the NLIT fluxes. During the amplification, the NLIT gains come mainly from triads 3(5,2) and 3(1,2), from which wave 3 gains about 230 $Jm^{-2}mb^{-1}$. The course of these triads during E5 is graphed in figure 5.15. Wave 3 peaks as wave 1 decays. The NLIT shows a loss for wave 1 and this is mainly into triad 1(3,4). See figure 5.15. Thus wave 1 loses to a triad containing wave 3, and wave 3 gains from a triad containing wave 1, suggesting that wave 3 gains a substantial amount of energy from wave 1's decay.

Wave 5 peaks as wave 3 begins to decay. Wave 5's amplification is consistent with the simultaneous NLIT gain which is in the form of a short peak lasting one day.

This is caused by a high value of gain ($1.1 \times 10^{-3} Wm^{-2} mb^{-1}$) in the triad 5(3,8). Thus wave 3 appears to feed wave 5.

A type of 'cascade' mechanism is therefore evident in this block; a longer wave passes energy to a shorter wave before decaying.

Block E6.

During E6 there is little activity until mid-way through when the energy of wave 0 drops sharply. This can be accounted for by the NLIT which ceases to supply its normal flux. Since wave 0 is normally supplied through the NLIT (Saltzman), the zonal wind decelerates when this energy supply stops. This deceleration signals an amplification and peaking of waves 6 and 7. The 6 and 7 event is not fully accounted for by the gains via the NLITs for they are only about two thirds of the required size. So, waves 6 and 7 cannot be purely forced by the non-linear interactions. Amplifying more slowly after the wave 0 collapse, waves 3 and 4 together reach a strong peak two days after the finish of the block. This amplification is not explained by the NLIT fluxes which, though of the correct sign, are smaller than is required.

It can be seen that this block, whose principal event is the wave 0 decline, is not of an Egger type. No wave has a peak central to the block. Those peaks that do occur are in the second half and are not explained by the NLITs. The block is more of a cascade type.

The abrupt decays of waves 3 and 4 after the block are described by the NLIT fluxes. Simultaneously, waves 6 and 7 experience strong peaking and this too is explained

by strong NLIT fluxes into each wave. Wave 6 and wave 7 are maintained against strong dissipation by the NLIT fluxes which, during the days of the peak, daily deliver nearly one and a half times the energy in each peak. When the NLIT fluxes fall, the kinetic energy peaks fall also.

Block E8.

During E8, wave 2 amplifies strongly to peak on the last day of the block falling sharply thereafter. All is consistent with the NLIT fluxes. The main contributors to these fluxes are the triads 2(1,1) and 2(3,1). The course of these during E8 is graphed in figure 5.16. E8 is seen to fit Egger's mechanism closely with a wave 2 amplification being caused by non-linear interaction with waves 1 and 3. Wave 2 decays when the strong interactions with waves 1 and 3 cease. Thereafter, wave 2 loses its energy to all waves. However, there are also important contributions to the block which are not described by the NLIT fluxes. These are the contributions from waves 6 and 7. Once again, as in E3, Egger's mechanism is not a complete explanation.

Block E11.

The sole event of importance during E11 is a wave 2 peak. Both the amplification and the decay of this are consistent with the NLIT fluxes. The main contributor to the amplification is the triad 2(1,1) but there are also important contributions from triads 2(2,4) and 2(3,5). The decay is into slightly different triads viz: 2(1,1), 2(4,6) and 2(6,8). The time series of the values of the interaction in triad 2(1,1) are shown in figure 5.17.

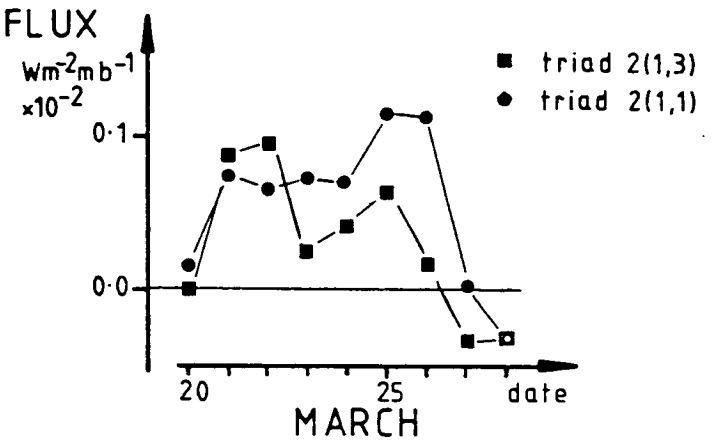

Figure 5.16 Time evolution of the energy fluxes in triads 2(1,3) and 2(1,1) during E8.

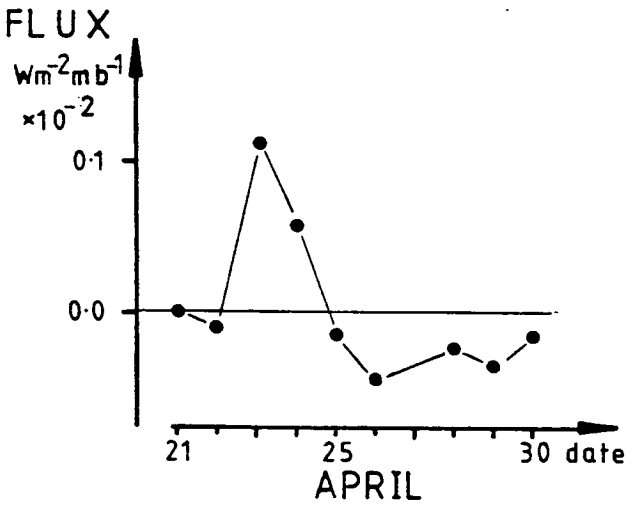

Figure 5.17 Time evolution of the energy fluxes in triads 2(1,1) during E11.

Only blocks E8 and E11 have wave 2 events which are describable by the NLITs. It may be significant that they occurred in late March and in April. These timings are after the final seasonal reversal in the stratosphere which suggests that on both occasions wave 2 is a trapped wave and, therefore, not transporting the NLIT gains vertically, but growing in situ.

5.7.4 Summary of section 5.7.3.

The blocks E3, E4, E4B, E5, E6, E8 and E11 all have their most important events described by the NLIT's, but only three display Egger type mechanisms. Of the three that do viz: E3, E8 and E11, E8 is especially close to Egger's model, having a wave 2 gaining from waves 1 and 3. In E11 wave 2 is again the principal wave and wave 1 the main forcing wave. In E3, the principal wave, wave 4, can be explained by the NLIT, whereas wave 2, which is also prominent, is independent of the NLIT. It is also observed that Egger's model fits these three blocks provided it is generalised to allow waves other than just wave 2.

Two others, E4B and E5, are superficially of the Egger type, with their principal waves being explained by the non-linear interactions. But here, and with E4 and E6 as well, the energy transfer mechanism involves a cascade effect through which energy from one decaying wave is passed on to another. This is not Egger's mechanism which is concerned with forcing free waves from stationary waves but another which concerns forcing one wave by depleting energy stored in others. It is also apparent that Egger's

mechanism cannot account for blocking fully since there are other wave events (e.g. during E3 and E8) which are important but not explained by the NLIT.

5.7.5 Blocks where the major energy events are only partly explained by the NLIT.

There are five blocks in this category - E2, A2, E5A, A4 and E10. They are described in order.

Block E2.

Wave 4 is the most important wave in E2 and it peaks in energy during the block. The decay of the peak is consistent with the NLIT fluxes, but during the amplification the NLIT shows a loss. This block is not Egger like because wave 4's amplification is not due to an NLIT flux. Also during this block wave 3 is seen to amplify simultaneously with a decay of wave 1. The amplification of wave 3 can be explained by the NLIT but wave 1's decay cannot. Thus the energy for wave 3 does not appear to come from the decaying wave 1.

Block A2.

None of the components in A2 is fully consistent with the NLIT fluxes. The main event is a peak of waves 5 and 6. The NLITs show gains during the amplification and losses during the decay of this peak, but they (except for wave 5's decay) are only about three quarters of the size required to explain the energy changes. This block is therefore not of Egger's type. An energy producing mechanism of another sort is implied.

Block E5A.

Block E5A is due to a sharp peak in wave 3 together with a high level of wave 4. The amplification of wave 3 is explained by more than adequate gains through the NLIT. Hence, the block appears to fit an Egger mechanism. However, the subsequent decay of wave 3 is accompanied, not by losses in the NLIT, but by moderate gains. In this block, therefore, wave 3 is responding to energy changing mechanisms other than the non-linear interactions and so the block cannot be altogether of Egger's type.

Block A4.

The principal wave of A4 is wave 5 which experiences a strong peak during the block. The next most important is wave 2. Only the decay of wave 5 is describable by the NLITs. Wave 4, the next again in importance, is described by the NLIT but it does not peak within the block itself. It peaks in the 'grey' period after the block proper has finished. Hence the block A4 alone is not of the Egger type, but the block plus 'grey' period is a possible candidate.

Block E10.

E10 occurs when, previously strong, waves 4 and 6 drop of a minimum. In their place, a wave 5 amplifies to a peak. The amplification can be explained by the NLITs but the subsequent decay is not accompanied by NLIT losses of sufficient strength. Because wave 5's decay is not entirely explained by the NLIT fluxes it is concluded that wave 5 is controlled by other mechanisms and this block, like E5A, is not immediately classifiable as of Egger's type.

5.7.6 Summary of section 5.7.5.

Of these five blocks, E10 and E5A appear to fit an Egger type mechanism most closely except that the decays of the energy peaks are not consistent with the NLIT fluxes. A2 and A4 are very similar. Both have important peaks in waves 5 and 6. In both, the NLIT fluxes are not sufficient to explain the changes and energy must be coming from other sources. This is also implied in E2, where wave 4 is seen to amplify in spite of losses in the NLIT.

In A4 wave 2 is important but its behaviour is not explained by the NLIT fluxes. This echoes the situation in E3, E4 and E4B and reinforces the conclusion that, although they are important in blocking, the NLITs provide only a partial explanation.

5.7.7 Blocks where the major energy events are not explained by the NLIT.

The three blocks remaining to be described do not fit an Egger type mechanism because the important events are not explained by the NLITs. The blocks are A1, E7 and A5/E9.

Block A1.

Block A1 has wave 2 as its principal wave with a less energetic wave 3 next in importance. The behaviour of wave 2 is not explicable by the NLIT, but that of wave 3 is, and Egger's mechanism is seen to operate in wave 3. Here, in A1, one has a situation similar to that in E3 in which a strong wave 2 is not describable by the NLITs, though Egger's mechanism fits the other wave of the block.

Block E7.

This block has no energy event of particular significance, though wave 5 peaks briefly, as does wave 6, and wave 3 amplifies throughout. None of the events is consistent with the NLIT fluxes. The NLIT gain during wave 3's amplification is not of the required strength to explain the amplification.

Block A5/E9.

The double block A5/E9 is caused by high amplitudes of waves 4, 6 and 7. During most of the events, the NLIT's are opposite to the changes in kinetic energy. The NLIT's are acting as a dissipative mechanism. A5/E9 is therefore definitely not an Egger type block. A possible mechanism for this block is that of Tung and Lindzen. In their theory, wave 4 becomes resonant growing to high amplitude with only small energy input. For such a resonance to occur, wave 4 needs to be trapped. A vertical section of the zonal mean wind at 60^{o}N, figure 5.18, shows easterly winds down to 60mb. This implies that wave 4 is indeed trapped in the troposphere. However, the strong dissipation which the losses in the NLIT represent implies that the forcing mechanism of wave 4 must be strongly enhanced over normal to cope with the increase in losses. Tung and Lindzen's formulation does not take account of such strong dissipation - but also does not include enhanced forcing.

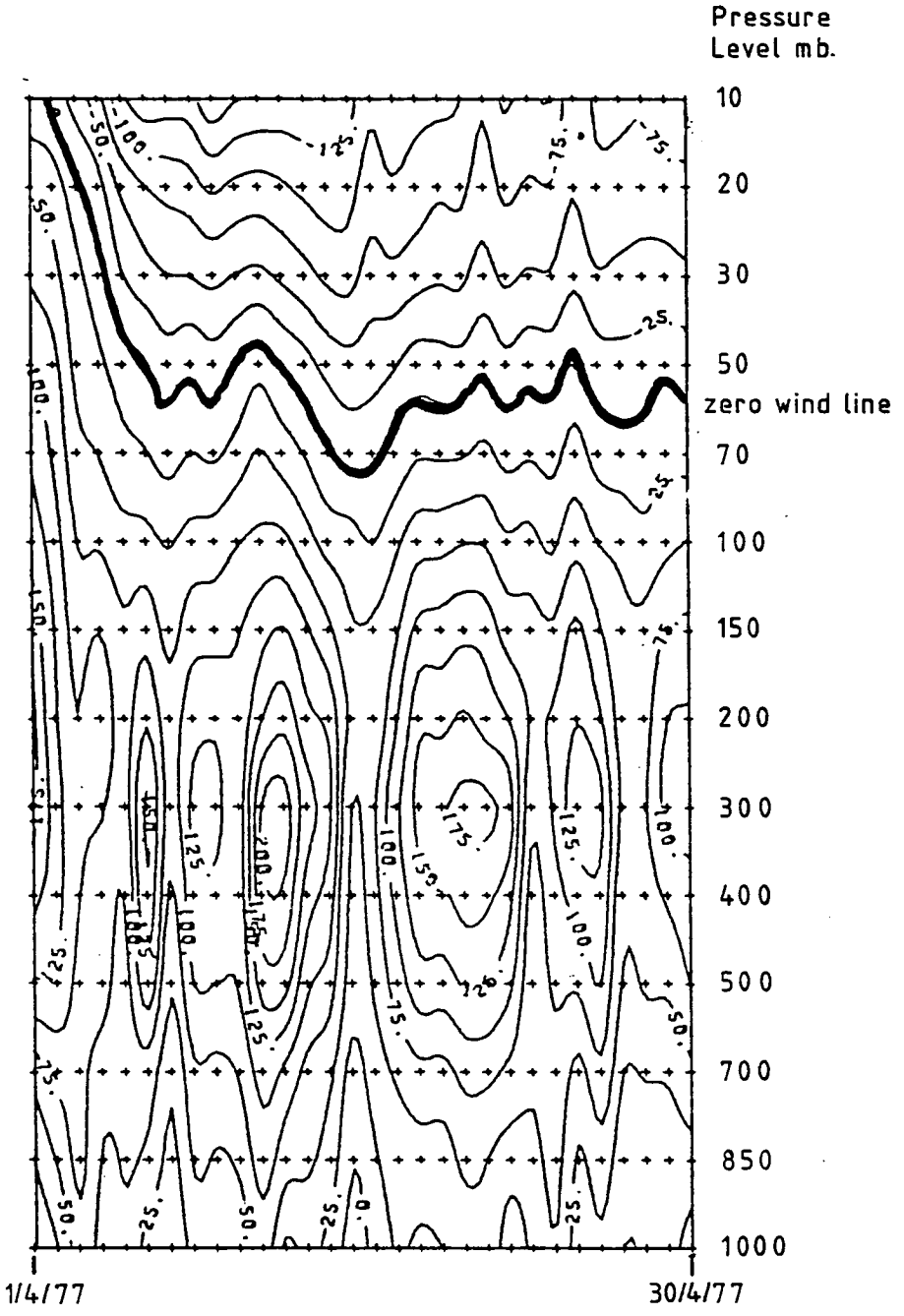

Figure 5.18

Time/height section of the zonal wind between 55° and 60°N for April 1977. Westerly winds are positive; contours are in cm/s. The data are described in chapter 2 and the results are obtained as in chapter 4 but extended to include the additional levels.

5.7.8 Summary of section 5.7.7.

These last three blocks, A1, E7 and A5/E9, show that the non-linear interactions do not even offer partial explanations for some blocking events. As the evidence of A1 shows, and this is supported by evidence from other blocks in earlier sections, wave 2 can be singled out especially as being of importance but not often explained by the NLIT.

Evidence of a non-Egger mechanism is apparent in A5/E9 where, instead, the theory of Tung and Lindzen is possibly an explanation. However, this is only a tentative identification. Although wave 4 is trapped beneath the easterly stratospheric winds, the magnitude of the energy loss to wave 4 via the NLIT is greatly in excess of dissipations envisaged by Tung and Lindzen.

5.8 Discussion of the results.

5.8.1 The importance of barotropic, horizontal non-linear interactions is evident from the analysis. The NLITs provide explanations of important events in nine out of the fifteeen blocks in the study. Egger's mechanism is operative clearly on three occasions - in E8, E11 and E3. On two more occasions, E5A and E10, the mechanism is possibly occurring, but not clearly,because the decays of the waves are not fully explained.

In two other blocks, E4B and E5, an Egger mechanism is apparent, e.g. a major peak in energy is caused by the NLIT, but the energy does not come from the same source as

in Egger's model. Instead of coming from increased interaction with stationary waves of relatively constant energy, it comes from the decaying energy peak of a wave of lower wavenumber. This might be called a cascade event.

There are two other cascade events, blocks E4 and E6, which both involve the zonal mean wind. These events are not Egger like because the major event is not an energy peak during the block. Finally there were six blocks E2, A2, A4 A1, A5/E9 and E7 for which the non-linear interactions have no explanation because they show fluxes of inadequate magnitude or of opposite sign.

5.8.2 The failure of the NLIT to explain wave 2 events.

The Egger and cascade mechanisms, even during blocks where they are dominant, do not furnish complete descriptions. The prominent failures are the lack of descriptions of events in wave 2 and in waves 5 to 7. Overall, of nine occasions, wave 2 is fully explained only twice and both of these occur towards the end of the period.

The stratospheric wind completed its spring reversal around the beginning of April (O'Neil and Taylor 1979). Thus it appears that wave 2 can be explained only when it is trapped by easterly stratospheric winds and, so, is at its most barotropic. During the winter, when wave 2 can propagate, other energy conversions than barotropic non-linear ones are operative. This agrees with the work of Tsay and Kao. In a winter period, they found wave 2 to be unique in that it always loses energy via the barotropic non-linear interactions. It gains energy mostly via

baroclinic processes. More study of wave 2's energy cycle is required to give a fuller understanding of blocking.

5.8.3 The failure of the NLIT to explain waves 5, 6 and 7.

Egger's study, limited by truncation at wave 3, gives no information about any short wave effects. As seen in blocks A2, A4 and others, waves 5, 6 and 7 can have an important and decisive role yet are not explained by the NLITs.

These waves generally grow by baroclinic processes (Tsay and Kao), and to explain their behaviour would require the calculation of the conversions between potential and kinetic energy by which these waves appear to grow. Nevertheless, this agrees with the suggestion put forward in chapter 3, that these short wave peaks during blocking are evidence of long wave/short wave interaction. The evidence of this chapter shows that, if such an interaction is operative, it is not via horizontal barotropic processes. It must therefore be via channels not considered in this study, i.e. conversions via vertical velocities and thermal effects. Frederiksen (1979) shows evidence from a model that the presence of planetary waves creates preferred areas of generation of baroclinic disturbances. These lie immediately downstream of the long wave troughs. The interaction between planetary waves and the short waves in A2 and A4 may thus be a phase effect whereby the preferred area of baroclinic disturbance growth due to the long waves is situated over a geographical area also optimal to baroclinic growth, hence the production of a strong

baroclinic disturbance. Further, the statement that the area of preferred growth lies just downstream of the long wave trough implies that the ridge of the growing baroclinic disturbance lies close to the first long wave ridge downstream of the trough, explaining the observation in A2 and A4 that the ridges of waves 5 and 6 are in close proximity to the long wave ridges at the blocking position.

5.8.4 Mechanisms other than Egger's.

Two recent theories for blocking can be assessed with this data. The first, by Tung and Lindzen, suggests that blocking consists of a single wave in resonance with the boundary forcing and the vertical state of the atmosphere. Block A5/E9 is the candidate best fitting such a mechanism. The stratosphere has easterly winds so that wave energy is trapped, a necessary condition for this mechanism. The vertical structure of wave 4, during A5/E9 shows one simple amplitude maximum in the upper troposphere, figure 5.19. The analysis shows the wave 4 peak in energy to be accompanied by NLIT losses, but the growth of a resonant wave would not necessarily be explained by the NLIT fluxes since only small forcings are required. However, as pointed out in section 5.7.8, during the amplitude peak of wave 4, the NLIT shows losses of a strength able to remove the peak of energy in one day. This is in excess of the damping rate of 4 days considered by Tung and Lindzen. But these authors only consider constant forcing: if, instead, the forcing were also increased, resonance could still occur even in the presence of stronger

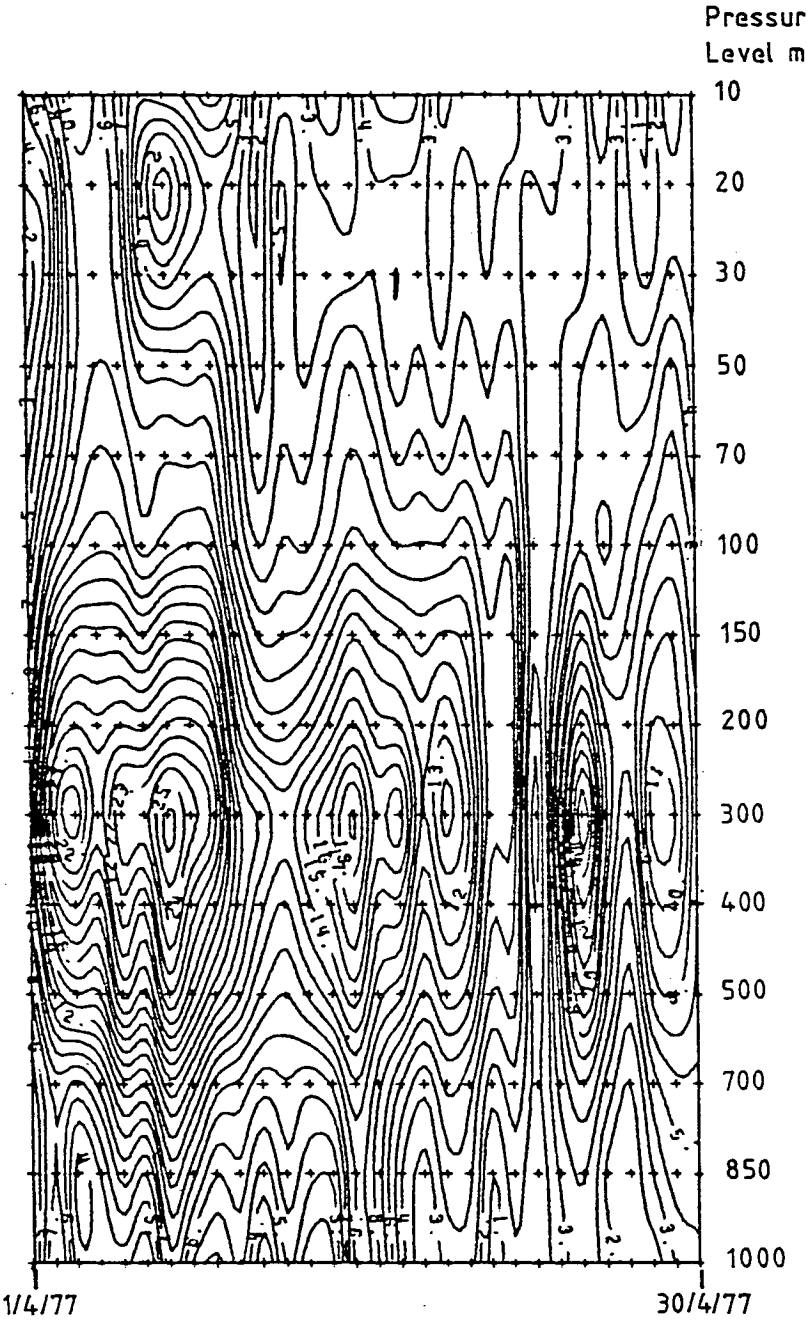

Figure 5.19 Time/height section of wave 4 at 55°N during April 1977. The contours are in dcm. The data are described in chapter 2 and the results are obtained as in chapter 4 but extended to include the additional levels.

dissipation. In A5/E9 the forcing of wave 4 must be greatly increased over its normal value. Wave 4 may, of course, have been produced by other mechanisms. To resolve the question requires further study of the full energy budget of wave 4 to see if it gained its energy from thermal sources, or, as is consistent with a boundary forced resonance, from vertical pumping. The theory states that the wave becomes resonant only if the free wave state of the atmosphere has a phase velocity of zero. Finding whether, in the case of A5/E9, this is so requires solving the equations governing the structure of the free wave, such as are presented by Tung and Lindzen, using the atmospheric conditions applicable to A5/E9.

The second theory, put forward by Charney and De Vore, suggests that blocking may be a quasi-equilibrium state of low zonal index. The block is effectively the highly meridional stage of a vacillation cycle where a single wavenumber interacts non-linearly with the zonal mean wind. E6 might be such a vacillation. In it, the zonal mean wind falls, and subsequently waves 3 and 4 amplify. For this to be a vacillation, wave 0 energy must be transferred by the NLIT into waves 3 and 4, but this is not observed and hence the E6 event is not a vacillation of the Charney and DeVore type. A better example might be the cascade type block E4B where a wave 0 decline forces a wave 6 peak, and the NLIT explains both. However, both E4B and E6 are one-off events and do not represent evidence of a stable oscillation between the long waves and the mean wind.

It is not clear how direct evidence of quasi-stability might be uncovered, although evidence of the interaction between waves and zonal wind might be found if the forcing terms through which the interaction takes place could be calculated directly.

5.9 Conclusions.

Egger's mechanism for blocking has been shown to be operative in real data. It is, however, neither a complete explanation nor a universal one. Analysis shows another mechanism at work, similar to Egger's, but one in which the energy for the forced wave comes from the collapse of a wave of lower wavenumber via a cascade. Significant deviations from Egger's model occur when, the non-linear interactions fail to explain important energy events. To explain these failures requires a study of the complete energy cycle of all the waves, but of waves 2, 4, 5, 6 and 7 in particular. The lack of an explanation of waves 2 and 4 suggests that changes in orographic forcing or wave structure is important. The evidence of waves 5, 6 and 7 shows that there is an important short wave component during blocking whose energy processes need further study. The theories of blocking as a wave resonance or as a vaccilation have possible examples in this study period but more investigation is required before any conclusions can be reached.

Chapter 6. BLOCKING AS A ROTOR IN A ROSSBY WAVE.

6.1 The case for a block as a Rossby wave rotor.

6.1.1 Introduction.

The possibility that blocks might be rotors was put forward by Scorer in 1979, but, to my knowledge, has not been investigated with reference to real data on blocking prior to this study. The idea provides a relatively simple mechanism for blocking. Simple, that is, to visualize though less simple to describe. Yet it is important, in the context of a search for blocking mechanisms, that the idea be developed. Previous theories of Rossby waves - see references in Madden 1979 and Shutts 1978 - have simplified the flow equations by staying within the limits of small perturbations, thereby eliminating the very conditions which give rise to rotors.

This chapter presents a simple, and what must be considered a preliminary investigation of Rossby wave rotors and of their connection with blocking. In the first part of the chapter, Scorer's simple theory of rotors is reworked in Rossby wave terms. In the second part, some possible examples of rotors taken from the period 1/11/76 to 30/4/77 are described and their connection with blocking discussed. Due to the simple nature of the theory, it is not compared directly with the real examples. Such a comparison must await a more complex development of the theory.

6.1.2 What is a rotor?

A rotor is a local reversal of the wind velocity, and is characterised by streamlines in the form of closed loops. Rotors occur in association with high amplitude waves and have been mostly studied in connection with gravity waves (Scorer).

The definition of blocking adopted by Treidl, Birch and Sajecki includes the requirement of a closed streamline around the anticyclone. Thus it includes rotors. However, as mentioned in chapter 1, not all real blocks show such a contour. Thus they may not always be rotors.

6.1.3 The similarity in appearance of blocking anticyclones and rotors.

An example will serve to show the similarity: see figure 6.1, in which the upper chart shows the 500 mb height field for 12/11/76. The block A1 is present at 120°W 50°N. The anticyclone, with its closed circulation, and the strongly meandering jet form a pattern resembling a rotor type flow pattern. The correspondence is made clearer when all but the dominant planetary wave of the block, wave 2, and the zonal mean are filtered from the field, as in the lower chart. Now, the pattern resembles a rotor pattern closely. Additionally, the ridge of wave 2 at 120°W accurately matches the blocking anticyclone. Thus, in this example, there is,at least in the dominant wave component, a visual similarity between the blocking anticyclone and a rotor flow pattern.

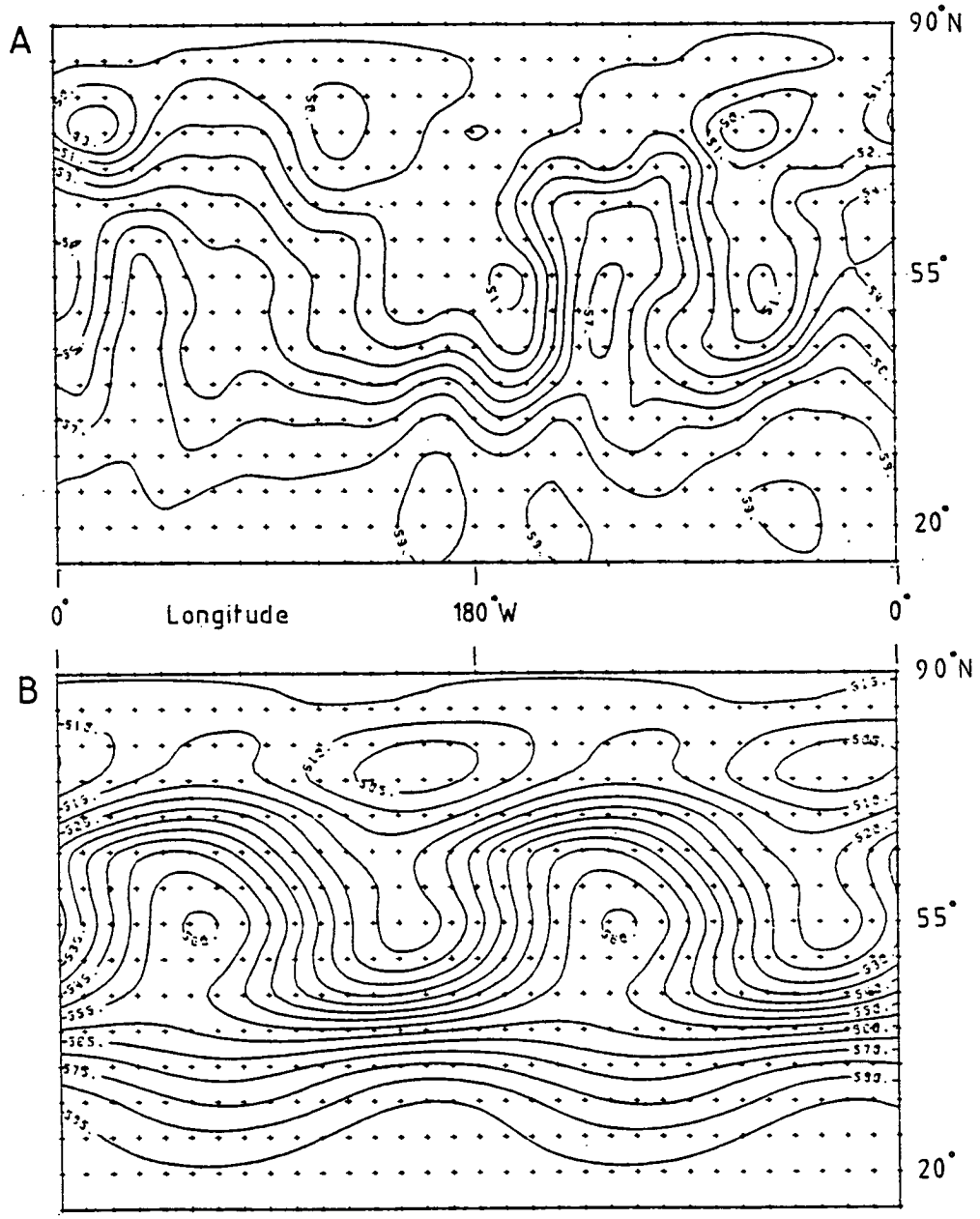

Figure 6.1 Charts of the 500 mb surface for 12/11/76. 'A' shows the actual chart; contours are marked in dcm x 10. 'B' shows the filtered data with only wave 2 and the zonal mean present; contours are in dcm.

6.1.4 The similarity of the theories of Rossby waves and of gravity waves.

Scorer (1979) points out that the description of simple gravity wave flow results in a conservation equation similar to that found in describing Rossby waves on a beta plane.

For steady gravity waves, the quantity $\eta - \frac{B g}{U_o} z$ is conserved along a streamline where η is the y component of vorticity and z is height. The simplifying assumptions are: the flow is two dimensional in the x and z directions, frictionless and incompressible: the upstream velocity U_o is uniform: the density stratification B depends only on the initial undisturbed streamline position.

For Rossby waves on a beta plane, in an incompressible and frictionless fluid, the quantity $\zeta + \beta y$ is conserved along a streamline, where ζ is the vertical component of vorticity, and β is the latitudinal gradient of Coriolis parameter.

In the case of gravity waves, a simple linear equation can be found which describes waves of unlimited amplitude: Scorer suggests that it ought to be possible to find a similar simple linear equation to describe rotors in Rossby waves.

6.2 The theoretical treatment of rotors in a simple planetary wave.

6.2.1 The failure of the usual derivation of a Rossby wave to describe rotors.

The conventional derivation of Rossby waves is given in many texts, e.g. Fleagle and Businger (1980). This fails to describe rotors because of the linearisation of the vorticity equation. The vorticity equation for simple Rossby wave is $\frac{D}{Dt}(\zeta + f) = 0$

where $\frac{D}{Dt}$ is the substantive derivative,

ζ is the vertical component of vorticity, and

f is the Coriolis parameter.

Because of the advection term $\underline{V}.\nabla$ in the substantive derivative, this equation is non-linear. Normally the term is linearised to $\bar{U}\frac{\partial}{\partial x}$ on the assumption that the perturbation velocities induced by the wave are small in comparison with the zonal mean wind $\bar{U}$. Rotors occur when, locally, the wave induced velocity is greater than (and opposite to) the zonal mean velocity. Since the linearisation assumption specifically excludes this situation, the usual treatment cannot deal with rotors.

6.2.2 The derivation of rotors in Rossby waves.

In this derivation, I follow Scorer's simple derivation for gravity waves in a stratified flow (Environmental Aerodynamics 1978) but translate it into Rossby wave terms. The flow pattern is taken to be stationary and time evolution is not considered. Additionally, the density is everywhere the same and the vertical velocity is everywhere zero.

Assume the horizontal component of vorticity on a beta plane, $\zeta + \beta y$, to be constant along a streamline. Take for simplicity orthogonal co-ordinates x,y , with respect to an origin in the middle of the plane, and examine the continuity of mass flow between two streamlines.

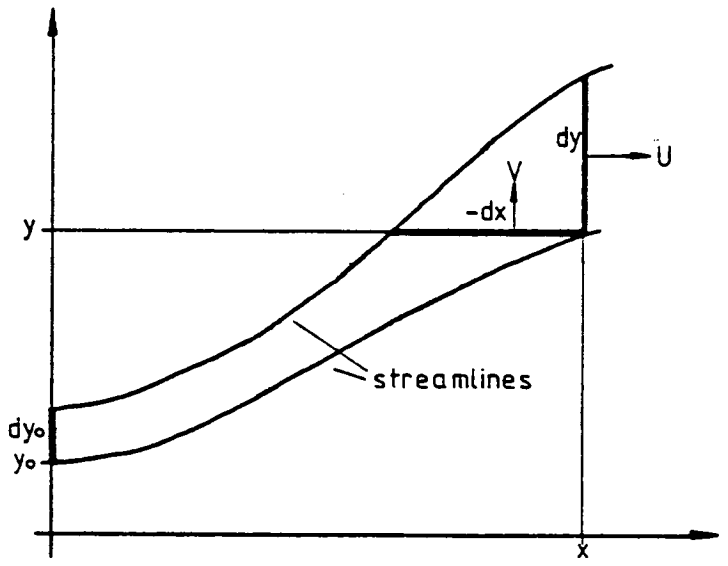

Figure 6.2

Take the subscript '0' to refer to the value of each quantity at an initial position. Referring to figure 6.2, the continuity of mass requires

$$U_o dy_o = -V dx = U dy \qquad \text{eqn. 6.1}$$

from which $U = U_o \frac{dy_o}{dy}$; $V = -U_o \frac{dy_o}{dx}$ eqn. 6.2

Then $\zeta = \frac{\partial V}{\partial x} - \frac{\partial U}{\partial y} = -U_o \nabla^2 y_o - \frac{\partial U_o}{\partial y_o}(\nabla y_o)^2$ eqn. 6.3

Hence $\zeta + \beta y = -U_o \nabla^2 y_o - \frac{\partial U_o}{\partial y_o}(\nabla y_o)^2 + \beta y$

$$= \text{constant along a streamline} \qquad \text{eqn. 6.4}$$

Putting $\alpha = \frac{1}{U_o}\frac{\partial U_o}{\partial y_o}$ eqn. 6.5

in equation 6.4 leads to

$$\nabla^2 y_o + \alpha(\nabla y_o)^2 - \frac{\beta}{U_o} y = \text{constant} \qquad \text{eqn. 6.6}$$

Considering the following diagram, y is expressed in terms of the deviation of a streamline from its y co'ordinate, y_o , at $x = 0$ as $y_o = y - \xi$ eqn. 6.7

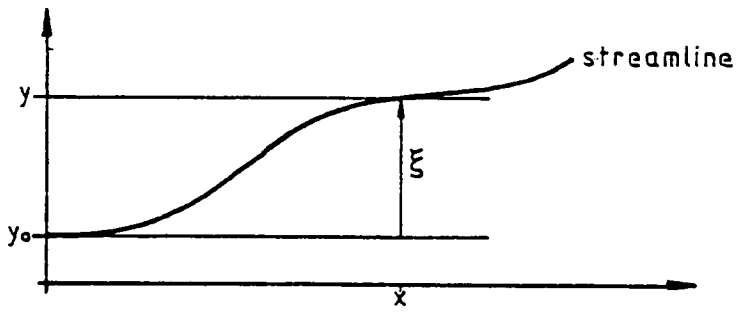

From which $\nabla^2 y_o = -\nabla^2 \xi$ eqn. 6.8

and $(\nabla y_o)^2 = (\nabla \xi)^2 - 2\frac{\partial \xi}{\partial y} + 1$ eqn. 6.9

substituting from eqns 6.8 and 6.9 in 6.6 gives

$$\nabla^2 \xi + \alpha\left((\nabla \xi)^2 + 1 - 2\frac{\partial \xi}{\partial y}\right) + \frac{\beta \xi}{U_o} = \text{constant} \qquad \text{eqn. 6.10}$$

Now assume that somewhere upstream the velocity is constant across the channel and that ξ and its derivatives are zero. In this case equation 6.10 reduces to

$$\nabla^2\xi + \frac{\beta\xi}{U_o} = 0 \qquad \text{eqn. 6.11}$$

This equation is linear. Yet, it can describe waves of unrestricted amplitude because none of the assumptions have limited the possible amplitude of ξ .

At the boundary of the channel of width 'h' ; $\xi = 0$. A wave like solution for ξ satisfying this requirement is

$$\xi = A.\cos ly.\cos kx \ :$$

$$\text{where } l = \frac{n\pi}{h} \ : \ n=1,2,3.... \qquad \text{eqn. 6.12}$$

In this chapter only $n=1$ will be considered since this is the most appropriate as will be seen later.

Substituting 6.12 into 6.11 results in the dispersion relation

$$l^2 = \frac{\beta}{U_o} - k^2 \qquad \text{eqn. 6.13}$$

This is identical to the dispersion relation derived through the usual linearised method.

This new derivation shows that simple Rossby waves on a beta plane need not be restricted to small amplitudes. It shows too that the same simple dispersion relation applies to unrestricted amplitudes as well as to small amplitudes, and therefore can be applied to a flow including rotors.

6.2.3 Conditions for the formation of rotors.

The necessary and sufficient condition for rotors to occur in a flow as described in the previous section is that somewhere the zonal velocity is negative.
Now, from equations 6.2 and 6.7

$$U = U_o\left(1 - \frac{\partial \xi}{\partial y}\right)$$

This becomes negative if $\frac{\partial \xi}{\partial y} > 1$, which can only occur in this example if

$$Al \geq 1 \qquad \text{eqn. 6.14}$$

6.2.4 Examples of the flow pattern.

Four examples show the pattern of the flow for different values of amplitude A . See figure 6.3. For these examples, the latitude of the beta plane is set at 55°N, and the zonal wind at 8 ms^{-1}. Using equations 6.12 and 6.13 the width of the channel h is chosen to be 4.72×10^3km, equivalent to 42° of latitude, to suit a wave 4 pattern. The critical amplitude A_c for this flow is 1.5×10^3 km. In order to include the pattern of the zonal wind, the several plots in figure 6.3 show contours of ψ , where

$$\psi = \xi - y$$

Thus

$$U = -U_o \frac{\partial \psi}{\partial y} \qquad V = U_o \frac{\partial \psi}{\partial y}$$

The values of amplitude are chosen to show, subcritical, critical and rotor flows.

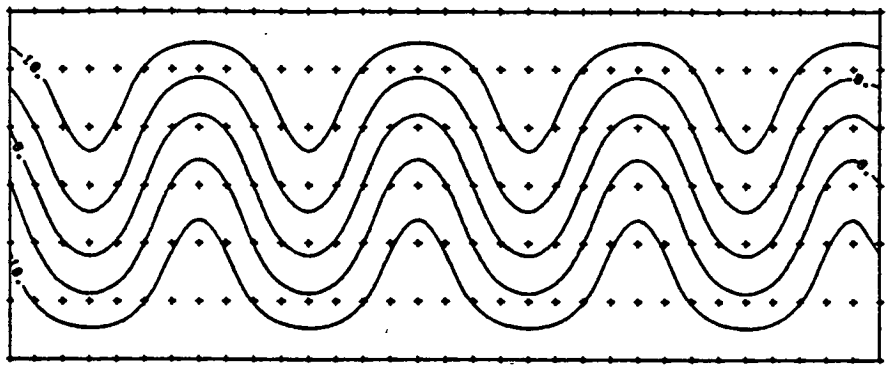

A= 1·2×10^{3}km

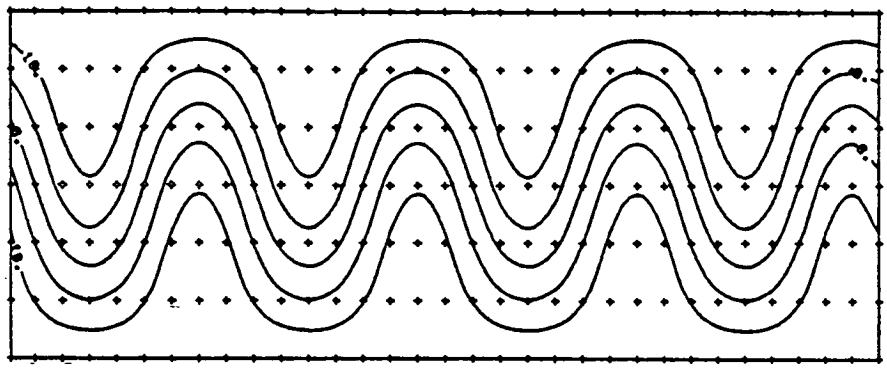

A= 1·5×10^{3}km

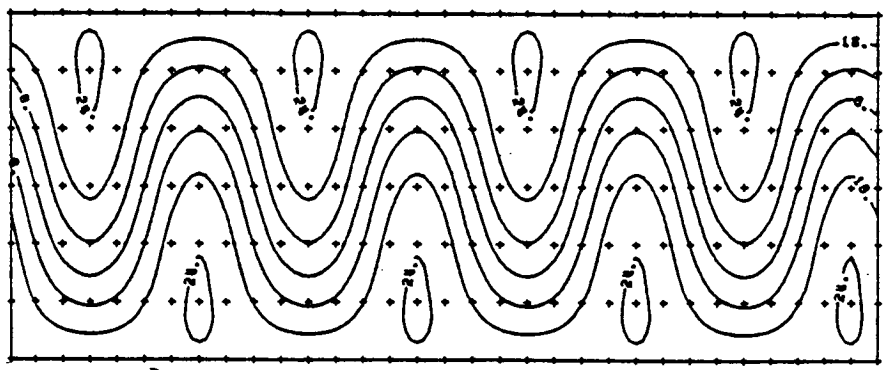

A= 1·8×10^{3}km

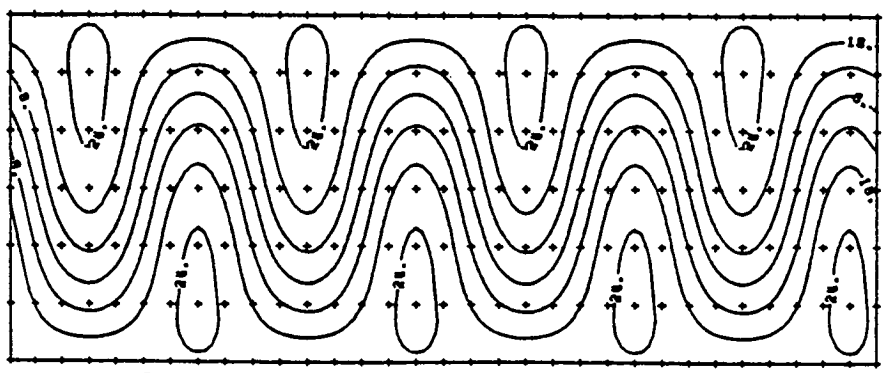

A= 2·0×10^{3}km

Figure 6.3 Contours of ψ x 1.25 x 10^{-7} m^2s^{-1} for various amplitudes 'A' as shown.

6.2.5 Summary and conclusions of section 6.2.

Working Scorer's suggestions through has resulted in a simple theory in which Rossby waves can have amplitudes large enough to produce rotors. The resulting dispersion relation is identical to that obtained in the usual linearised derivation. However, the present formulation has no time dependence and so is limited to steady and stationary waves. Additionally there are other important simplifications, viz. lack of sphericity, constant density and lack of latitudinal variation of the zonal wind. This latter can be allowed to vary, but then the equations become non-linear once more, eliminating the useful quality of superposeable wave solutions present in the linear case. Before critical comparisons of this theory and actual planetary wave events can be undertaken, the simplifications must be addressed.

6.3 A search for rotors in observed waves.

6.3.1 The data and analysis.

The theoretical description of rotors given earlier is followed up here by a simple visual search for their occurrence in real data. This visual search takes the form of examining charts of the 500 mb flow filtered to show only the zonal mean and dominant wave component, as in figure 6.1. Such charts are, in one aspect, similar to the conditions of the theory in having only a single wave

present on a zonal current.

The theoretical situation differs from the real by allowing no latitudinal variations of phase of the wave, or variations in the zonal wind. If zonal wind variations were allowed, the theory would be non-linear, and,so, harmonic wave solutions to the equations would not be independent. Nevertheless, examining separate harmonic waves - as in the filtered charts - is still valid, particularly if one wave is predominant, though,for a full understanding of the flow,all waves would need to be considered simultaneously. This search is only exploratory and therefore is confined to examining the filtered charts, but,if there is evidence of rotors forming in a single wave, then it is most likely that they form in multiple wave flows also. This is illustrated further in section 6.5, where the connection between rotors and blocking is discussed.

Charts were prepared for a number of days specially selected for the search: days were chosen which had a dominant wave of high amplitude, as seen in figures 3.1 to 3.9. Also, days were selected specially to have, as far as possible, a uniform zonal wind over the area where the dominant wave had high amplitude. Such days are not common. Presented below are eight charts showing the best developed rotors in the period. Also, to show the variations possible, some examples of waves 1 and 4 with a range of amplitudes from weak to strong are included. Finally, the consecutive wave 4 examples show three stages in the development of a rotor system over a period of eight days.

In the cases presented, the waves are not strictly steady as in the theory. Further differences from the theory arise because the contours of geopotential height displayed on the charts, due to the variation with time and the variation of the Coriolis parameter with latitude, do not strictly correspond to the streamlines of the theory.

6.3.2 Charts for selected days, showing various stages in the development of closed circulations in planetary waves.

Events involving wave 1.

11/3/77 - See figure 6.4

Above 70°N the closed circulations are caused by the large rate of change of the phase of wave 1 with latitude and are not relevant to this search. Below 70°N a small wave 1 perturbation is seen. The width of the disturbance appears to be from about 25°N to 70°N.

25/3/77 - See figure 6.5

A large rotor-like disturbance is present between 40°N and 70°N with a closed anticyclonic circulation centred at 10°W, 55°N. The latitudinal extent of the disturbance appears to be about 30°.

The planetary waves can have large phase changes with latitude, wave 1 showing the effect most strongly. On this day, the rotor disturbance is not affected by any phase change with latitude, but above 70°N the effects of a strong phase change with latitude is seen in the west-east orientation of the trough at 120°E 70°N. Throughout the procedure of selecting days for presentation, care was taken

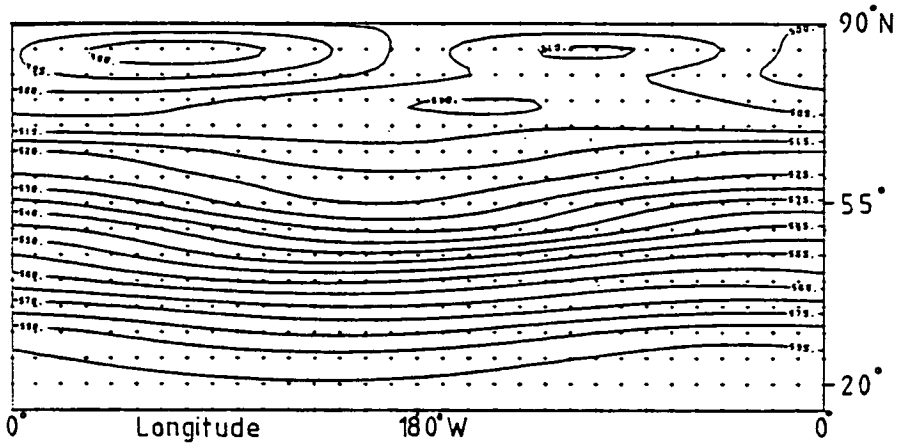

Figure 6.4 Chart of wave 1 plus the zonal mean for 11/3/77. Contours in dcm.

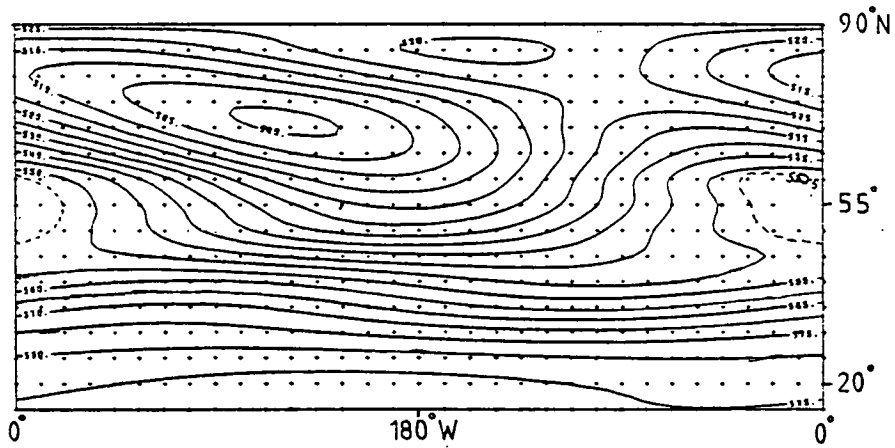

Figure 6.5 Chart of wave 1 plus the zonal mean for 25/3/77. Contours in dcm.

to exclude effects arising from phase changes with latitude.

18/11/76 - See figure 6.6.

A disturbance of 30° width is seen between 40°N and 70°N with a closed cyclonic circulation at 180°W 60°N, but this is not a rotor of the type relevant to this search. It is caused by the eastward change of phase of wave 1 with latitude above 65°N. The alignment of the ridge from 0°W 65°N to 110°W 80°N shows this.

There are anticyclonic ridges present, as in 25/3/77, but no rotors are apparent. The wave seems to be just below the rotor forming amplitude.

A disturbance of wave 2.

12/11/76 - See figure 6.1.

This, one of the best developed rotors in the study, has already been displayed in section 6.13 as figure 6.1. The well developed rotors are present between 40°N and 75°N. Most striking is the sharp cut off in streamline deviations at 40°N which shows much similarity to the fixed boundary conditions of the channel flow of the theory. A northern edge is not apparent.

On this day, a double jet structure is present in the zonal mean with jet maxima located at 35°N and 65°N. So, the real conditions deviate markedly from those of the theory.

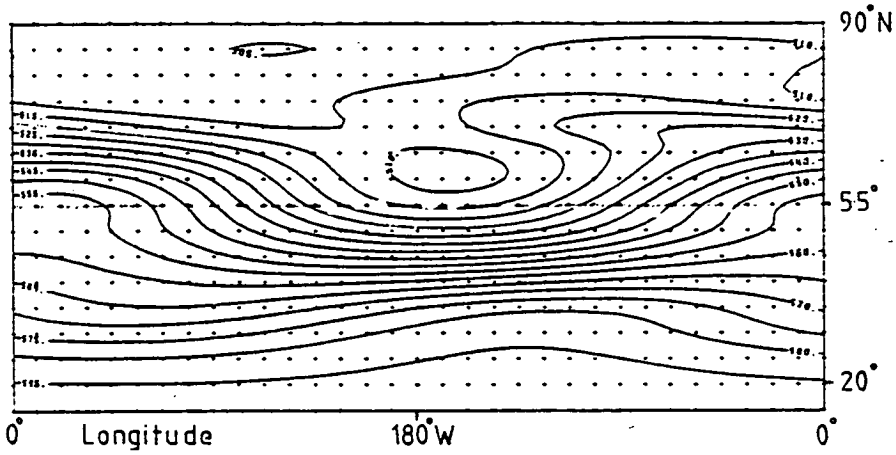

Figure 6.6 Chart of wave 1 plus the zonal mean for 18/11/76. Contours in dcm.

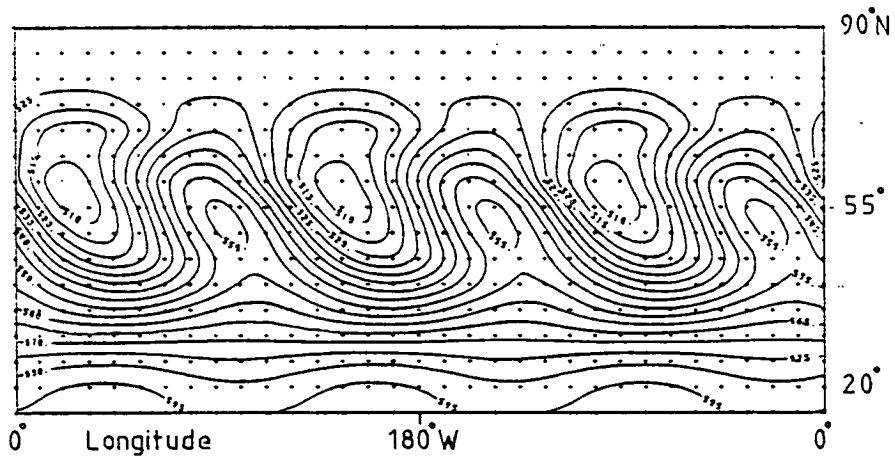

Figure 6.7 Chart of wave 3 plus the zonal mean for 9/1/77. Contours in dcm.

A disturbance of wave 3.

9/1/77 - See figure 6.7

This well developed wave 3 disturbance occurs in very low and deccelerating, mid latitude zonal winds. The wave shows a distinct eastward phase change with latitude, which, from theory, implies a transport of zonal momentum south and a decceleration of the zonal mean wind in the north. Wave 3 is therefore connected with the observed decceleration of the zonal wind in high latitudes occurring on this day.

Events involving wave 4.

29/3/77: 4/4/77: 7/4/77 - See figure 6.8

This series of three charts shows the development of a rotor flow over a period of nine days.

On the chart for 29/3/77, only low amplitude waves are seen and they are not organised, having little latitudinal continuity.

On the chart for 4/4/77, the waves have amplified and become organised with a distinct disturbance band between 40^{o}N and 70^{o}N.

On the chart for 7/4/77, wave 4 has amplified further, and well developed cyclonic rotors are now present. The width of the disturbance, and the strengths of the zonal winds are the same as on 4/4/77. Note again, as for wave 2 on 12/11/76, the similarity of the flow pattern at 40^{o}N to a fixed boundary condition.

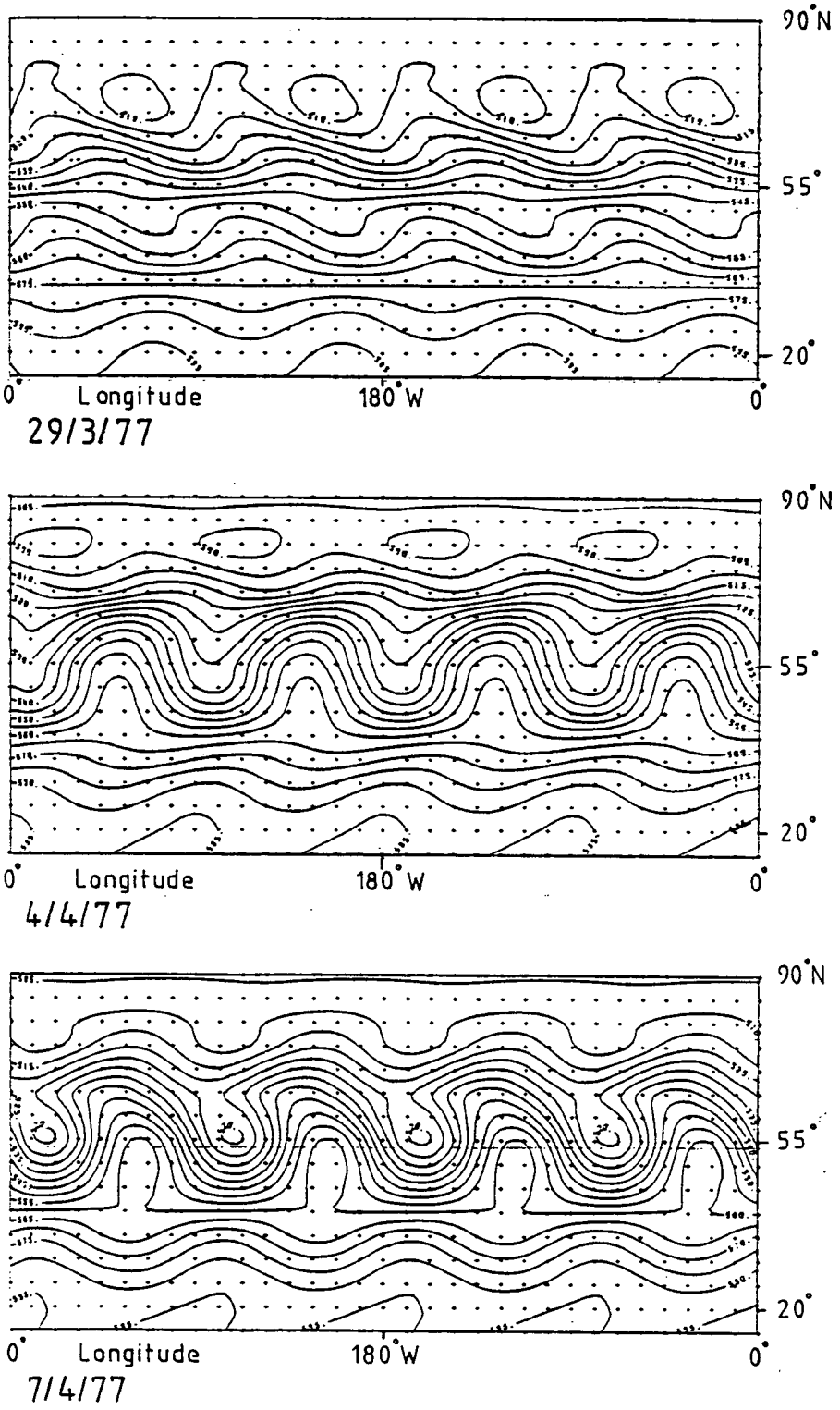

Figure 6.8 Charts of wave 4 plus the zonal mean for the dates shown; the contours are in dcm.

6.3.3 Discussion of the results of the analysis of section 6.3.

This analysis of real data was undertaken to find if rotors occurred in real planetary waves. This objective has been satisfied, i.e. individual waves have been found which display closed streamlines. Thus, wave velocities can become as large as the mean wind velocity and therefore cannot be described by the normal perturbation theory.

Overall, however, cases of rotor behaviour are not common. Of the thirty two days picked out initially for study, only the four presented show distinct rotor flow, while two more show less clear examples. Although this was not an exhaustive search,its results serve to show that rotors both exist and are important in only isolated cases.

The disturbances are found to lie between 40^{o}N and 70^{o}N in all examples, and show a similarity to the pattern of disturbances confined in a channel. The southern boundary, especially, appears to be quite distinct. The wave 4 example in figure 6.8 illustrates this well. However, this apparent boundary may be quite dissimilar in structure to the solid wall of the theory.

6.4 The generalisation of the results of sections 6.2 and 6.3 to describe the blocking events.

The waves in which rotors are seen in the examples of section 6.3.2 are all from blocking events. In only two cases - wave 2 in block A1 and wave 3 in block E5 - is the rotor of the dominant wave visible on the actual chart as the blocking anticyclone. In the other two cases the rotors seen in the examples are not found positioned identically on the actual charts for the day. The actual charts for 9/1/77, 25/3/77 and 7/4/77 are given in figure 6.9 for comparison with the filtered charts presented in section 6.3.2.

Altogether, the simple, single wavenumber rotors investigated in the previous section are not generally applicable to actual blocking events. To be able to give a complete account of blocking, the simple theory of section 6.2,which allows only a uniform zonal current and specifies a rigid walled channel, must be expanded to take into account: -

(1) Changes with latitude of the phases of waves such as occurs with wave 3 on 9/1/77.

(2) Latitudinal structure in the zonal mean wind, e.g. in A1 the wave 2 rotors cannot be addressed by the theory of section 6.2 because the zonal mean wind is not constant with latitude, an extra high latitude jet being present. By equation 6.10, if variations of the zonal mean wind are allowed, then the equation of the motion becomes strongly non-linear. This affects the next condition.

(3) Blocks which are composed of more than one

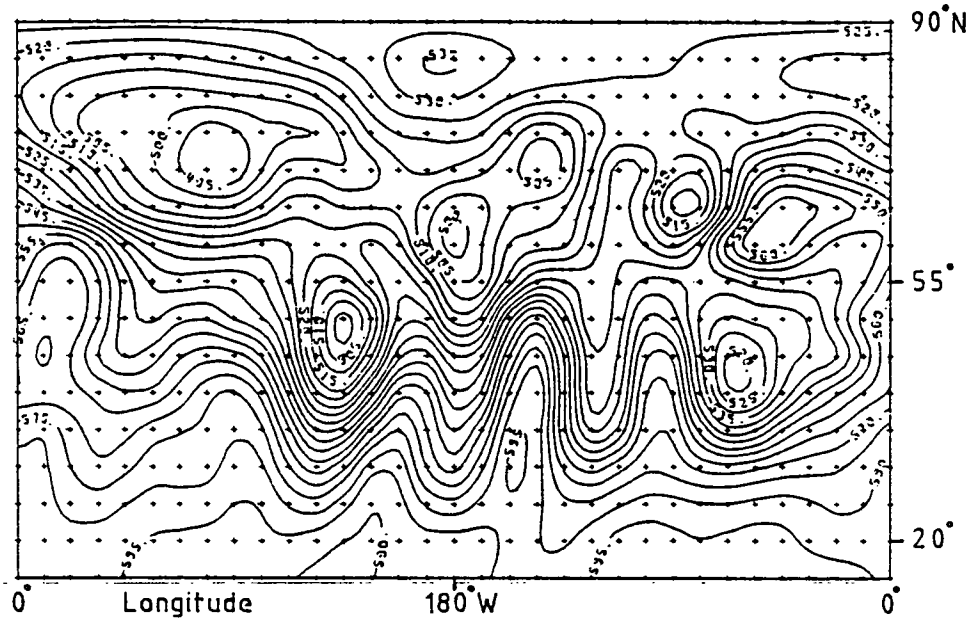

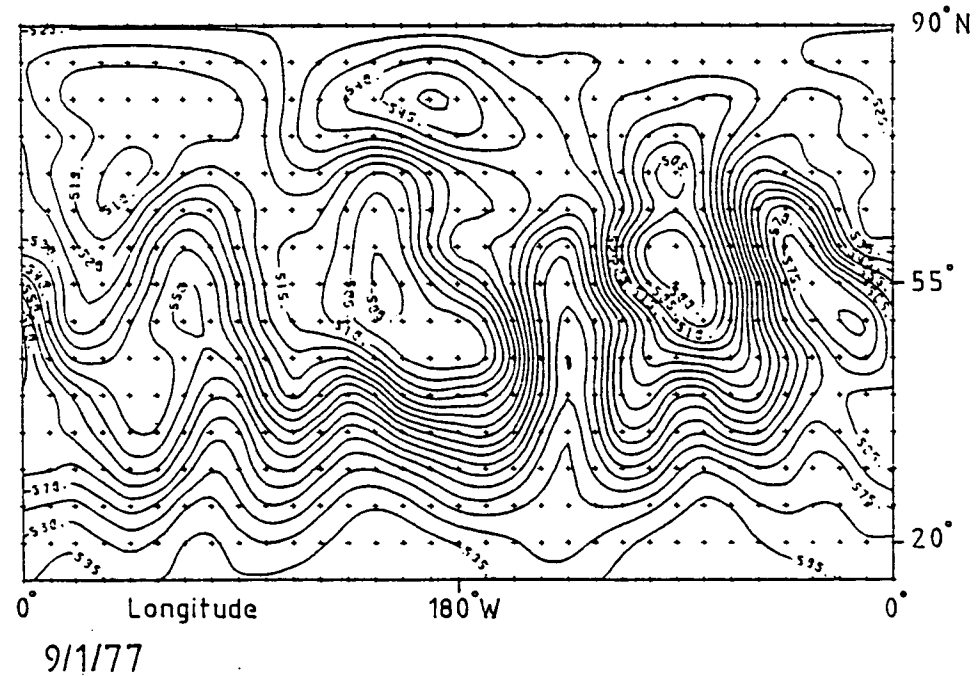

Figure 6.9 Unfiltered 500 mb. charts for 9/1/77 and 25/3/77; contours in dcm.; and 7/4/77, contours in dcm x 10.

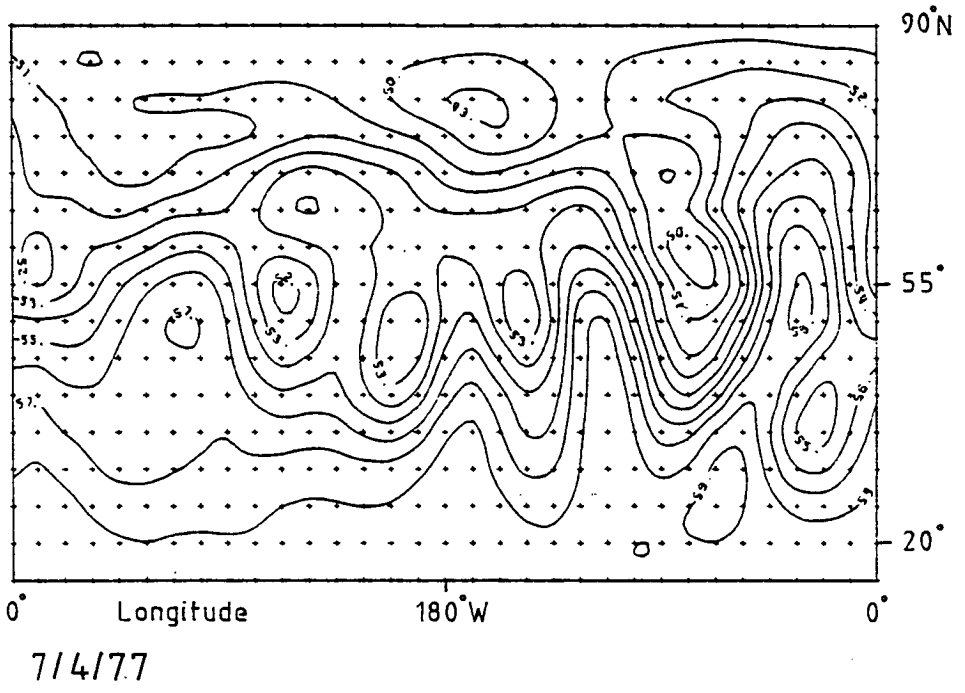

Figure 6.9 continued.

wavenumber. When the actual charts for 25/3/77 and 7/4/77 are compared with the corresponding filtered charts for waves 1 and 4, it is seen that the blocking anticyclone on each actual chart does not match directly with the rotor on the single wave. The shift between the actual blocking anticyclone and the wave rotor arises in each case from the presence of other waves of significant amplitude and different phase. These interfere with the main wave to change the streamline pattern. However, because of condition 2, the theory must be non-linear with the consequence that solutions for discrete wavenumbers are not superposable: the solution in every case must involve all wavenumbers. So, against a fully developed theory, the simple, single wavenumber analysis of section 6.3.2 would not yield results of general applicability.

To sum up, the simple theory of 6.2 has too many limitations to give more than a preliminary description of blocking.

6.5 Conclusions.

In this chapter, the suggestion that Rossby waves can form rotors, and the further suggestion that these rotors can form blocking anticyclones are reviewed.

It is found that individual planetary waves, on occasion, have amplitudes which, in the absence of other waves, will form rotors. The simple Rossby wave theory allows for the possibility of rotor formation, but before any close comparison between theory and real events is attempted, account must be taken of the simplifications of the theory,

viz. the non spherical geometry, the constant zonal wind, the absence of phase velocity and the restriction to a single wavenumber. Some anticyclones in the charts of actual blocks are quite similar in appearance to rotors, but, in other cases, rotors apparent in the dominant wave are not apparent in the actual blocking pattern. Thus, for a proper description of blocking, the effects of all wavenumbers must be taken into account.

CHAPTER 7. CONCLUSIONS.

7.1 Summary of Conclusions.

This study has employed dynamically important parameters in investigating blocking situations identified in an extensive real data set. In particular, three current theories have been examined, viz. Austin's, where blocking is considered to be a superposition of planetary waves; Egger's, where blocking is assumed to be caused by an interaction between planetary waves, and Scorer's where blocking is considered to be a rotor in a planetary wave.

Chapter 3 investigated Austin's theory that blocking is caused by a superposition of waves 1, 2 and 3. There, it is concluded that Austin's suggestions agree with the cases of American blocking in the present data set but not with the cases of European blocking. Generally in this study, waves 3 and 4 play a more prominent role than Austin suggests. Overall, no distinct blocking 'signature' is found. Instead, a variety of wave combinations and histories are found.

In chapter 4, the study of individual wave kinetic energy agrees with Austin's statement that blocking waves are higher in amplitude than normal. However, they are not higher by a large margin. It is found that, generally, the effects of blocking on the kinetic energy are variable, sometimes being large and sometimes not visible. On average, the total eddy kinetic energy varies over the blocking

period in a manner in agreement with the suggestions of Lejenas. Also,this kinetic energy analysis brings out clearly, in agreement with chapter 3, the occasional events where the shorter waves 5 and 6 make important contributions and which are indicative of interaction between the shorter baroclinic waves and the planetary waves.

The kinetic energy analysis shows the low sensitivity of the kinetic energy of the hemisphere as a whole to the effects of blocking. This insensitivity may imply that the blocking phenomenon, as a mechanism, is restricted to higher latitudes, i.e. particularly to north of the sub-tropical jet. By examining only a narrow band of latitudes centred on the blocking area, one could obtain a kinetic energy more sensitive to blocking.

The study of barotropic horizontal non-linear interactions, in chapter 5, suggests that Egger's model of blocking is slightly simple and not entirely general. That is to say that the non-linear interactions do not explain many of the blocks in the study completely. Often they explain single waves while failing to explain the behaviour of other important waves. Foremost among the unexplained is wave 2; wave 2 has a different energy cycle to other planetary waves.

In summing up the study of Egger's model, it appears that many different interaction mechanisms operate during blocking. Again, a variety of blocking histories is present. In some cases an Egger like mechanism is found. In others, different processes occur.

The search for rotor behaviour in planetary waves, in chapter 6, suggests,first, that rotors occur, and second, that rotors occur in association with blocking, but that a more complex rotor theory than the linear derivation presented must be developed to be properly applicable to the real atmosphere. The planetary waves are all found to reach amplitudes which would cause rotors were these waves on their own. However on real charts the superposition of the other wavenumbers present masks the effect to the extent that rotors do not appear often, and seldom as the observed blocking anticyclone.

7.2 Further conclusions.

While the validities of the theories of blocking were being examined, an attempt was also being made to identify a dominant blocking 'signature'. That such a 'signature' was not evident might suggest that blocks are due, not to particular patterns of waves, but to some organising mechanism which can operate within a variety of wave groupings, as, for instance, in depressions, where the organising mechanism is the baroclinic process, which, in the event, produces a disturbance composed of a range of wavenumbers. Related to such a blocking mechanism could be the apparent connection between wave 4's importance and the block's longevity, suggesting that the preferred scale for the 'blocking instability' would be of wavenumber 4. Deciding between the cause of blocking being individual planetary waves, or being a 'blocking instability' must await either the full elucidation of the wave/wave/block

interactions or a successful 'blocking instability' mechanism.

It is also apparent that the current blocking models viz. Egger's, Charney and DeVore's and Tung and Lindzen's are individually too simple in describing only one mechanism each. The real phenomenon probably makes use of all of these mechanisms alternately or even simultaneously. Of course, if blocking is not a planetary wave phenomenon, then no description in terms of harmonically analysed energetics - and mechanisms dealing with individual planetary waves - is going to yield a clear and simple picture.

7.3 Further work.

A major objective of any future study must be the construction of an objective definition of blocking which could then be applied to a larger data set. Such a definition could use, either wave parameters, such as amplitude and phase, or, as in some current studies (e.g. Hartmann and Ghan, 1980), anomalies in the original height field. Investigation of a large data set should yield the full variety of blocking histories and so enable the overall frequency and planetary wave signature of each pattern to be ascertained. Additionally, superpositions of many blocks of similar history should yield more definite conclusions about the energetics and the role of each wave during blocking.

In further studies of the energetics of blocking, a full budget will be required: this must include

the baroclinic conversions and vertical convergences as well as the barotropic conversions. In this respect, wave 2 needs particular study, since it appears to have a different energy cycle to the other waves, and to be important in many blocks.

Noted, in this study, but not explained, is the occasional importance and prominence of the short waves. Further general investigation of the processes involved in the block/baroclinic wave interaction is desirable since important synoptic effects of blocking are due to this effect.

Finally, theories, such as Tung and Lindzen's, and Charney and DeVore's, which have not been dealt with fully here, and Scorer's, which has only been investigated simply, need to be fully studied. It may be that the method Scorer uses to derive rotor theory could be applied to other theories - such as Charney and DeVore's, etc. allowing the analytical solutions to describe high amplitude waves. Where the investigators use numerical methods, of course, high amplitude waves and non-linearity are automatically dealt with.

Appendix 1. THE BLOCKING CATALOGUE.

This appendix lists and describes the blocking events in the period 1/11/76 to 30/4/77. The blocks are selected, according to the definition of blocking described in chapter 2, from the daily 500 mb and surface charts of the European Meteorological Bulletin. The blocks are dealt with in chronological order and each is identified by a reference letter and number; the 'E'group are in the European sector, and the 'A' group in the American sector.

There is an entry for each block. The heading consists of the reference number; the dates of the first and last days of the block, and the characteristic longitude of the anticyclone. Then, there follows a detailed description of the event as observed on the 500mb chart. Finally, there is a table giving the longitude of the main ridges at both 60°N and 45°N. This last is for direct comparison with figures 3.11 to 3.14.

Block E1 13/10/77 - 5/11/76.

This block is discounted in this study because the objective data set does not cover the whole episode. Only a partial description follows.

A very long lived block starting well before the study period, it is centred in high latitudes 70°N . At the opening of the study period, a ridge is present over Europe at 38°E. This dissipates by collapsing south, and brings the block to an end. From the 1st to the 4th, the ridge over Europe is not large, but the main centre of the blocking anticyclone is north at 40°E 70°N. A high latitude jet is present during the block and this returns south after the block ends.

Block A1 10/11/76 - 15/11/76 120°W.

This block is of the usual American ridge type. It starts when, at 120°W, a ridge pushes up strongly and blocks the jet. By the 12th, a small cut off low moves in to the south of the main block and the jet becomes split around the combination of blocking high and cut off low. The main part of the ridge now forms a closed anticyclone centred at 120°W 53°N. The block finishes when the anticyclone, losing its closed circulation, subsides south at 110°W finally becoming too weak.

Phases of the main ridges.

Date	10	11	12	13	14	15
60°N	125°W	120°W	116°W	116°W	120°W	110°W
45°N	118°W	118°W	120°W	120°W	120°W	110°W

Block E2 19/11/76 - 26/11/76 20°W.

This is a very good example of a block. It starts when a strong ridge pushes up over Ireland at 16°W. The northern tip of the ridge dilates and this extends its influence until the 21st; its centre is at 15°W 55°N. From the 22nd until the 26th the ridge is collapsing slowly south. In lower latitudes the ridge moves first a little west then it moves east. In high latitudes, north of 60°N, the top of the ridge moves strongly west. By the 22nd it is at 25°W. Then it returns east so that after the 25th it passes 0°W. The block finishes on the 26th when the ridge becomes too weak.

Phases of the main ridges.

Date	19	20	21	22	23	24	25	26
60°N	10°W	0°	35°W	25°W	20°W	18°W	6°W	5°E
45°N	16°W	15°W	18°W	20°W	20°W	20°W	11°W	4°W

Block A2 26/11/76 - 1/12/76 135°W

This block is of the ridge type. The ridge, pushing up at 135°W on the 26th moves slightly east during its life to be at 125°W on the 1st. The finish comes after the 1st when the peak of the ridge at 50°N collapses allowing the passage of a depression. At lower latitudes, and at the surface, the ridge continues to be present until the 6th. The period from the 1st until the 6th is not considered blocked because depressions are not being brought to a halt by the ridge. This period is described in other chapters as being a 'grey' period.

Phases of the main ridges.

Date	26	27	28	29	30	1
60°N	140°W	135°W	133°W	130°W	135°W	125°W
45°N	138°W	135°W	133°W	133°W	130°W	128°W

Date	2	3	4	5	6
60°N					
45°N	130°W	133°W	140°W	138°W	135°W

Block E3 11/12/76 - 20/12/76 0°E

This is a very large block in the Atlantic sector. It starts when two ridges push up into the jet at 10°W and at 50°E. These ridges join at 0°W 70°N. On the first day the most prominent feature is a very large cut off low centred at 20°E 58°N and covering most of western Europe. From the 11th to the 13th, the western ridge developes strongly. A closed anti-cyclone appears on the 13th at 30°E 70°N. On the 14th, the eastern ridge becomes the stronger. On the 15th, the cut off low moves south and east, the flanking ridges then becoming broader. On the 16th, 17th and 18th the block becomes symmetric in type, the anti-cyclone being at 20°E 70°N and the cut off low being at 10°E and south of the anticyclone; the jet splits to the west of and flows to north and south of the block. On the 19th and 20th the high latitude anticyclone again breaks into eastern and western ridges at 20°W and 40°E. The central cut off low moves north and fills. This block ends on the 20th when a new block E4 takes over. E4 originates as an amplification of the western ridge in the Atlantic. The eastern ridge becomes weak and no longer supports a surface anticyclone.

Phases of the main ridges.

Date	11		12		13		14	
60°N	17°W	55°E	7°W	55°E	5°W	55°E	5°W	50°E
45°N	15°W	75°E	8°W	70°E	7°W	50°E	5°W	50°E

Phases..... contd.

Date	15		16		17		18	
60°N	10°W	48°E	15°W	50°E		50°E		50°E
45°N	10°W	55°E	10°W	60°E		60°E	40°W	

Date	19		20	
60°N	30°W	45°E	20°W	40°E
45°N	33°W	33°E	20°W	30°E

Block E4 22/12/76 - 30/12/77 30°W

This block starts as the development of the ridge remaining in the Atlantic from block E3. The ridge, at 20°W on the 20th, cuts off to form a closed anticyclone over Iceland on the 21st. This amplifies until on the 22nd blocking is considered to have started. From the 22nd to the 26th the anticyclone expands south and east becoming a strong ridge. This ridge retrogresses to 50°W by the 30th though the portion of the ridge north of 60°N moves much more swiftly west reaching 65°W by then, carrying the centre of the anticyclone into northern Canada and therefore to the north of the cut off low centred over the U.S.A. at 92°W 48°N. Blocking finishes on the 30th by which date the ridge in the Atlantic has become too weak. The anticyclone has moved to 70°N, away from the normal depression tracks and is still moving swiftly west. After the 30th, the anticyclone continues westwards, finally passing into western America before dissipating

Phases of the main ridges.

Date	22	23	24	25	26
60°N	10°E	0°	6°W	15°W	15°W
45°N	20°E	20°E	5°E	8°E	15°W

Date	27	28	29	30
60°N	35°W	40°W	48°W	50°W
45°N	10°W	30°W	35°W	45°W

Block E4A 27/12/76 - 31/12/76 75°E.

This has the appearance of a ridge incidental to E4 and starts when a ridge, already present, pushes further north into the jet extending the Siberian anticyclone westwards. The blocking ridge is centred at 80°E 65°N. The block ends when the ridge, south of 60°N, moves swiftly west to become another European block at 40°E on the 31st.

Phases of the main ridges.

Date	27	28	29	30	31
60°N	72°E	78°E	80°E	70°E	73°E
45°N	73°E	75°E	60°E	55°E	43°E

Block E4B 31/12/76 - 7/1/77 40°E

This block forms from the westward moving ridge remaining at the conclusion of block E4A. This ridge moves westwards throughout the period. The block starts on the 31st when the ridge is 50°E and ends on the 7th when the ridge is at 10°W. This is a different block to E4A because it forms a new closed anticyclonic centre which takes over from the ridge of E4A when that decays. The block is of the omega type but the jet is not evenly split to north and south: the stronger jet passes to the north of the block over Scandinavia. The effect of this is not to hinder the passage of depressions westwards but to cause them to travel further north than is normal. The block finishes when the ridge decays southwards. The western part of E4B enlarges on the 7th to become E5.

Phases of the main ridges.

Date	31	1	2	3		4	
60°W	73°E	52°E	45°E		40°E	0°W	30°E
45°W	43°E	40°E	25°E	20°W	25°E	15°W	22°E

Date	5		6		7		
60°W		25°E		30°E	20°W	45°E	
45°W	12°W	20°E	12°W	20°E		5°E	

Block E5 7/1/77 - 14/1/77 40°W

This block begins as an amplification of the western ridge of E4B. On the 7th a closed anticyclone is formed with its centre at 15°W 50°N. On the 9th, however, the centre shifts to 35°W due to the growth of a strong ridge at this longitude. The ridge continues to grow until the tip reaches the pole creating an anticyclone there. It also retrogresses slightly to be along 40°W. This block coincides with a major stratospheric warming of which the anticyclone and easterly winds at the pole are a consequence (O'Neil and Taylor 1979). The block finishes when the ridge becomes too thin and weak, and, in mid latitudes, the connection with the polar anticyclone breaks and depressions push the surface ridge aside.

Phases of main ridges.

Date	7	8	9	10
60°N	20°W	12°W	40°W	37°W
45°N	12°W	10°W	25°W	30°W

Date				
60°N	40°W	43°W	45°W	45°W
45°N	33°W	33°W	38°W	30°W

Block A3 4/1/77 - 16/1/77 135°W

This block starts on the 4th with a ridge at 140°W pushing into the jet and disrupting the zonal regeme. The ridge maintains a position close to 135°W until the 14th when it starts to move east, reaching 120°W on the 16th. Like E5 the ridge extends to the pole. By the 16th the connection with the pole becomes very weak and, by the 17th, the blocking is finished. A depression moves through the area on the 18th. Prominent throughout the block is a deep cut off low over middle and eastern America.

Phases of main ridges.

Date	4	5	6	7	8
60°N	140°W	133°W	130°W	145°W	135°W
45°N	142°W	135°W	134°W	133°W	135°W

Date	9	10	11	12
60°N	140°W	145°W	140°W	145°W
45°N	133°W	130°W	128°W	140°W

Date	13	14	15	16
60°N	145°W	140°W	133°W	130°W
45°N	130°W	127°W	125°W	125°W

Block E5A 13/1/77 - 19/1/77 30°E

This an omega type block which appears as a growing ridge at 40°E on the 13th. By the 17th the ridge has retrogressed a little to 30°E and extended its influence to the north. The block finishes when the cut off low to the west moves east and undercuts the ridge which then steadily collapses.

Phases of the main ridges.

Date	13	14	15	16	17	18	19
60°N	40°E	38°E	35°E	35°E	27°E	25°E	25°E
45°N	37°E	36°E	38°E	30°E	30°E	5°W	5°E

Block A4 23/1/77 - 30/1/77 130°W

This block appears when an anticyclone at 135°W develops into a strong ridge including a closed contour. After the 27th the part of the ridge north of 60°N moves west whereas the part near 45°N moves east. This movement continues until, on the 29th, the ridge is lying from 145°W 60°N to 125°W 45°N. The block ends when the ridge collapses.

Connected with block A4 there is a secondary 'grey' period from 3/2/77 to 7/2/77 which is too short lived to be a block in its own right. It occurs as a rebuilding of the remnants of the ridge of A4 at 123°W until, on 3/2/77, the westerlies are again disrupted. The ridge slowly decays from then until the 7th. On the 8th the mid-latitude portion of the ridge moves east ending the episode.

Phases of the main ridges.

Date	23	24	25	26	27	28
60°N	135°W	138°W	138°W	135°W	140°W	150°W
45°N	133°W	133°W	134°W	133°W	133°W	128°W

Date	29	30	31	1	2	3
60°N	147°W	130°W	130°W	120°W	135°W	125°W
45°N	128°W	124°W	120°W	140°W	130°W	123°W

Date	4	5	6	7
60°N	130°W	120°W	120°W	127°W
45°N	115°W	115°W	123°W	120°W

Block E6 22/2/77 - 2/3/77 20°W

Prior to this block there is a large area over Scandenavia, Iceland and the eastern Atlantic of slack gradients in the height field with the jet stream passing to the south of the British Isles. On the day before a weak jet is established which branches from the main jet over Newfoundland and travels north over Greenland and thence directly into Siberia. The block starts on the 22nd when the main jet ridges at 40°W. This ridge then progresses and amplifies until a large anticyclone becomes established over Iceland at 20°W 67°N on the 24th. The associated ridge to the south becomes established over the U.K. The block finishes when the system decays, subsiding south.

Phases of the main ridges.

Date	22	23	24	25	26
60°N	35°W	30°W	20°W	18°W	15°W
45°N	42°W	33°W	25°W	15°W	10°W

Date	27	28	1	2
60°N	10°W	7°W	7°W	5°W
45°N	3°W	1°W	7°W	5°W

Block E7 11/3/77 - 20/3/77 40°E

This is not a strong block and it is situated further south than is normal. It does split the jet but all depressions follow the northern part of the jet over Scandinavia. The block starts as a ridge over the Mediterranian centred at 20°E 50°N, which, on the 11th, extends its influence northwards. The block takes a symmetrical pattern when the anticyclone progresses to 45°E 50°N by the 17th and develops a closed circulation. On the 18th it weakens becoming a mere ridge on the eastern flank of the cut off low centred at 33°E 38°N. The block finishes on the 20th as the system weakens. On the 21st a new ridge builds in the Atlantic to form another block there.

Phases of the main ridges.

Date	11	12	13	14	15	16	
60°N	30°E	27°E	33°E	45°E	35°E	40°E	
45°N	15°E	22°E	30°E	40°E	35°E	7°E	60°E

Date	17		18		19	20
60°N	30°E		40°E		40°E	45°E
45°N	10°E	50°E	17°E	55°E	58°E	68°E

Block E8 21/3/77 - 26/3/77 20°W

This block starts as a ridge in the Atlantic at 25°W which moves to be at 20°W on the 22nd and amplifies to form an anticyclone north of 60°N. To the south, a cut off low is present at 5°W 48°N. The high latitude anticyclone continues to move east but the cut off low retrogresses a little as a ridge builds at 15°E connecting with the anticyclone on the 23rd and 24th. On the 25th the anticyclone, now at 65°N, moves west to 45°W while the ridge over Europe weakens. On the 26th the high latitude anticyclone weakens leaving only a ridge lying between 15°E 45°N and 40°W 65°N. On the 27th the ridging over Europe is no more, while the anticyclone at 65°N realigns north/south in the Atlantic at 25°W. The block finishes on the 26th with the decay of the European ridge. However, the ridge at 25°W strengthens and, though slow moving, crosses into Europe over the next four days. This ridge is considered too short lived to be called a block.

Phases of the main ridges.

Date	21	22	23	24	25
60°N	22°W	18°W	0°W	15°E	18°E
45°N	28°W	25°W	20°E	15°E	20°E

Date	26	27	28	29	30
60°N	20°W	25°W	25°W	18°W	0°W
45°N	15°E	25°W	30°W	25°W	20°W

Block A5 30/3/77 - 7/4/77 135°W

This is a ridge type block which starts at 145°W by amplifying and extending northwards. It then moves slowly east to be at 120°W on the 7th. After the 7th the ridge persists, continuing to move east, but blocking is considered finished because the surface anticyclone is pushed aside on the 7th by an oncoming depression. The ridge finally subsides on the 10th.

Phases of the main ridges.

Date	30	31	1	2	3	4
60°N	140°W	145°W	150°W	140°W	135°W	135°W
45°N	150°W	145°W	145°W	140°W	135°W	133°W

Date	5	6	7	8	9	10
60°N	128°W	128°W	123°W	115°W	107°W	95°W
45°N	128°W	123°W	123°W	113°W	104°W	97°W

Block E9 2/4/77 - 9/4/77 30°W

This block starts as an amplifying ridge at 40°W with a corresponding surface anticyclone. The ridge continues to grow, forming into an omega type block by the 4th with the anticyclone centred at 30°W 50°N. The anticyclone continues to spread north and west and, from the 6th to the 8th, the portion north of 60°N moves east while the main anticyclone moves west resulting, by the 8th, in a long ridge extending from the centre at 33°W 47°N to the tip at 25°W 70°N. On the 9th the system weakens and the anticyclonic centre is lost. The block finishes then because the ridge north of 55°N moves off east, but a deep trough remains at 10°E. More ridging takes place later on either side of this trough leading eventually to further blocking.

Phases of the main ridges.

Date	2	3	4	5	6
60°N	40°W	33°W	22°W	20°W	33°W
45°N	42°W	36°W	30°W	25°W	25°W

Date	7	8	9
60°N	30°W	24°W	17°W
45°N	47°W	36°W	35°W

Block E10 11/4/77 - 16/4/77 55°E

During the period 9/4/77 to 11/4/77 ridging takes place in the Atlantic at 30°W 40°N and over Europe at 40°E. These flank a deep cut off low at 10°E. The eastern ridge amplifies more than does the Atlantic ridge to become, on the 11th, a block of an omega pattern with the anticyclone centred on 35°W 65°N. The anticyclone then moves steadily east, passing to the north of the eastern cut off low present at 55°E 55°N and finishes as a decaying ridge at 80°E on the 16th. After this the ridge moves further east and declines, but, since it is not in an area where it can disrupt the depression tracks, it is not considered to be a block at this stage.

Phases of the main ridges.

Date	11	12	13	14	15	16
60°N	35°E	35°E	35°E	72°E	78°E	85°E
45°N	40°E	40°E	80°E	75°E	75°E	75°E

Block E11 21/4/77 - 29/4/77 70°E.

This block starts on the 21st when a ridge, which had been moving east, amplifies. On the 24th the block develops into the symmetrical type with the anticyclone centred at 75°E 55°N. It remains in this position until the 26th before retrogressing to 63°E where it remains until the 29th. This block finishes on the 29th but a new ridge builds up at 35°E, which, on the 30th, takes over causing another block. However, this new block lasts beyond the period covered by the objective data set and is not considered further.

Phases of the main ridges.

Date	21	22	23	24	25
60°N	65°E	73°E	80°E	75°E	80°E
45°N	65°E	70°E	70°E	65°E	60°E

Date	26	27	28	29
60°N	57°E	62°E	65°E	60°E
45°N	65°E	65°E	60°E	35°E

Appendix 2 THE DETAILED WAVE HISTORY OF EACH BLOCK.

This appendix contains the detailed history for each block and is the data from which the results in chapter 3 are produced. The method of compilation is described in chapter 3 and involves comparing the amplitude and phase behaviour of each wave with the observed behaviour of the blocking anticyclone. The descriptions use the data presented in figures 3.1 to 3.14.

After each description, those waves which are considered most important over the period of the block are listed. This gives the wave combination that is thought to cause the block. The phases of the waves at $60^{\circ}N$ and $45^{\circ}N$ can be directly compared with the phases of the main ridges given in appendix 1.

Block A1 10/11/76 - 15/11/76

As the period of the block approaches wave 1 moves into a minimum of amplitude leaving a strong wave 2 whose phase puts a ridge of wave 2 over the blocking area. Also, early in the week before, wave 3 is weak and mobile, but a few days before the block starts becomes stationary at 60°N with a phase of 120°E. Blocking starts when, at 45°N, the weak and moving wave 3 aligns north/south and in phase with itself at 60°N and amplifies at 50°N. On the first day of the block, wave 4, which had been moving east at 60°N, also comes into phase with itself at 45°N and into phase with waves 3 and 2. At 45°N wave 4 is as high in amplitude as wave 3.

During the block, wave 4 at 60°N moves west but waves 3 and 2 remain stationary.

The block finishes when the amplitude of wave 4 at 50°N falls, wave 4 moves away from close coincidence with 2 and 3 at 60°N, wave 1 amplifies and wave 2 decays in mid-latitudes.

The conclusion is that this block is caused by wave 3 superposing on wave 2 and on wave 4. The block appears to start when mobile waves line up so that their ridge lies north and south. The block ends when amplitudes fall and the waves move away from coincidence.

A double jet lasts throughout this block decaying at the finish, the second jet lying near 70°N. To the south, on the first two days, easterlies are present.

The important waves for block A1 are - 2,3,4.

Block E2 19/11/76 - 26/11/76.

The block appears while wave 1 is strong and wave 2 is weak. Wave 1 moves swiftly west at latitudes north of 60°N during the first half of the period. Afterwards, the amplitude falls and wave 1 moves swiftly east. At 55°N wave 1 has a phase close to 0°E. The block starts when wave 4, earlier at 60°N and moving east, comes into the same phase as itself at 45°N and amplifies. Wave 3 is in phase with wave 4 and amplifies during the block. The block finishes when the high amplitude of wave 4 decays and the wave moves away from the blocking area.

Additionally, late in the period, wave 2 amplifies and, with the support of wave 3 in the American sector, leads to block A2 which starts on the 26th.

In the first half of this block, a double jet is formed with a brief easterly between the northern jet at 65°N and the subtropical jet which shows an acceleration at this time. The double jet breaks down in the second half.

The important waves for block E2 are - 4, 3, 1

Block A2 26/11/76 - 1/12/76.

A2 follows immediately after E2. E2 is caused by a strong wave 4 supported in the closing stages by wave 3. During these closing stages wave 2 amplifies north of 50°N and it is the combination of wave 2 with wave 3 - wave 3 being most important south of 50°N - that supports A2. However, the block only appears when wave 4 collapses, for the phase of wave 4 at 60°N is such as to produce a masking trough at the longitudes of A2 as long as wave 4 remains strong during E2. The phases of waves 2 and 3 are both slightly west of the blocking ridge throughout. The most striking components of the block are waves 5 and 6. They display, for them, very large amplitudes during the block (10 decametres). They are also slow moving and in phase with the observed ridge. Wave 5 extends further north than wave 6.

In the first half of the block a double jet is formed which breaks down again in the second half. During the second half the subtropical jet becomes very broad. In the 'grey' period after the end of A2 the northern jet forms again and there is deceleration evident south of this at 55°N.

The important waves for block A2 are - 2, 3, 5, 6

Block E3 11/12/76 - 20/12/76

This block starts when wave 1 comes into phase with wave 2 in the region between 65°N and 70°N, and both amplify strongly. Wave 1 continues to move steadily west throughout the block, though this wave is of importance only in latitudes north of 60°N. In the southern area, below 65°N, the block is caused by a combination of waves 4 and 2, with the assistance of wave 3. In these latitudes, the block has the form of two ridges, the western being supported by wave 4 with wave 3 in phase whilst the eastern consists of waves 4 and 2.

The zonal wind shows no northern jet in this block. In the second half, easterly winds develop at 67°N.

The important waves for block E3 are - 1,2,4.

Block E4 22/12/76 - 30/12/76.

This block appears to be caused by a very strong amplification of wave 3, which slowly retrogresses during the period. In latitudes north of 60°N, wave 2 is also very strong, and it retrogresses across the ridge of wave 3. During the last two days, when wave 3 is decaying, it is the ridge of wave 2 that is responsible for carrying the high latitude anticyclone swiftly west. Wave 1 too is strong in very high latitudes but it has phases which, being east of 0°, are such that wave 1 does not affect the block by the addition to it of either peak or trough.

In the first third of E4, a northern jet is present at 80°N with easterlies to the south. In the second third this northern limb of a double jet decays and easterlies move south from the pole. In the final third the double jet reforms at 80°N and moves south, ending at 70°N with strong easterlies to the south.

The important waves for block E4 are - 3, 2.

Block E4A 27/12/76 - 31/12/76.

This ridge at 80°E appears during E4 and is in phase with a ridge of wave 3 which is of high amplitude at this time. It appears independently on the 27th as a rapidly moving wave 2 at 60°N and moves into phase with wave 3. Waves 3 and 2 also move into phase with wave 4 at 60°N. The block finishes when wave 3 decays and the swiftly moving wave 2 carries the ridge east to become block E4B

A marked double jet is present throughout this block with strong easterlies present at 58°N.

The important waves for block E4A are - 3, 2.

Block E4B 31/12/76 - 7/1/77.

This block occurs in a period of low amplitudes of both waves 3 and 4. Following directly upon the previous block, it starts when waves 3 and 4 die away and wave 2 amplifies at all latitudes from 40°N to 80°N. Wave 2 reaches high amplitude during this block, the peak being in the band between 60°N and 70°N. As for phase, wave 2 at 45°N is stationary at 40°E, whereas at 60°N it retrogresses from 75°E at the start to 30°E at the close. The second component of this block appears on the 2nd when wave 1 starts to amplify around 50°N. It continues to strengthen throughout the remaining period and achieves its highest amplitude of 27 decametres on the final day. Wave 1 at 45°N retrogresses from 10°E to 20°W and, like wave 2, it retrogresses around 60°N, being slightly west of wave 2. The block ends when wave 2 decays and waves 3 and 4 amplify to cause the next block, E5. Note that the very large amplitudesof wave 1 merely appear to have the effect of displacing the jet north over a wide band of longitude.

A distinct double jet with the northern portion at 70°N is present at the start. During the block, this moves south and merges with the subtropical jet.

The important waves for block E4B are - 2, 1.

Block E5 7/1/77 - 14/1/77.

This block has similarities to block E4, the main wave being a high amplitude wave 3 which again extends north to the pole. However, in this block, wave 4 plays a stronger role than in E4. Before the block, the phase of wave 3 is east of the phase of wave 4. At the onset of blocking, wave 3 moves to the longitude of the blocking ridge and amplifies strongly. Wave 4 remains stationary throughout, being in phase with wave 3 over the blocking ridge. The block ends when wave 3 decays and its phase moves abruptly away from coincidence with wave 4.

Easterly winds become established at all latitudes down to 55°N during this block. No double jet is formed.

The important waves for block E5 are - 3, 4.

Block A3 4/1/77 - 16/1/77.

This block is contemporaneous with parts of E4B, E5 and E5A. It appears when a high latitude, high amplitude, retrogressive wave 2 moves into phase with, and to the north of, a moderate and stationary wave 3. This happens immediately after the amplitude of wave 1 above 60°N falls. In mid-latitudes, wave 1 continues strong. However, the phase being around 0°, wave 1 is near zero at the blocking longitude and does not affect the height field substantially.

On the 7th, wave 3 at 60°N moves a little west and into phase with the blocking ridge. With a subsequent strong amplification, wave 3 becomes dominant over wave 2. Wave 4, which is earlier very low in amplitude, now amplifies. It is most closely in phase with wave 3 over the Atlantic ridge of E5 at 60°N, and it is most closely in phase with wave 3 over A3 at 45°N. It therefore aids the maintainance of both blocks and the large and deep cut off low over the U.S.A.

On the 14th, in higher latitudes, wave 3 decays leaving wave 4 as the principle blocking wave at 60°N. On the last day of the block wave 4 at 60°N decays and its phase begins to progress eastwards. These breakdowns of waves 3 and 4 at 60°N remove the northerly portion of the blocking ridge allowing depressions to pass, and thus end the block. At lower latitudes, waves 3 and 4 remain stationary in the blocking area, but, being south of the main jet, they have little influence.

On the first few days the double jet of E4B merges with the subtropical jet. Thereafter easterly winds are established down to 55°N. These return north at the close of the block.

The important waves for block A3 are - 3, 4.

Block E5A 13/1/77 - 19/1/77.

In the area north of 55°N, the block starts when the very strong wave 3 decays leaving a stationary wave 4 whose phase is 40°E. This wave 4 remains in position until the 16th when it decays. Its place as the blocking agent is taken by a newly amplified wave 3 whose phase is 20°E. Hence the blocking ridge is seen to retrogress as the wave 4 ridge gives way to the wave 3 ridge. The block ends on the 19th when wave 3 decays.

South of 55°N, waves 3 and 4 are out of phase with the block: wave 3 lies 40° to the west and wave 4 lies 30° to the east. The southern portion of the block is produced by wave 6 in the first half and wave 5 in the second half of the period. Both waves progress slowly, with wave 5 taking over in importance when wave 6 moves too far east. Note that the zonal mean wind is very low throughout the block.

Block E5A starts with strong easterlies as far south as 55°N. These return north at the close.

The important waves for block E5A are - 3,4,5,6.

Block A4 23/1/77 - 30/1/77.

This block occurs during a period when wave 1 has low amplitudes everywhere and when wave 2 has a long living maximum of amplitude in mid-latitudes. The block starts when a strong and westerly moving wave 3, at 60°N, moves into phase with the ridge of wave 2 over the blocking longitude. Wave 5 then amplifies, achieving amplitudes of 12 decametres. It progresses slowly east from 144°W to 114°W when, on the 30th, it decays. Wave 4 is in phase with the established block when,on the second day of blocking, it amplifies and becomes stationary. During the earlier part of the block the strong wave 3 together with the wave 2 moves west in northern latitudes pulling the ridge west. However, when wave 3 decays later, the ridge returns east to be in phase with the stationary wave 4. The block ends when wave 5 decays and wave 3 moves out of phase at 60°N.

The secondary period of A4, the 'grey' period - from 3/2/77 - 7/2/77 - is caused by wave 3, which, having moved out of phase with wave 2 on decaying earlier in the block, now comes into phase with wave 4 and amplifies once more. This episode ends when wave 4 decays and moves away and wave 3 decays at 60°N.

Easterlies are present around 75°N throughout A4. Otherwise the zonal wind is weak. In the 'grey' period a double jet is formed with the northern jet at 83°N.

The important waves for block A4 are - 2,3,4,5.

Block E6 22/2/77 - 2/3/77

This block occurs during a large amplitude pulse of wave 1 which has its peak at 60°N. Before blocking commences, wave 1 is mobile, but where it amplifies it becomes slow moving and in phase with the block. At the outset, wave 2 is high in amplitude. However, it decays in the first few days and in any case its phase is 60°E of the block. The block is initiated by amplitude pulses in waves 3 and 4. Wave 3 is in phase with the block at 45°N and 60°N, but wave 4 is only in phase at 60°N. They both decay in amplitude to moderate levels after the first day, but remain in phase with the block throughout. The main observed ridge has a large wave 6 component, and the phase of this wave matches the observed progression of the ridge. Figures 3.13 and 3.14 show that wave 6 is most probably due to the strong trough lying immediately to the west of the block. The block ends when waves 1 and 6 decay.

This block starts with light eastery winds at 60°N. These return to light westerlies before the end.

The important waves for block E6 are - 1,5,4,6.

Block E7 11/3/77 - 20/3/77.

This block is initiated in a minimum of wave 1. It begins as a ridge of an easterly moving wave 4 crosses a ridge of a westerly moving wave 2 at 60°N, the longitude of the block. Wave 4 has a continuous period of eastward progression beginning many weeks prior to this block and continuing throughout the block. This progressive wave 4 carries the anticyclone east. Also, before blocking commences, wave 2 moves west to the blocking longitude and amplifies. As the block commences wave 3 decays. During the block wave 2 continues to retrogress slowly. Both waves 2 and 4 have their amplitude peaks at 55°N. Farther north the moderate wave 3 is in phase with the stronger wave 4. The block ends when wave 2 and wave 4 decay in mid-latitudes, and wave 1 amplifies to reach high amplitudes in the 60° to 65°N band.

The zonal wind shows no special behaviour during this block.

The important waves for block E7 are - 2,4.

Block E8 21/3/77 - 26/3/77.

The ridge which builds up to start this block is caused by a brief amplification of waves 3 and 4 on the 19th. Wave 3 peaks at 40° - 45°N to the south of wave 4 which peaks between 45° and 60°N. At this time the peaks of waves 4 and 3 are progressing and close to each other over the Atlantic. When amplification occurs, wave 3 stops at 35°W and comes into phase with wave 4. Subsequently, as waves 4 and 3 of the initial period decay on the 22nd a wave 3 amplifies instead in the band 60 - 65°N with phases which match the eastward movment of the observed anticyclone. This continues until the 24th when wave 3 decays to low amplitudes. During this block, wave 1 experiences high amplitudes with maxima in the latitudes 55° to 70°N while wave 2 has moderate amplitudes peaking in the 60 to 70°N band. Both retrogress through the blocking area, wave 2 being about 15°west of wave 1. However, on the 25th, wave 2 moves more swiftly west taking over the blocking anticyclone from wave 3 and carrying it farther west. On this same day wave 1 passes 0°E, and, on the 24th and 25th, its phase matches the observed ridge which appears at 15°E. In high latitudes waves 2 and 1 remain strong and become nearly stationary with phases around 40°W after the 26th. There is no clear end to this block. In the disturbed period after the 26th, the slow moving ridge is matched by a wave 6.

The zonal wind shows no particular behaviour in this block. At the end there is a general acceleration at all latitudes up to 70°N.

The important waves in block E8 are - 1, 2, 3.

Block A5 30/3/77 - 7/4/77.

This block starts as the amplitudes of wave 1 are falling to low low levels. Wave 2 subsequently amplifies in mid-latitudes with phases coincident with the block. The main component of the block is a strongly amplifying wave 4 which reaches an amplitude of 15 decametres in the latitude band between 55° and 60°N. The amplification starts on the 1st. This main component progresses slowly throughout the block, its phase being over the observed ridge. Throughout, wave 2 in latitudes below 55°N is in phase with wave 4. Wave 2 decays on the 6th but, in phase with wave 4, its place is taken by wave 3 which amplifies briefly. However, wave 3 at 60°N is eastward moving and moves out of coincidence with wave 4 with the result that the ridge caused by the superposition falls in amplitude and moves east and the block ends.

During A5 a strong double jet is present. The northern jet starts at 60°N and moves north to end at 70°N by the end of the block.

The important waves for block A5 are - 4, 3, 2.

Block E9 2/4/77 - 9/4/77.

This block is caused by an amplification of wave 4 to very high amplitudes - the highest in this study. Wave 2 is of moderate amplitude but its phase at 45°N is such as to give reinforcement with wave 4 over the American block A5, and correspondingly a trough of wave 2 in the Atlantic area. At 60°N and above, wave 2 is low in amplitude but nearly in phase with the block. Wave 3 has some moderate amplitude pulses during the block which are in phase with wave 4 in the Atlantic. On the 7th, however, wave 3 at 60°N moves east swiftly. This, coupled with the decays of waves 4 and 2, causes the end of the block.

The double jet established in the first days of A5 is present throughout E5. The northern jet moves north throughout the block, ending at 70°N.

The important waves for block E9 are - 4, 3.

Block E10 11/4/77 - 16/4/77.

In this block all the wave events happen at or north of 60°N. The block is mainly a wave 3 feature which appears on the 11th when wave 3 amplifies as it moves swiftly east. Wave 2 amplifies, in high latitudes, during the block and parallels wave 3's eastward movement but its phase lies east of wave 3 by 15°. Wave 2 becomes more prominent towards the end but the block finishes when wave 3 decays. At the end of the block a minor supporting wave 4 also decays.

A strong double jet is present during E10. The northern jet is centred on 70°N.

The important waves for block E10 are - 3, 2.

Block E11 21/4/77 - 29/4/77.

The wave events of this block occur north of mid-latitudes, the principle component being a high amplitude wave 2 between 50°and 70°N. At the start of the block wave 3 amplifies and has a phase 25° east of wave 2. After the start wave 4 also amplifies and is in phase with wave 2. Wave 3 decays on the 26th and then moves west, phasing in with the block and reamplifying. In the first half of the blocking period wave 1 is low but it amplifies and moves west to reach the blocking longitude on the 28th at which time the block is seen to broaden. The block weakens as waves 2 and 4 decay on the last day though wave 1 remains.

Since the data set for this analysis finishes at this date, the exact ending of the block is unclear.

The zonal wind during E10 shows two periods of weak double jets - at the beginning and at the end of the block.

The important waves for block E11 are - 2,4,3.

APPENDIX 3. THE KINETIC ENERGY HISTORY OF EACH BLOCK.

This appendix outlines the important kinetic energy events associated with each block. The method of compiling the histories and assessing importance is described in chapter 4. The events of importance are listed twice at the end of each history. They are ranked in order of assessed importance in the first list and in order of decreasing energy in the second.

Blocks E4A and A3 are not described separately; they occur simultaneously with E4 and E5 respectively and are described with them. Blocks A5 and E9 are also described together because they are simultaneous.

Block A1.

Wave 2, which strengthens for a week before the block starts, comes to a strong maximum during the block. Wave 3 is much weaker beginning to amplify only one day before the start yet reaching a peak at the same time as wave 2. Wave 4 does not show much significant activity but tends to move through a minimum. Waves 5 and 6 are low during the block though both amplify strongly through the last day to peak immediately after the block finishes.

The events in order.

Subjective importance	Decreasing energy
Wave 2 peak, wave 3 peak, wave 5 and wave 6 peaks following the end.	2, 3 and at the end 6,5 .

Block E2.

The most important event in this period is the very high maximum of wave 4; no other wave peak is as high in this block. Wave 1 is moderate in the early part but falls abruptly to a minimum in the middle of the period whereas wave 3 does the opposite. It amplifies from a low value exactly as wave 1 decays. Wave 0 has a small peak during this block.

The events in order.

Subjective importance	Decreasing energy
wave 4 peak, wave 3 amplification in mid period, wave 1 decay in mid-period.	4, 3, 1

Block A2.

The analysis of the actual synoptic charts leads to the dates given for the block period, but, as explained in appendix 1, there is a consecutive 'grey' period. The kinetic energy series separates these two periods well. The blocking period is dominated by very strong peaks of wave 5 and wave 6 which fit the starting and ending dates precisely, while the entire episode of block plus 'grey' period is better fitted by the long waves 1 to 4. Wave 1 amplifies very strongly during the block to peak on the last day, and falls during the 'grey' period to a minimum at the end. Wave 2 amplifies throughout both blocks and 'grey' periods to peak at the end. Waves 3 and 4 behave similarly, coming to a minimum in mid block before amplifying to peak simultaneously with wave 1 as the 'grey' period begins.

Note that wave 1 and wave 2 do not peak together but that the wave 1 peak is closely associated with the peaks of waves 3 and 4. Also waves 5 and 6 peak during the minima of waves 3 and 4.

The events in order.

Subjective importance	Decreasing energy
wave 5 and wave 6 peaks, wave 1 peak, wave 3 and wave 4 dips during the block.	5,1,3,6,4

Block E3.

During this block, waves 4 and 2 amplify simultaneously. However, wave 4 peaks earlier than wave 2 and leads wave 2 in decaying.

Between this block and the previous block, A2, there is a very large pulse of wave 7, but this collapses on the day E2 commences.

The events in order.

Subjective importance	Decreasing energy
wave 4 peak, wave 2 peak	4,2

Block E4.

The TEKE peaks during the second half of this block, and, as it falls, the zonal kinetic energy rises to peak after the last day. This strong and well defined peak of wave 0 is a unique event in this study. Of the other waves, waves 1,3, 4 and 5, of which wave 3 is the most energetic, peak simultaneously to cause the peaks in the TEKE while wave 2 peaks simultaneously with wave 0.

The events in order.

Subjective importance	Decreasing energy
wave 0 peak, TEKE peak, wave 3 peak, wave 2 peak.	0,3,2

Block E4B.

Waves 1 and 2 display asynchrony of their peaking. Wave 2 falls from a peak on the first day, and wave 1 amplifies to a very high peak on the last. Waves 3, 4 and 5 pass through minima. Wave 6 and, though much smaller, wave 8 peak strongly within the block. Wave 0,which peaks on the first day, subsequently decays and the TEKE goes through a minimum.

The events in order.

Subjective importance	Decreasing energy
wave 6 peak, wave 0 peak, wave 2 decay, wave 1 amplification, wave 8 peak.	2, 0, 1, 6, 8

Block E5 and main portion of A3.

The very strong wave 1 peak on the first day decays to a minimum before the end of the block. Taking wave 1's place, wave 3 amplifies as wave 1 falls, reaching a very high level in mid period before decaying to reach a minimum by the end. As wave 3 decays, wave 5 amplifies to peak just before the last day. Wave 4 amplifies steadily throughout.

The events in order.

Subjective importance	Decreasing energy
wave 3 peak, wave 1 decay, wave 5 peak, wave 4 amplification.	3, 1, 4, 5

Block E5A.

This period is dominated by a very high wave 3 peak which decays before the end of the block. Wave 4 is high throughout the block but falls sharply after the end. Wave 1 has a broad maximum while wave 2 has a low period. Wave 5 shows a moderate peak, which is simultaneous with the high peak in wave 3.

The events in order.

Subjective importance	Decreasing energy
wave 3 peak, wave 4 high wave 5 peak, wave 1 high	3, 4, 1, 5

Block A4.

This block, like A2, has two distinct periods: the blocking and a subsequent 'grey' period which includes a mini-block. Waves 4 and 2 have peaks centred on the entire episode. Waves 5 and 6 peak in the first blocking period, whereas waves 6 and 1 peak in the 'grey' period and mini-block.

The events in order.

Subjective importance	Decreasing energy
wave 5 peak, wave 2 peak, wave 4 peak, wave 6 peak.	2, 4, 5, 6

Block E6.

Except for a broad moderate maximum in wave 1, no wave has a peak that can be associated with the entire block. The other waves, e.g. waves 2, 3 and 4, exhibit short lived peaks. The energy of wave 0 falls sharply during the last days of this block. Simultaneously waves 3 and 4 amplify very swiftly past the last day of the block to peak simultaneously and strongly two days later. In the last days of the block, waves 6 and 7 also peak strongly.

The events in order.

Subjective importance	Decreasing energy
wave 0 fall, wave 1 maximum, wave 2 pulse, wave 4 pulse, wave 6 and wave 7 pulses, waves 3 and 4 very strong peaks after the block.	0, 2, 1, 4, 6

Block E7.

There is no behaviour attributable to this block and of any significance in the kinetic energy of any of the waves. Waves 2 and 4 show only small pulses. Waves 1 and 3 amplify on the last days, and wave 5 and wave 6 show short-lived peaks. None of these appear to be specific to E7.

The events in order.

Subjective importance	Decreasing energy
wave 5 peak, wave 3 peak at end, wave 6 peak.	5, 3, 6

Block E8.

The major feature of this block is an amplification of wave 2 to peak on the final day of the block, followed by a sharp fall later. This amplification is matched by a peaking of wave 6 in mid period. Wave 7, unusually, has a broad maximum of high kinetic energy throughout the period.

The events in order.

Subjective importance	Decreasing energy
wave 2 peak, wave 6 peak, wave 7 peak	2, 6, 7

Block A5/E9.

Waves 4 and 6 overshadow all others during this block. Wave 6 has a period of generally high energy, something unique in this study, but it also comes to a high peak towards the end of the block. Wave 4 amplifies very strongly from the first day of the block and, after peaking simultaneously with wave 6 on the final day, falls off past the end of the block. Wave 7 and wave 2 also peak within the period. Wave 7 is strong but wave 2 is not.

The events in order.

Subjective importance	Decreasing energy
wave 4 peak, wave 6 peak and high period, wave 7 peak, wave 2 peak.	4, 6, 2, 7

Block E10.

Waves 4 and 6, which peak on the last day of E9, fall off, pass through a minimum during this block, and recover by the end of E10 to their levels at the end of E9. Wave 3 has a peak on the first day, then declines throughout. Wave 1 starts high, rises to a peak in mid block and then falls off to a minimum by the end. The wave whose behaviour appears most individual to this block is wave 5 which shows a double peak within the period, its amplitude falling sharply at the end of the block.

The events in order.

Subjective importance	Decreasing energy
wave 5 peaks, wave 4 and wave 6 dips, wave 3 decay, wave 1 peak.	3, 5, 4, 1, 6

Block E11.

Waves 7, 6, 5 and 4 are high before, but decay during the block. Only wave 2 peaks in the period and it reaches high levels. This peak falls in mid block. On the last days waves 5 and 7 show amplification.

The events in order.

Subjective importance	Decreasing energy
wave 2 peak.	2

APPENDIX 4. THE NLIT FLUXES AND THE KINETIC ENERGY SERIES COMPARED.

This appendix presents the data from which chapter 6 draws its results and conclusions. It is to be read in conjunction with, and as a guide to, the interpretation of the various NLIT series. The NLIT fluxes are to be compared with the simultaneous changes in kinetic energy; if the NLIT flux dominates the energy cycle then the energy changes will follow the NLIT series. In this appendix, a comparison between the NLIT fluxes and the kinetic energy behaviour is made for each energy event which is listed as important in the description of the kinetic energy events contained in appendix 3. For the purposes of comparison, the NLIT fluxes are assumed to be constant over the day for which they are calculated, and, on this basis, the total energy transferred by these fluxes is calculated for the duration of the kinetic energy event which is being interpreted.

In what follows, the comparisons are set out block by block. The behaviour of the NLIT versus that of the kinetic energy is described in detail for each significant kinetic energy event within the block under a heading briefly describing the kinetic energy event. For brevity, in these descriptions, the unit $Jm^{-2}mb^{-1}$ is represented throughout by eu.

The units of the vertical scales on the graphs of the time series are chosen for the convenience of display. When making comparisons between graphs the following

conversion factors apply. One unit on the NLIT graphs corresponds to 1.24 units per day on the kinetic energy graphs for waves 1 to 8, and 0.31 units per day for wave 0. A positive NLIT value represents energy gain to the wave.

Blocks A3 and A5 are dealt with under the heading of the corresponding simultaneous E blocks. E4A appears with E4.

Block A1.

Wave 2 peak. In the week before blocking, wave 2 amplifies strongly. During this time, the NLIT shows gains which are larger than are necessary to explain the amplification: wave 2 gained 175 eu, whereas the NLIT gains imply a change of 370 eu. At the start of the block the NLIT changes to loss whereas the KE amplifies. This loss is of the same size as the energy gained. In mid-block the NLIT again becomes positive. During the decay of the peak in KE, the NLIT shows brief losses - these are smaller than can explain the decay: the decay is 150 eu and the NLIT loss is equivalent to 85 eu.

Wave 3 peak. During the amplification of this small peak, the NLIT shows gains which are greater than the energy increase: the NLIT gain grossed over the four days is 390 eu and the observed increase is 125 eu. During the decay energy is lost via the NLIT: the losses amount to 120 eu: the observed energy fall is 100 eu.

Wave 5 peak. The amplification of wave 5 by 166 eu is accompanied by gains in the NLIT. These deliver 200 eu.

The decay of the peak, however, is not accompanied by comparable losses but by only 95 eu.

Wave 6 peak after block. The NLIT shows gains during the amplification,and losses during the decay, but in neither case is the NLIT flux strong enough to explain the energy events. The amplification is 250 eu, while the NLIT gain is 190 eu and the subsequent loss is 90 eu.

Block E2.

Wave 4 peak. The NLIT shows losses throughout wave 4's amplification and decay. During the decay the losses gross up to 390 eu whereas the actual fall in KE is 312 eu. The NLIT can therefore account for the decay of wave 4 but not the amplification.

Wave 3 amplification. The amplification of wave 3 half way through the period is accompanied by a strong gain peak in the NLIT of one day's duration. The gain due to this peak is 186 eu which is greater than the observed rise of 100 eu in the KE of wave 3.

Wave 1 decay. This is not fully explained by the NLIT losses which accompany it. These are just 100 eu whereas the decay is 160 eu. However, before the decay there are strong gains from the NLIT. If these are sustaining wave 1 against dissipation then the energy in wave 1 will fall when they stop. The rate of energy supply via the NLIT in this early period is 170 eu per day providing a daily supply comparable with the decay in wave 1.

Block A2.

Wave 5 peak. During the amplification the low NLIT gains gross only 155 eu whereas the energy rise is 208 eu. During the decay, the NLIT is losing and grosses a loss of 350 eu, which matches the fall in energy of 300 eu over the same period.

Wave 6 peak. The gain from the NLIT accompanying the amplification supplies 160 eu of the observed energy rise of 216 eu. The decay on the last day of the block of 200 eu is accompanied by a loss in the NLIT which accounts for 170 eu of the decay.

Wave 1 peak. The amplification cannot be explained by the NLIT which shows low losses. The decay is paralleled by NLIT losses which are much larger than required to produce the observed decay. The decay is 200 eu. The NLIT losses for the same period total 700 eu.

Wave 3 dip. Wave 3 peaks on the first day of the block, then falls by 75 eu. This is accompanied by a loss via the NLIT of 124 eu. The reamplification of wave 3 cannot be explained by the NLIT because it shows moderate losses - not gains.

Wave 4 dip. The energy loss of 312 eu is matched by a loss through the NLIT of 390 eu. However, the reamplification cannot be explained, since the NLIT shows only low gains or losses. The decay of wave 4 during the 'grey' period of 200 eu can be only partly explained by the NLIT loss, for the period, of 155 eu which lasts only one day.

Block E3.

Wave 4 peak. The amplification of wave 4 by 175 eu can be explained by the NLIT gains of 225 eu over the same period. The decay of wave 4 by 225 eu in mid block is paralleled by a large loss of 450 eu, twice that expected from the observed decay.

Wave 2 peak. The NLIT shows a flux opposite to the behaviour of the kinetic energy. During the amplification, there are losses in the NLIT which reach their peak when the kinetic energy of wave 2 is highest. The NLIT shows gain during the decay. On the last day of the block, the energy falls by 145 eu: this is accompanied by a strong NLIT loss of 490 eu.

Block E4.

Wave 0 peak. The amplification of wave 0 is accompanied by gains from the NLIT. Wave 0 normally gains from the NLIT but in this case there is an extra gain of about 400 eu from the NLIT during the period. The amplification of wave 0 is 350 eu. Thus the NLIT is able to explain this peak in the energy of wave 0.

TEKE peak. The explanation of this peak must be sought in the individual wave numbers.

Wave 3 peak. While wave 3 peaks during the decay, the NLIT shows a strong loss. Wave 3 decays by 100 eu. The loss rate in the NLIT is 200 eu per day.

Wave 2 peak. The wave 2 amplification, which is simultaneous with the wave 0 amplification, is accompanied by a gain peak on only one day. This gain supplies only 148 eu of the amplification of 250 eu.

Block E4B.

Wave 6 peak. The amplification of 220 eu is accompanied by very strong gains in the NLIT which gross 480 eu over the same period. The decay from the peak by 220 eu is accompanied by moderate NLIT losses, which, at 230 eu, match the observed decay.

Wave 0 decay. Wave 0 decays by 300 eu. The NLIT at this time is losing strongly - an unusual occurrence for wave 0. It loses 800eu during the period of wave 0 decay.

Wave 2 decay. In the first half of the block, the initial decay of wave 2 is not matched by any loss in the NLIT. In the second half, wave 2 continues to decay but now the NLIT losses become very large - 300 eu per day.

Wave 1 amplification. Over the entire amplification the NLIT shows only low gains grossing 60 eu. The amplification is 240 eu.

Wave 8 peak. The amplification of 120 eu is paralleled by NLIT gains of 280 eu. When the NLIT gains finish, the peak decays.

Block E5.

Wave 3 peak. Over the period of amplification, the wave gains via the NLIT. These gains imply an input of 540 eu to wave 3. Over the amplification, wave 3 is observed to gain 275 eu, hence the NLIT supplies nearly twice the energy gain observed. During the decay, wave 3 loses the 275 eu again, while the NLIT shows very strong losses equivalent to a decay of 850 eu, hence the NLIT is about three times stronger than required to explain the energy decay.

Wave 1 decay. This decay of 250 eu is paralleled by greater losses in the NLIT of 505 eu. But, during the second half of the block, the NLIT shows strong gains which are over four times the observed increases in the KE.

Wave 5 peak. The amplification of wave 5 by 200 eu is accompanied by a short NLIT gain of 250 eu. However, the NLIT changes from gain to loss on the day of wave 5's peak. Thereafter wave 5 decays by 200 eu, the NLIT showing losses of greater than this at 412 eu.

Wave 4 amplification. The initial amplification of 150 eu of wave 4, on the first day of the block, is matched by NLIT gains grossing 430 eu. Thereafter, the NLIT turns briefly negative. After a brief decay wave 4 reamplifies, continuing so until the last day. In mid-block, this amplification is matched by a brief NLIT gain pulse. Towards the end of the block a sharp, strong gain from the NLIT grosses 260 eu,but this is hardly reflected in the observed KE rise of 25 eu only.

Block E5A.

Wave 3 peak. Wave 3 amplifies by 350 eu while the NLIT shows gains which accumulate 520 eu. Also, as the peak in wave 3 decays, the NLIT continues to show strong gains.

Wave 4 high. The NLIT shows a series of gains and losses during this block which is followed generally by the kinetic energy series but with changes of only about one third of these implied by the NLIT.

Wave 5 peak. The amplification starts on the second day of blocking. The gain in energy is 108 eu. The amplification is paralleled by gains from the NLIT which amount to 130 eu over the same period. The decay of wave 5 of 50 eu is not matched by NLIT losses strong enough to explain the decay. They gross only 31 eu.

Wave 1 high. During this block wave 1 shows a moderate, flat peak lasting throughout the block. Over the same period, the NLIT shows strong gains and losses which are not paralleled by equally large variations in KE. The decay of the peak after the block is accompanied by NLIT gains.

Block A4.

Wave 5 peak. The NLIT cannot explain the peak in wave 5's kinetic energy because it shows moderate losses throughout both the amplification and decay. The maximum loss occurs on the day of the peak. The subsequent losses in the NLIT gross 300 eu which is larger than the KE decay of 200 eu.

Wave 2 peak. Wave 2 has a sustained period of high energy during A4. This is not explained by the NLIT which shows very strong losses peaking at 370 eu per day.

Wave 4 peak. The amplification can be explained by NLIT gains which at 240 eu are of the size necessary to match the energy gains of 240 eu. As wave 4 peaks, the NLIT turns to a high loss at nearly four times the observed energy decay of 150 eu. The grossed NLIT loss is 750 eu.

Wave 6 peak. Wave 6 peaks on the first day of the block and again in the 'grey' period. For the first peak, the amplification of 150 eu is paralleled by NLIT gains of only 130 eu. The decay is paralleled by NLIT losses of 135 eu. The second peak's amplification of 160 eu is accompanied by NLIT gains of 150 eu and the decay by NLIT losses of 190 eu.

Block E6.

Wave 0 fall. Wave 0 is normally supplied via the NLIT and it can be seen that the kinetic energy of wave 0 falls when the NLIT gains drop to zero and recover again when the NLIT returns to more normal values. The kinetic energy drops be 450 eu in five days whereas the NLIT drops from supplying 180 eu per day to zero.

Wave 1 maximum. Wave 1 shows a broad maximum during this block. The 60 eu amplification on the first day is accompanied by a gain from the NLIT of 245 eu. There follows a sequence of decay, amplification, decay and amplification. These are accompanied by NLIT losses and gains in the expected order but the NLIT fluxes are nearly three times the observed KE changes. The final decay by 140 eu on the last day of the block is accompanied by a loss in the NLIT of 560 eu.

Wave 2 peaks. The minor peak in wave 2 is accompanied by moderate to strong losses via the NLIT averaging 140 eu. The KE of wave 2 is around 290 eu.

Wave 4 pulses and amplification at end. Wave 4 has a minor peak in the first half of the block which is accompanied by moderate losses in the NLIT. The amplification at the end of the block is accompanied by gains from the NLIT totalling 175 eu which is less than the kinetic energy gain of 250 eu. The subsequent decay of this peak of 225 eu is matched by an NLIT loss of 240 eu.

Block E6 contd.

Wave 6 peak. Wave 6 peaks in the second half of the block, and it is accompanied at first by NLIT gains, then by losses. The peak is 184 eu above the ambient level. Over the amplification, the NLIT flux supplies 160 eu of this rise, and during the decay the NLIT flux withdraws 120 eu. Hence both the input and the drain are slightly less than the corresponding KE change. A second peak of wave 6 occurs after the block. This is accompanied by strong gains in the NLIT which peak at 280 eu. These gains are thus capable of forcing the observed rise in kinetic energy of 185 eu. When the NLIT gains drop to zero, the kinetic energy is seen to collapse.

Wave 7 peaks. Wave 7, like wave 6, peaks both within the block and then immediately after. In both peaks, wave 7 is similar to wave 6, i.e. in the peak during blocking, theNLIT flux is slightly less than the observed changes, and, during the peak after blocking, the NLIT shows enough gain to be able to force the peak.

Wave 3 peak after the block. The NLIT shows gains during wave 3's amplification but these are too small to explain the energy rises. During the decay, when the kinetic energy drops by 175 eu, the NLIT losses gross about 510 eu, i.e. nearly three times as much as the observed fall.

Block E7.

Wave 5 pulses. Wave 5 has a minor peak on the first day and another in mid block. The amplification for the first peak of 85 eu is accompanied by gains in the NLIT of 95 eu. The decay of this peak by 100 eu is accompanied by NLIT losses of 200 eu. The amplification for the second peak is 75 eu. It is accompanied by gains in the NLIT of only 30 eu. The subsequent decay of 110 eu is accompanied by NLIT losses of 150 eu. However, the NLIT then returns to gain whereas the energy continues to fall.

Wave 3 peak at end. Wave 3 amplifies strongly to peak on the last day. For most of this amplification of 210 eu, the NLIT shows gains which gross 150 eu. On the day of the peak, the NLIT turns to a strong loss which lasts only one day: thereafter the losses are moderate. These losses amount to 580 eu whereas the observed decay is 240 eu.

Wave 6 pulses. Wave 6 has a minor peak on the first day. The amplification is accompanied by NLIT losses. The decay of 160 eu is accompanied by NLIT losses which total 140 eu. The second minor peak of wave 6 has NLIT losses during the amplification and gains during the decay.

Block E8.

Wave 2 peak. Throughout E8, wave 2 shows gains from the NLIT amounting to 550 eu which are more than sufficient to explain the observed energy rises of 230 eu and, in detail, the pattern of kinetic energy rise matches the NLIT flux. When the NLIT gain falls off in mid-period, the kinetic energy ceases to rise and,when the NLIT gain again increases, the kinetic energy increases once more. The decay of this peak by 325 eu comes immediately after the block. It can be explained also by the NLIT flux which loses 375 eu.

Wave 6 peak. The very sharp amplification of 330 eu cannot be explained by the NLIT which shows only low gain. The decay of the peak by 220 eu can partly be explained by a strong but short lived loss in the NLIT of 350 eu which is somewhat offset by the NLIT returning to gains while the KE decay continues.

Wave 7 peak. The NLIT gives no explanation of the kinetic energy behaviour because it shows no fluxes powerful enough to match the observed changes.

Block A5/E9.

Wave 4 peak. In the first few days of the block the NLIT gains are of sufficient size, 200 eu, to explain the amplification 150 eu. However, after this, the NLIT changes to show strong losses yet wave 4 continues to gain kinetic energy. At their peak the NLIT losses are at a rate of 230 eu per day: wave 4's kinetic energy at its peak is 450 eu and the average rise during the block is 350 eu. During wave 4's decay, the NLIT shows only low and gaining fluxes.

Wave 6 very high period. The NLIT flux is opposite to the kinetic energy changes during this period. During the amplification of 140 eu, the losses are at the same rate as the amplification, and, towards the end of the block, the decay is accompanied by gains in the NLIT.

Wave 7 peak. The amplification is accompanied by only low gains in the NLIT. The decay is accompanied by losses in the NLIT; the observed drop in energy is 175 eu and the accumulated loss through the NLIT is 340 eu.

Wave 2 peak. The amplification of wave 2 by 110 eu at the beginning of this block is only partly, in the second half, paralleled by NLIT gains which gross 90 eu. During the decay of 110 eu at the end of the block, the NLIT shows low losses. These gross 150 eu over the period of the decay.

Block E10.

Wave 5 peak. Prior to this block, wave 5 has a peak with the amplification and decay matched by NLIT losses and gains respectively. The peak which occurs within the block has an amplification of 90 eu which is matched by the simultaneous NLIT gain of 90 eu. However, the decay of 180 eu is paralleled by NLIT losses of only 40 eu over the same period.

Wave 4 dip. Throughout this dip, the NLIT shows strong gains which peak as wave 4 passes through its lowest energy. The gains in the NLIT of 200 eu after the minimum in energy can explain wave 4's amplification of 180 eu.

Wave 6 dip. The general decline of wave 6 during the early stages of the block is masked by a sharp minor peak in energy on the first day of blocking. The NLIT shows strong losses throughout the first half of the block and over the period of the peak: the total losses in the NLIT of 390 eu are over twice the observed fall of 160 eu.

Wave 3 fall. This fall is accompanied by strong NLIT losses. These are over double the strength necessary to explain the energy falls. The energy fall is 150 eu; the total loss in the NLIT is 410 eu.

Wave 1 peak. The NLIT provides no explanation of this event; the NLIT is merely losing weakly. Prior to the minor peak, the NLIT shows a strong gain pulse which is not reflected in any increase in energy.

Block E11.

Wave 2 peak. The amplification by 125 eu of wave 2 is accompanied by NLIT gains which total 310 eu over same period. The decay of the peak is accompanied by NLIT losses which amount to 92 eu - slightly less than the energy fall of 100 eu.

REFERENCES.

AUSTIN, J.F. 1978 'The blocking of mid-latitude westerly winds by stationary anticyclones' Ph.D. Thesis, Univ. of London.

BATES, J.R. 1977 'Dynamics of stationary ultra-long waves in middle latitudes' Quart. J. Roy. Meteor. Soc. Vol 103, 397-430.

BENGTSSON, L. 1981 'Numerical prediction of atmospheric blocking - a case study' Tellus 33, 19-41.

CHARNEY, J.G. and DE VORE, J.G. 1979 'Multiple flow equilibria in the atmosphere and blocking' J. Atmos. Sci. Vol 36, 1205-1216.

CHARNEY, J.G. and DRAZEN, P.G. 1961 'Propagation of planetary-scale disturbances from the lower into the upper atmosphere' J. geophys. Res. Vol 66, 83-109.

CHARNEY, J.G. and ELIASSEN, A 1949 'A numerical method for predicting the perturbation of the middle latitude westerlies' Tellus 1, 38-54.

CRUTCHER, H.L. and MESERVE, J.M. 1970 'Selected level heights, temperatures and dew points for the northern hemisphere' Navair - 50 - 1C - 52, revised Chief of Naval Operations, Washington.

EVERSON, P.J. and DAVIS, D.R. 1970 'On the use of a simple two level model in general circulation studies' Quart. J. Roy.Meteor.Soc. Vol 96, 404 - 412.

FLEAGLE, R.G. and BUSINGER, J.A. 1980 'An introduction to Atmospheric Physics. International Geophysical Series' Vol 25, 2nd. edition. Academic Press Ltd. London.

FREDERIKSEN, J.S. 1979 'The effects of long planetary waves on the regions of cyclogenesis: Linear theory' J. Atmos. Sci. Vol 36, 195 - 204.

EGGER, J. 1978 'Dynamics of blocking highs' J. Atmos. Sci. Vol.35, 1788-1801

GREEN, J.S.A. 1977 'The weather during July, 1976: some dynamical considerations of the drought' Weather Vol 32, 120 - 126.

HARTMAN, D.L. and GHAN, S.J. 'A statistical study of the dynamics of blocking' Monthly Weather Review Vol 108, 1144 - 1159.

LEJENAS, H. 1977 'On the breakdown of the westerlies' Atmosphere Vol 15, 89 - 113.

LONGUET - HIGGINS, M.S. and GILL, A.E. 1967 'Resonant interactions between planetary waves' Proc. Roy. Soc. London A299, 120 - 140.

MADDEN, R.A. 1979 'Observations of large-scale travelling Rossby waves' Rev. Geophys. Space Phys. Vol 17, 1935 - 1949.

MATSUNO, T. 1971 'A dynamic model of the stratospheric sudden warming' J. Atmos. Sci. Vol 28, 1479 - 1494.

MURAKAMI, T. 1965 'Energy cycle of the stratospheric warming in early 1958' J. Meteor. Soc. Japan Vol 43, 262 - 283.

O'NEIL, A and TAYLOR, B.F. 1979 'A study of the major stratospheric warming of 1976/77' Quart. J. Roy. Meteor. Soc. Vol 105, 71 - 92.

PERRY, J.S. 1967 'Long wave energy processes in the 1963 sudden stratospheric warmings' J. Atmos. Sci. Vol 24, 539 - 550.

PETTERSSEN, S. 1956 'Weather Analysis and Forecasting', Vol 1 'Motion and Motion Systems' McGraw-Hill, New York.

REITER, E.R. 1969 'Atmospheric transport processes. Part 1; Energy transfers and transformations' Critical Review Series, US Atomic Energy Commission, Division of Technical Services.

REX, D.F. 1950 'Blocking action in the middle troposphere and its effect upon regional climate' Tellus 2, 196 - 211 and 275 - 301.

ROSSBY, C.G. 1950 'On the dynamics of certain types of blocking waves' J. Chin. Geophys. Soc. Vol 2, 1 - 13.

SALTZMAN, B. 1970 'Large scale atmospheric energetics in the wavenumber domain' Reviews of Geophysics and Space Physics Vol 8, 289 - 302.

SCORER, R.S. 1978 'Environmental Aerodynamics' Ellis Horwood, Chichester, England.

SCORER, R.S. 1979 'One further remark on blocking' Weather 34, 361 - 363.

SHAW, M.S. 1977 'The exceptional heat wave of 23rd June to 8th July, 1976' Meteor. Mag. Vol 106, 329 - 346.

SHUTTS, G.J. 1978 'Quasi-geostrophic planetary wave forcing' Quart. J. Roy. Meteor. Soc. Vol 104, 331 - 350.

SMAGORINSKY, J. 1953 'The dynamical influence of large-scale heat sources and sinks on the quasi-stationary mean motions of the atmosphere' Quart. J. Roy. Meteor. Soc. Vol 79, 342 - 366.

SUMNER, E.J. 1954 'A study of blocking in the Atlantic-European sector of the northern hemisphere' Quart. J. Roy. Meteor. Soc. Vol 80, 402 - 416.

SUMNER, E.J. 1959 'Blocking anticyclones in the Atlantic-European sector of the northern hemisphere' Meteor. Mag. Vol 88, p. 300 - 311.

TOMATSU, K. 1976 'Spectral atmospheric energy budget over the northern hemisphere'. Technical Report No. 1, The Meteorological Research Institute, Tokyo.

TREIDL, R.A, BIRCH, E.C. and SAJECKI, P. 1981 'Blocking action in the northern hemisphere: a climatological study' Atmosphere-Ocean Vol 19, 1 - 23.

TSAY, C-Y and KAO, S-K. 1978 'Linear and non-linear contributions to the growth and decay of the large-scale atmospheric waves and jet stream' Tellus 30, 1 - 14.

TUNG, K.K. and LINDZEN, R.S. 1979 'A theory of stationary long waves', parts 1 and 2. Monthly Weather Review Vol 107, 714 - 750.

WHITE, W.B. and CLARK, N.E. 1975 'On the development of blocking ridge activity over the central North Pacific' J. Atmos. Sci. Vol 32, 489 - 502.

TIME SERIES CHARTS.

	Time series of the kinetic energy of each wave at 500 mb and between 20°N and 80°N. (continued)	
4.6	wave 4	L
4.7	wave 5	M
4.8	wave 6	N
4.9	wave 7	O
4.10	wave 8	P
4.11	Time series of the total eddy kinetic energy of waves 1 to 8.	Q
4.11	Time series of the total kinetic energy.	Q
	Time series of the non-linear interaction of each wave with waves 1 to 8 at 500 mb and between 20°N and 80°N.	
5.3	wave 0	H
5.4	wave 1	I
5.5	wave 2	J
5.6	wave 3	K
5.7	wave 4	L
5.8	wave 5	M
5.9	wave 6	N
5.10	wave 7	O
5.11	wave 8	P
5.13	Time series of the results of filtering the NLIT for wave 4 (figure 5.7) with a three point unitary filter. (The first and last days, being lost in the filtering, are set to zero for plotting).	R
	The positions of each block in time and longitude plotted to the same scales as the other time series plots.	R

COLOUR SEQUENCE.

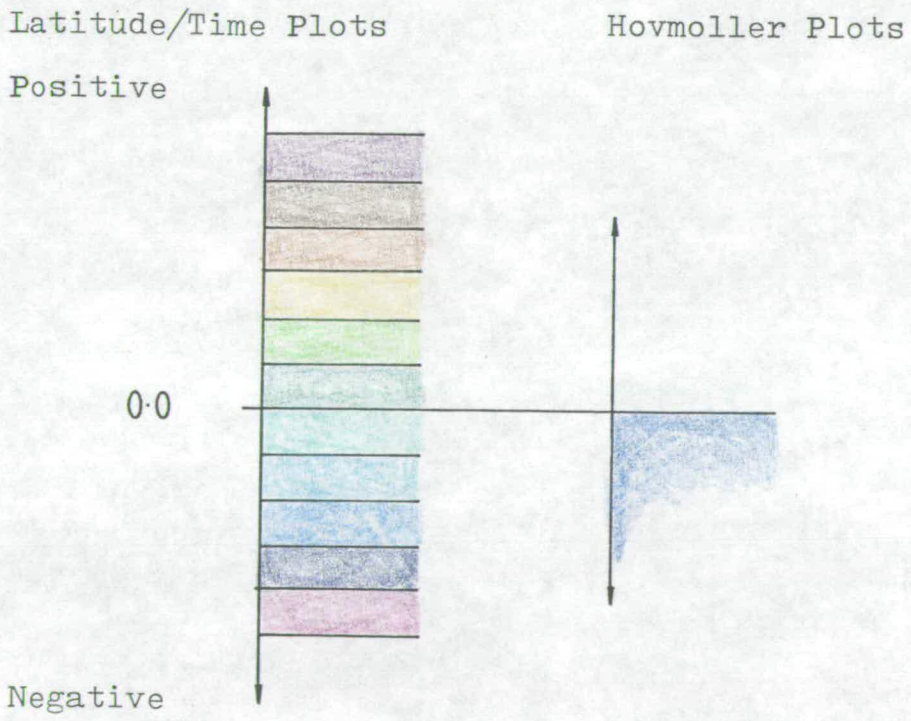

AMPLITUDE OF WAVE 1

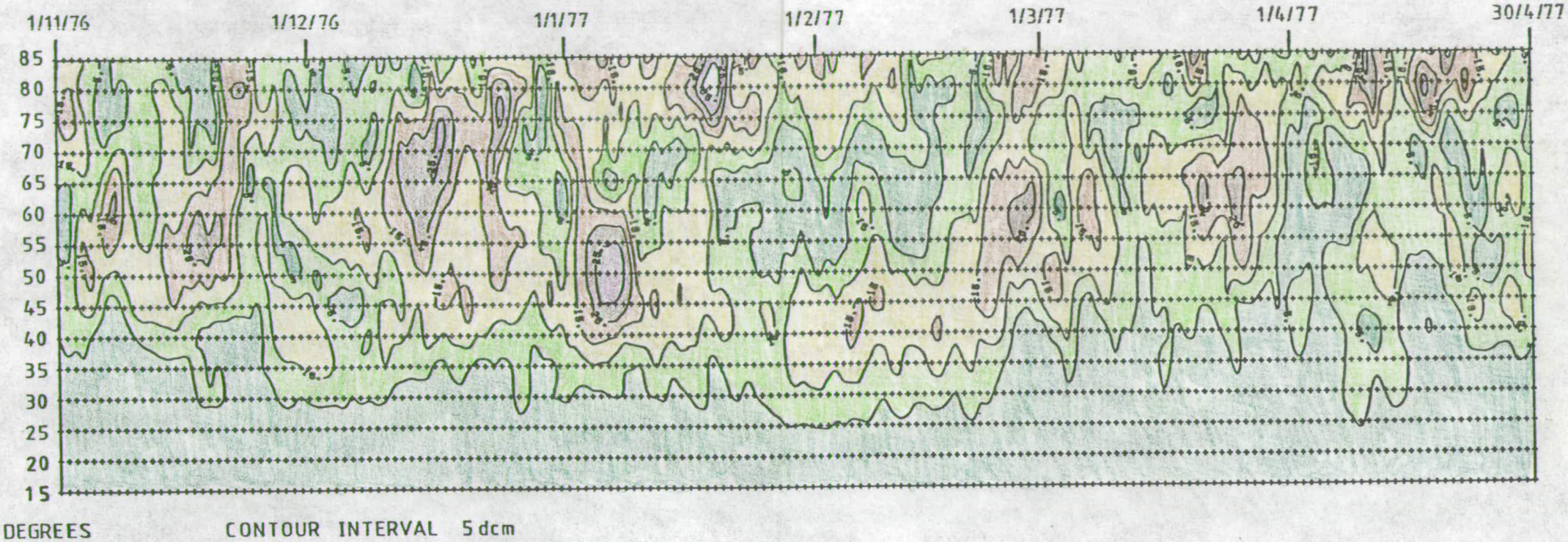

AMPLITUDE OF WAVE 2

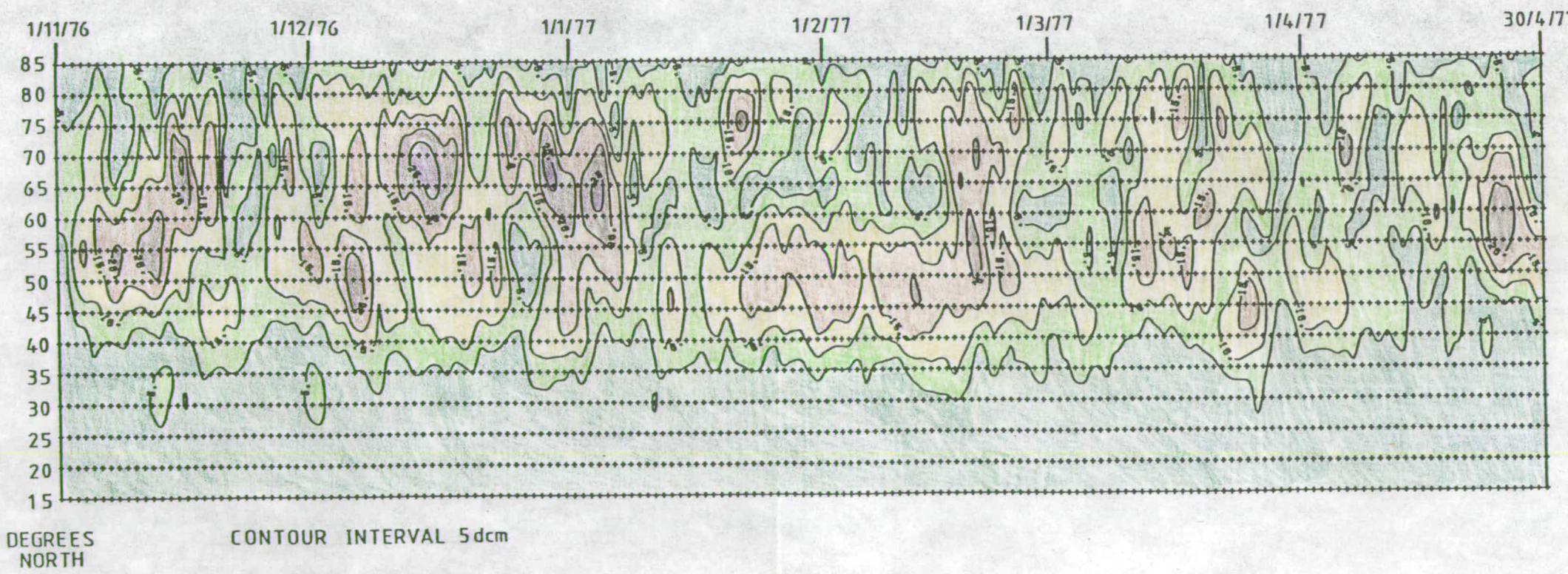

AMPLITUDE OF WAVE 3

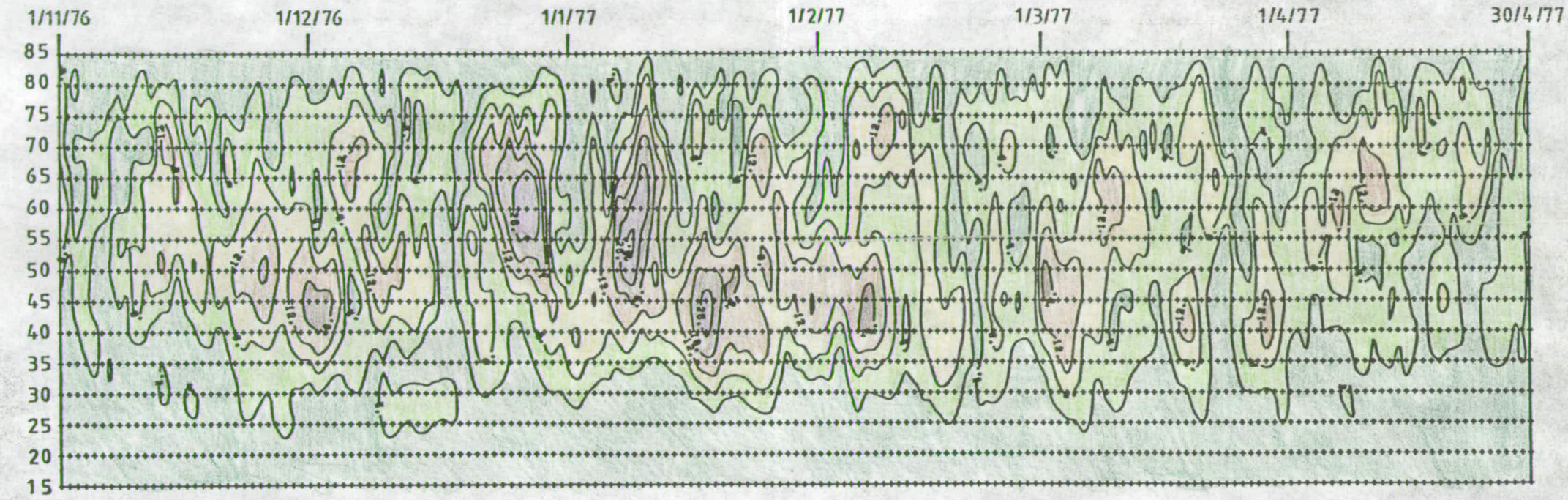

DEGREES NORTH

CONTOUR INTERVAL 4 dcm

AMPLITUDE OF WAVE 4

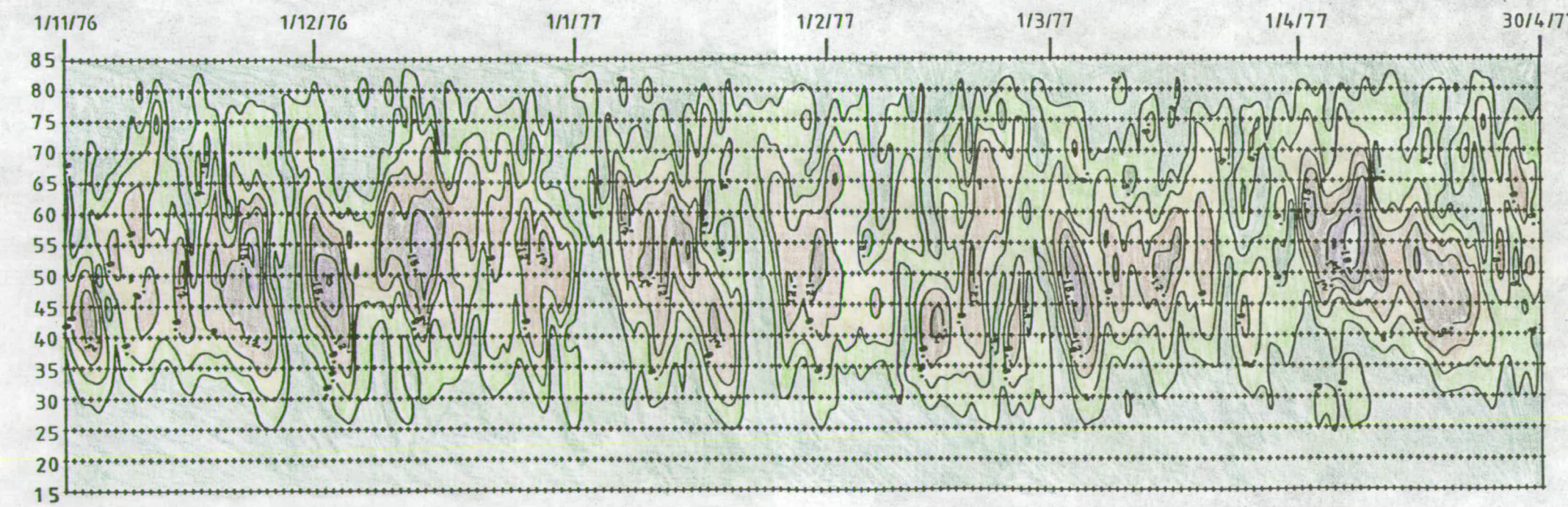

DEGREES NORTH

CONTOUR INTERVAL 3 dcm

AMPLITUDE OF WAVE 5

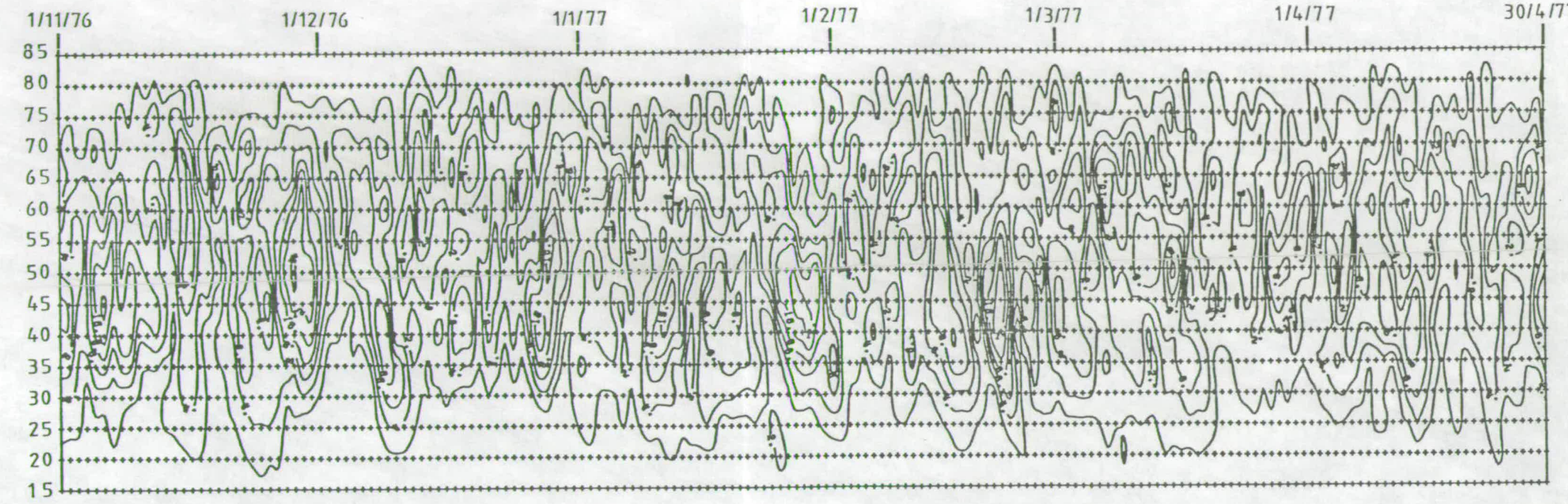

AMPLITUDE OF WAVE 6

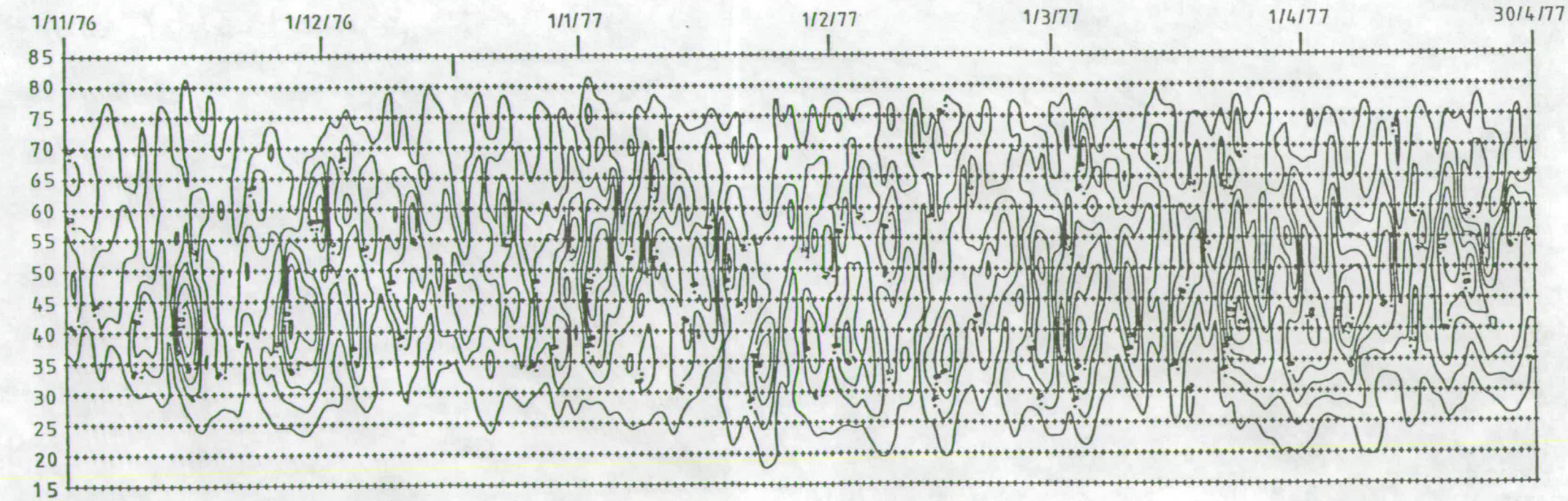

AMPLITUDE OF WAVE 7

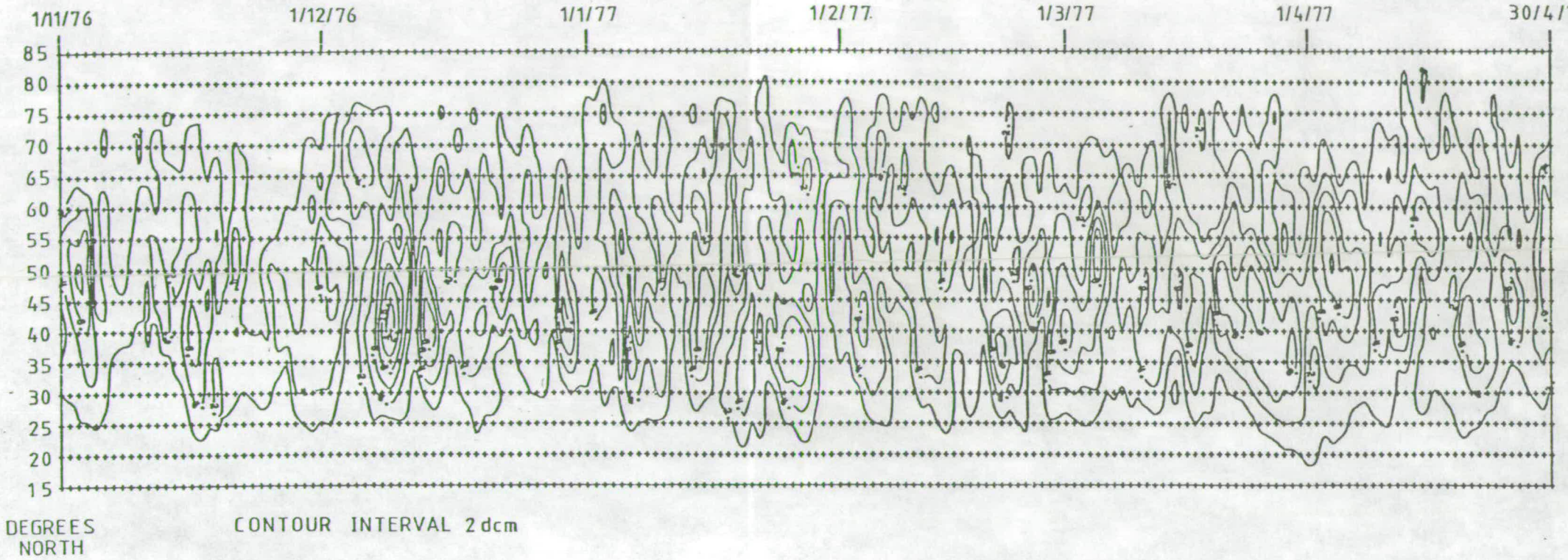

AMPLITUDE OF WAVE 8

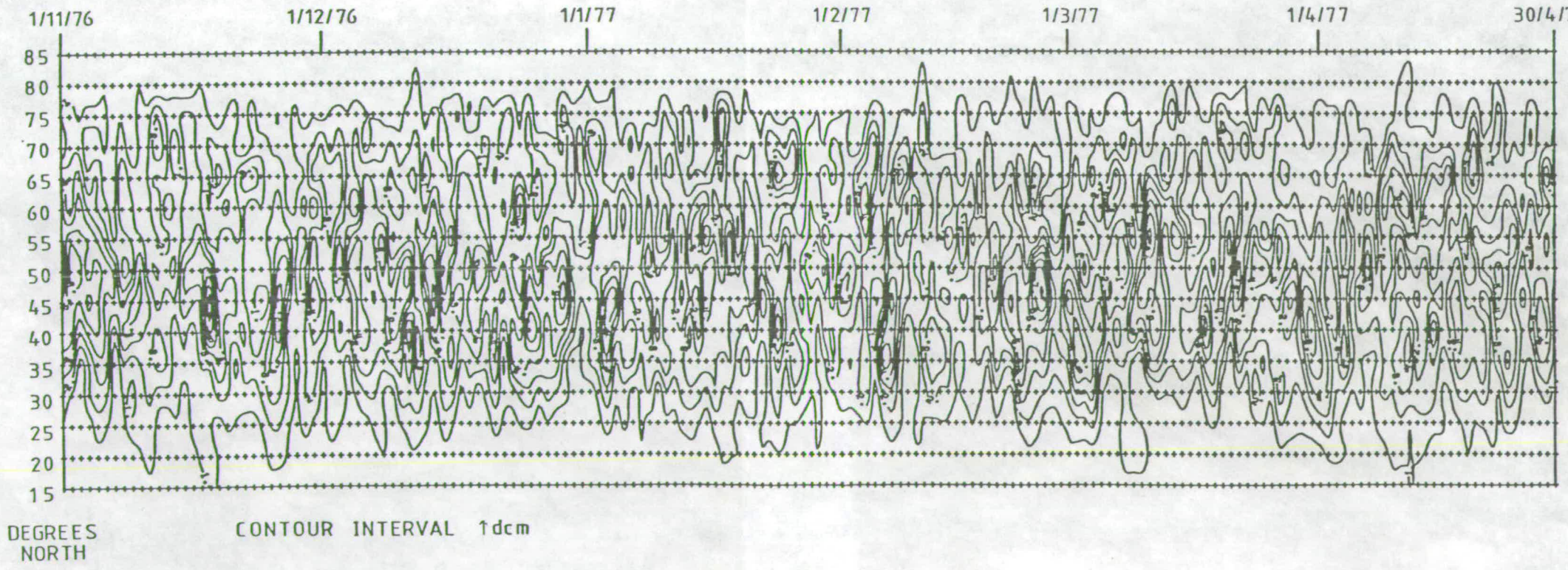

PHASES OF WAVES 1-4

60°N

180°W
135°W
90°W
45°W
0°
45°E
90°E
135°E

1/11/76 1/12/76 1/1/77 1/2/77 1/3/77 1/4/77 30/4/77

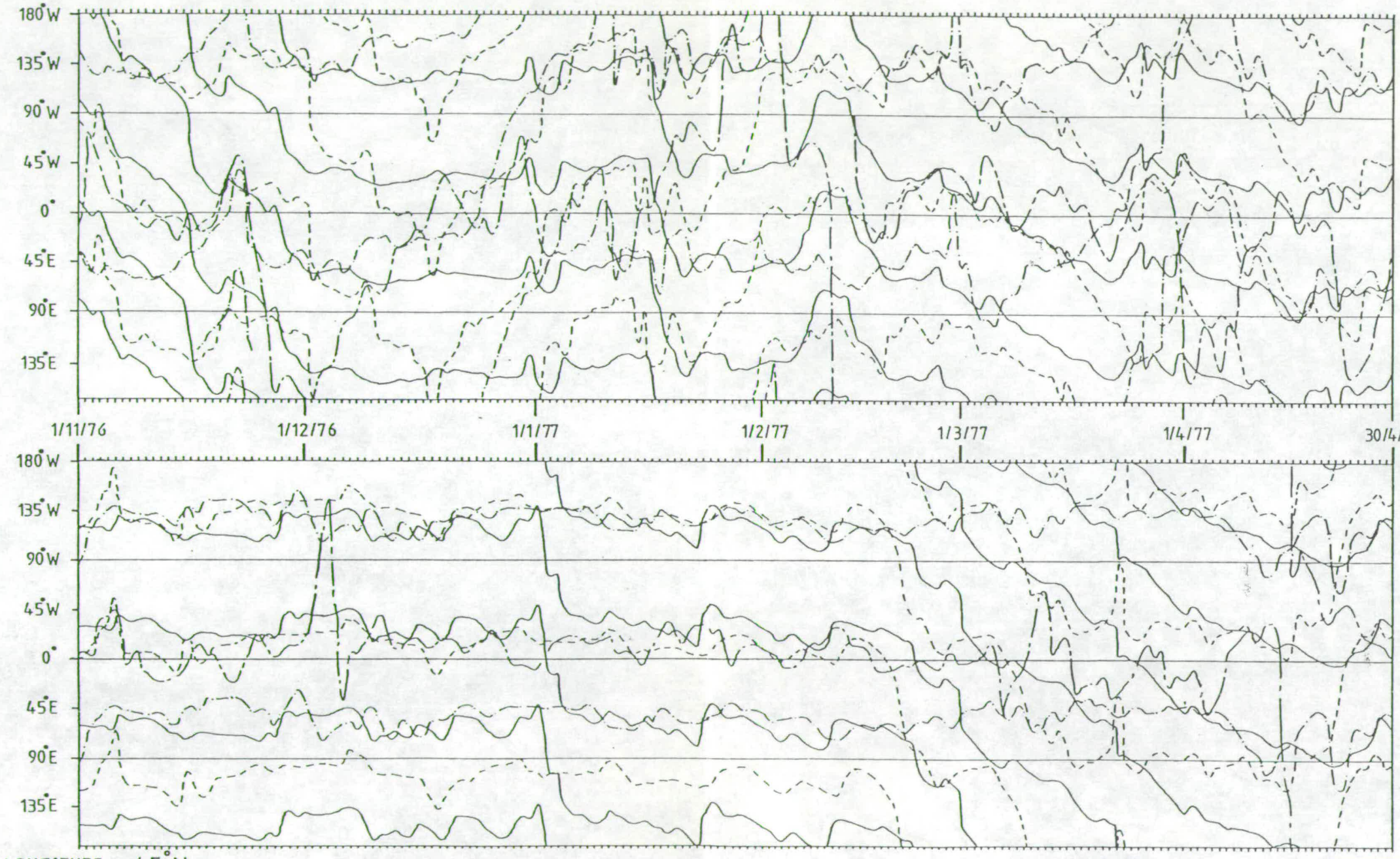

LONGITUDE 45°N

WAVE 1 —·— WAVE 2 —·—·— WAVE 3 - - - - - - WAVE 4 ———

HOVMÖLLER DIAGRAM OF WAVES 5-8

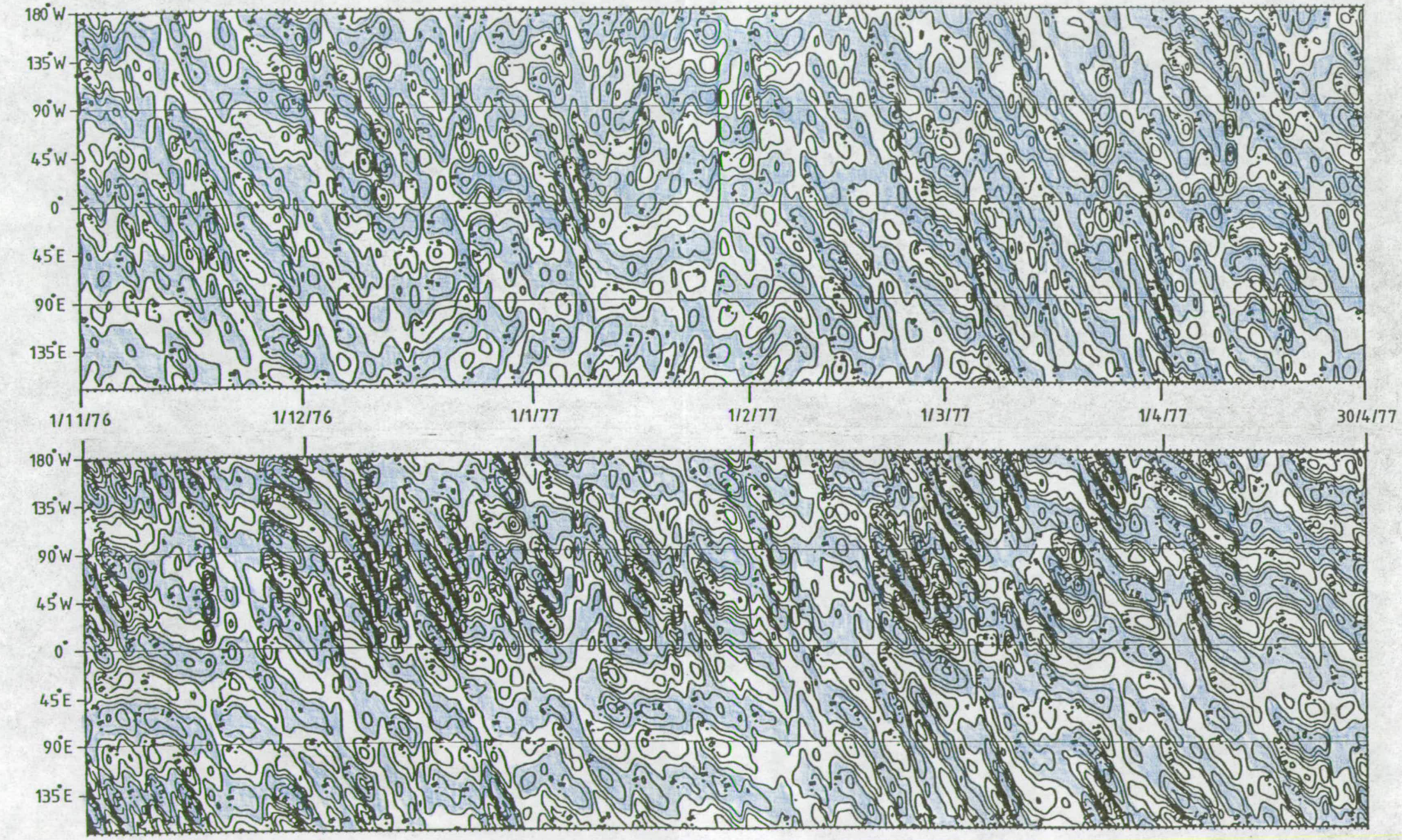

contour interval 5 dcm.

ZONAL WIND

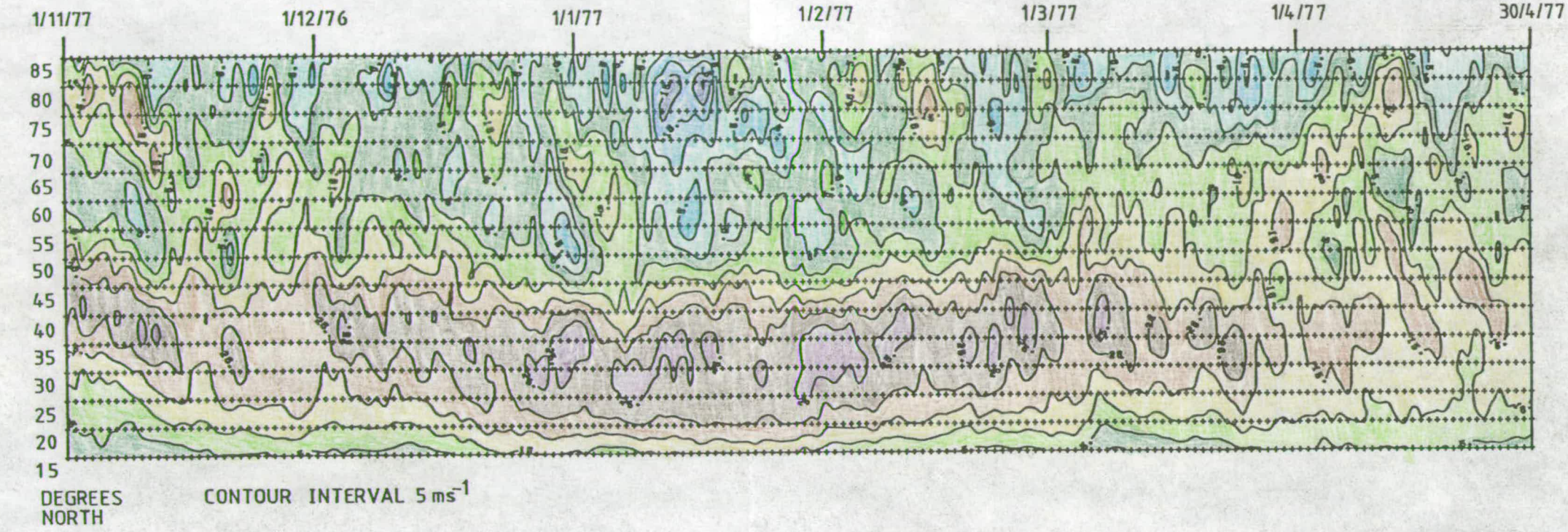

ZONAL INDEX 45°-60°N

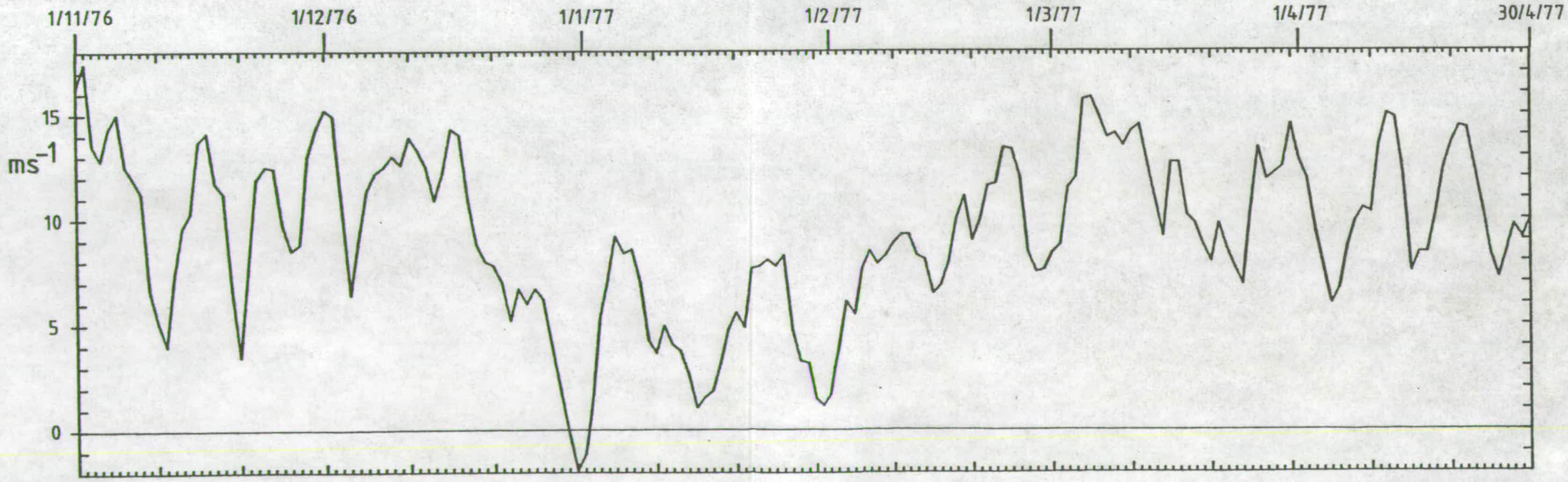

WAVE 0

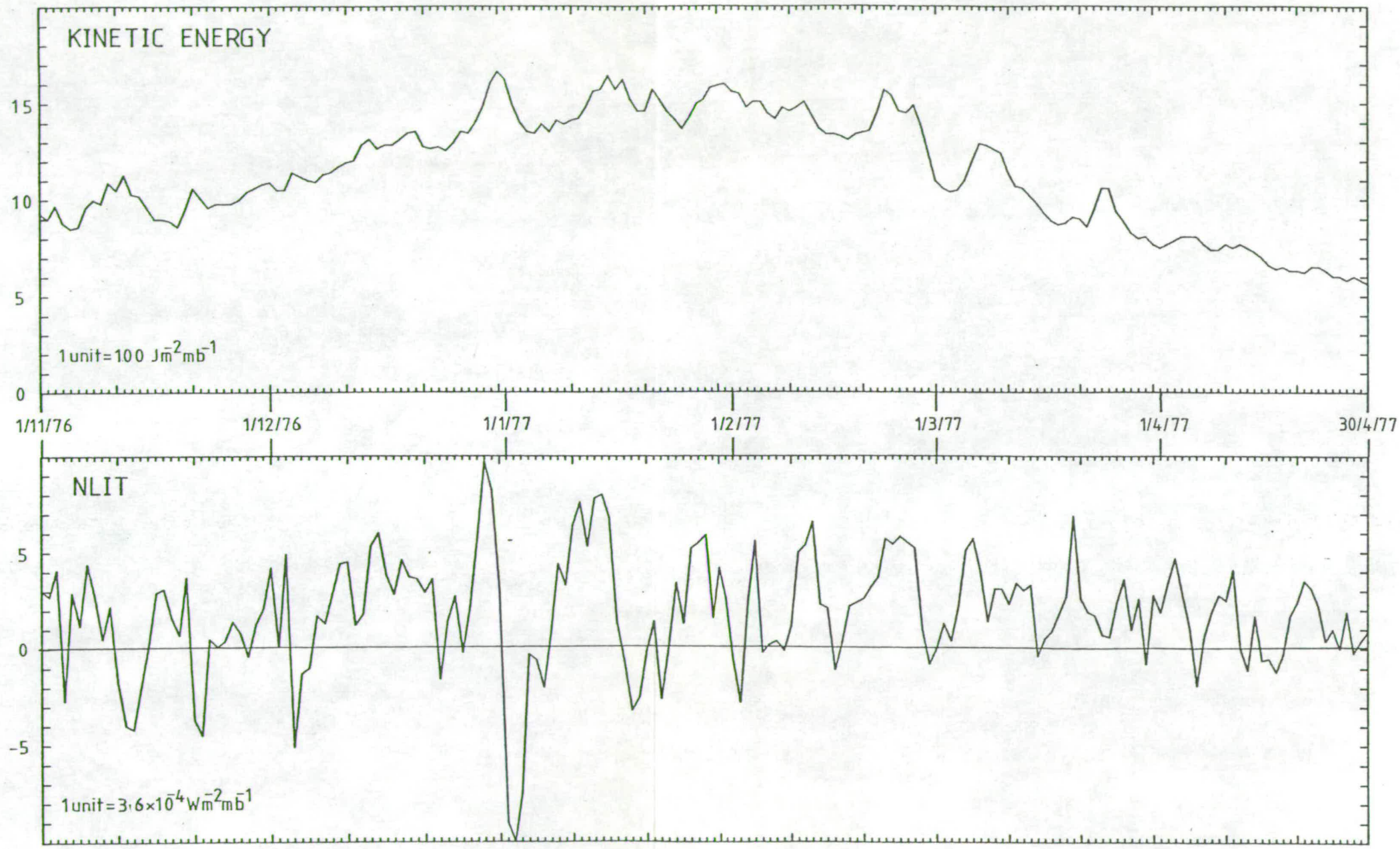
KINETIC ENERGY
15
10
5
0
1unit=100 Jm⁻²mb⁻¹
1/11/76
1/12/76
1/1/77
1/2/77
1/3/77
1/4/77
30/4/77
NLIT
5
0
-5
1unit=3·6×10⁻⁴Wm⁻²mb⁻¹

WAVE 1

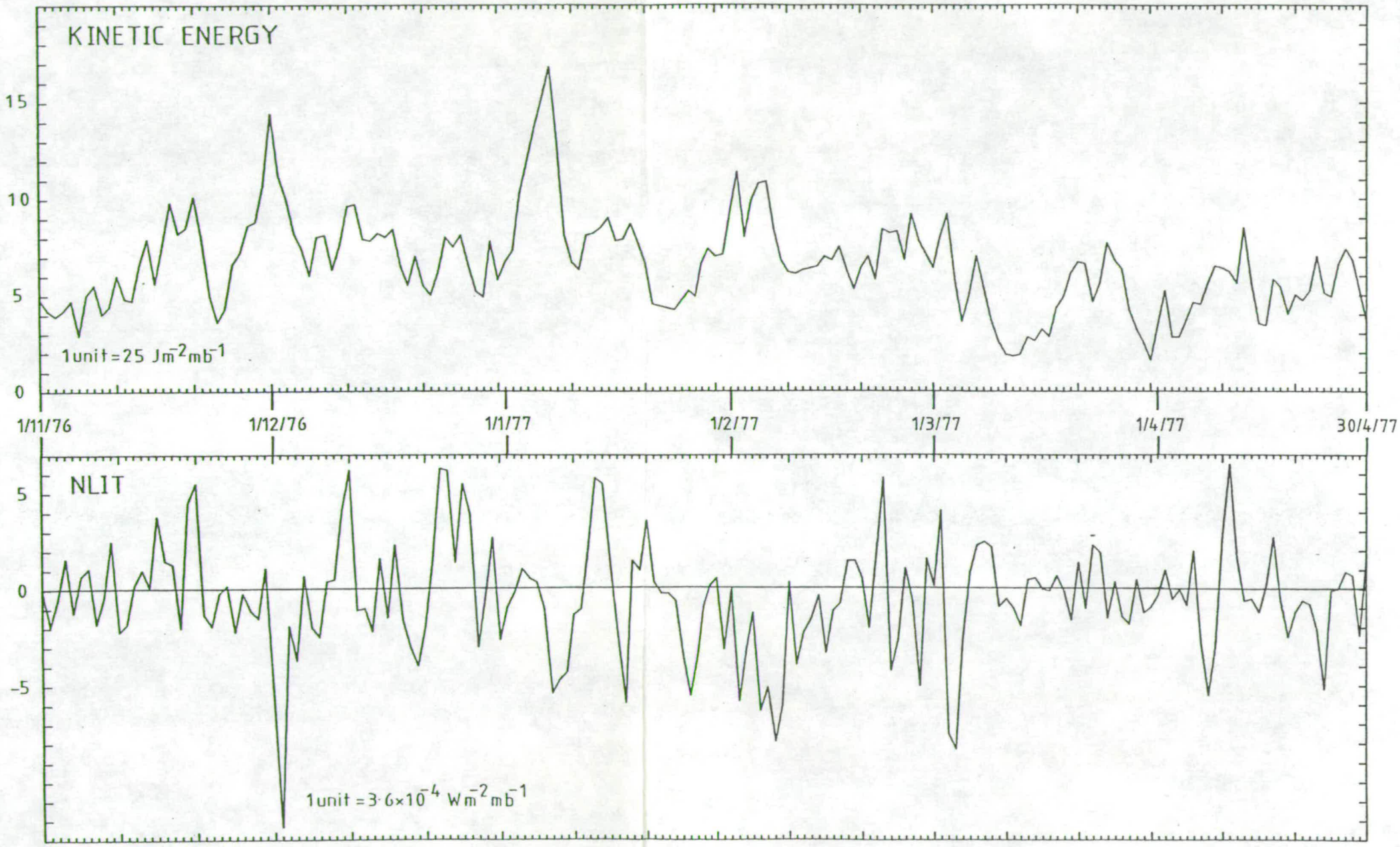
KINETIC ENERGY
15
10
5
0
1unit=25 Jm⁻²mb⁻¹
1/11/76
1/12/76
1/1/77
1/2/77
1/3/77
1/4/77
30/4/77
NLIT
5
0
-5
1unit = 3·6×10⁻⁴ Wm⁻²mb⁻¹

WAVE 2

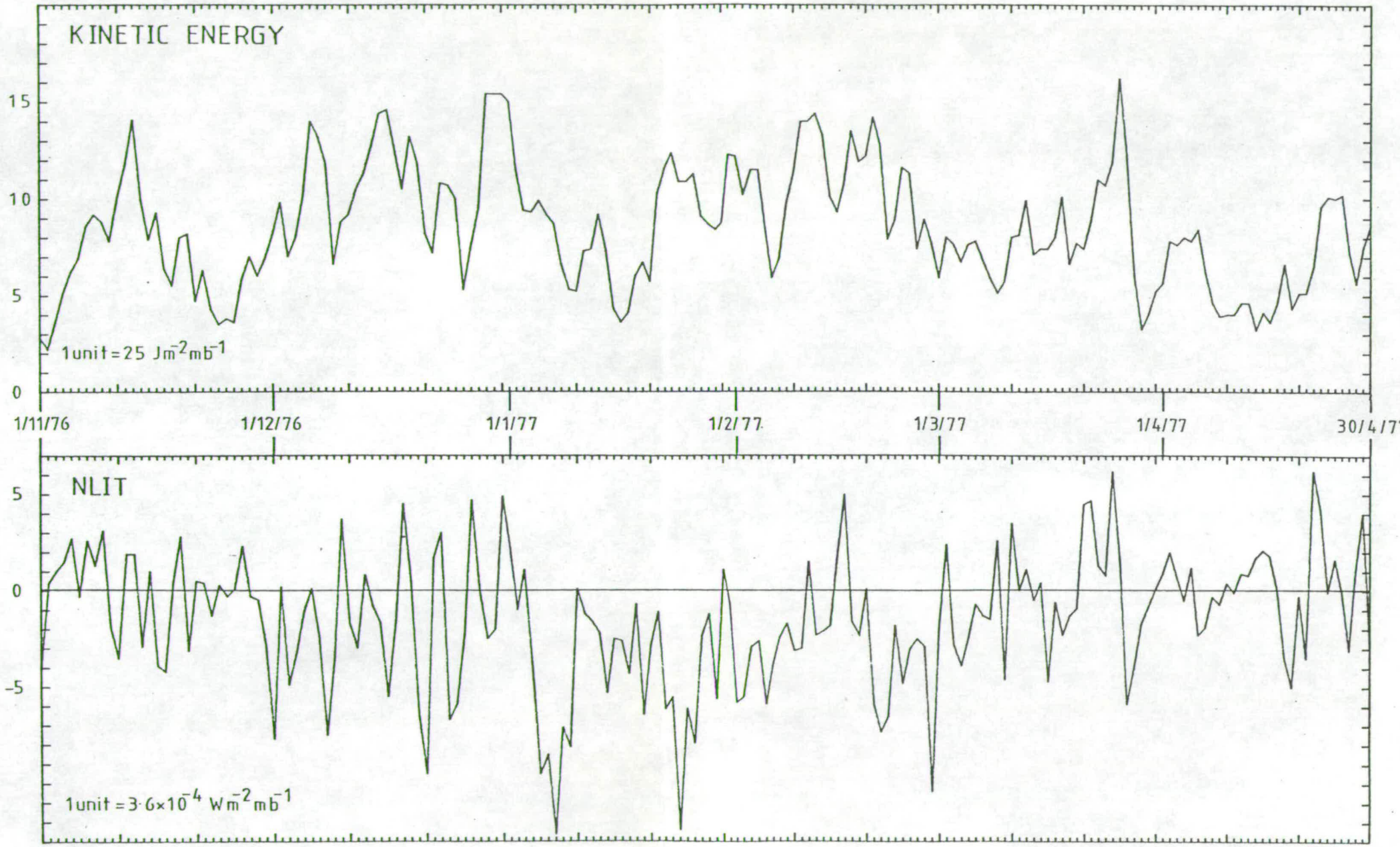
KINETIC ENERGY
15
10
5
0
1unit=25 Jm⁻²mb⁻¹
1/11/76
1/12/76
1/1/77
1/2/77
1/3/77
1/4/77
30/4/77
NLIT
5
0
-5
1unit = 3·6×10⁻⁴ Wm⁻²mb⁻¹

WAVE 3

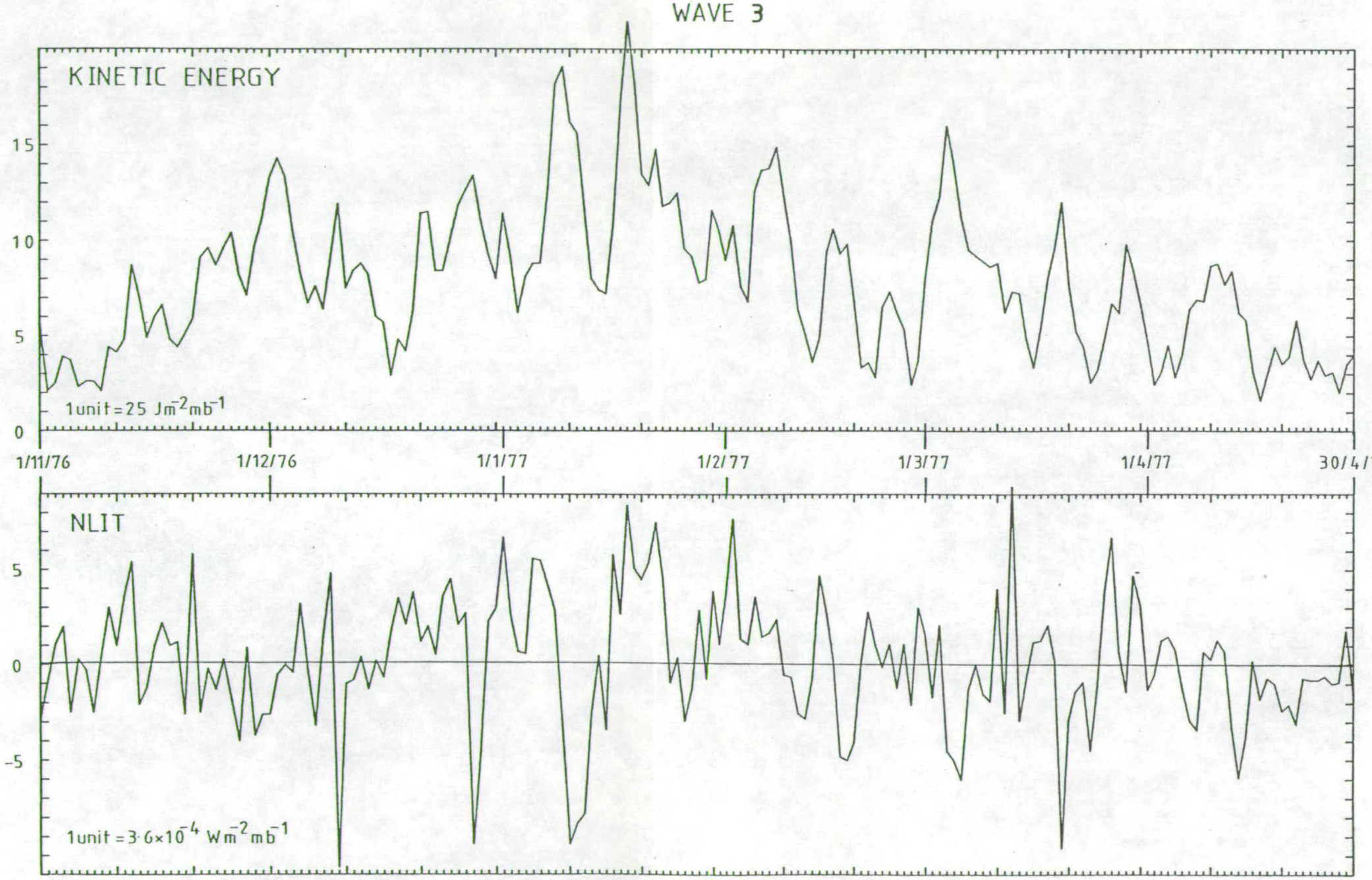
KINETIC ENERGY
15
10
5
0
1unit=25 Jm⁻²mb⁻¹
1/11/76
1/12/76
1/1/77
1/2/77
1/3/77
1/4/77
30/4/77
NLIT
5
0
-5
1unit = 3·6×10⁻⁴ Wm⁻²mb⁻¹

WAVE 4

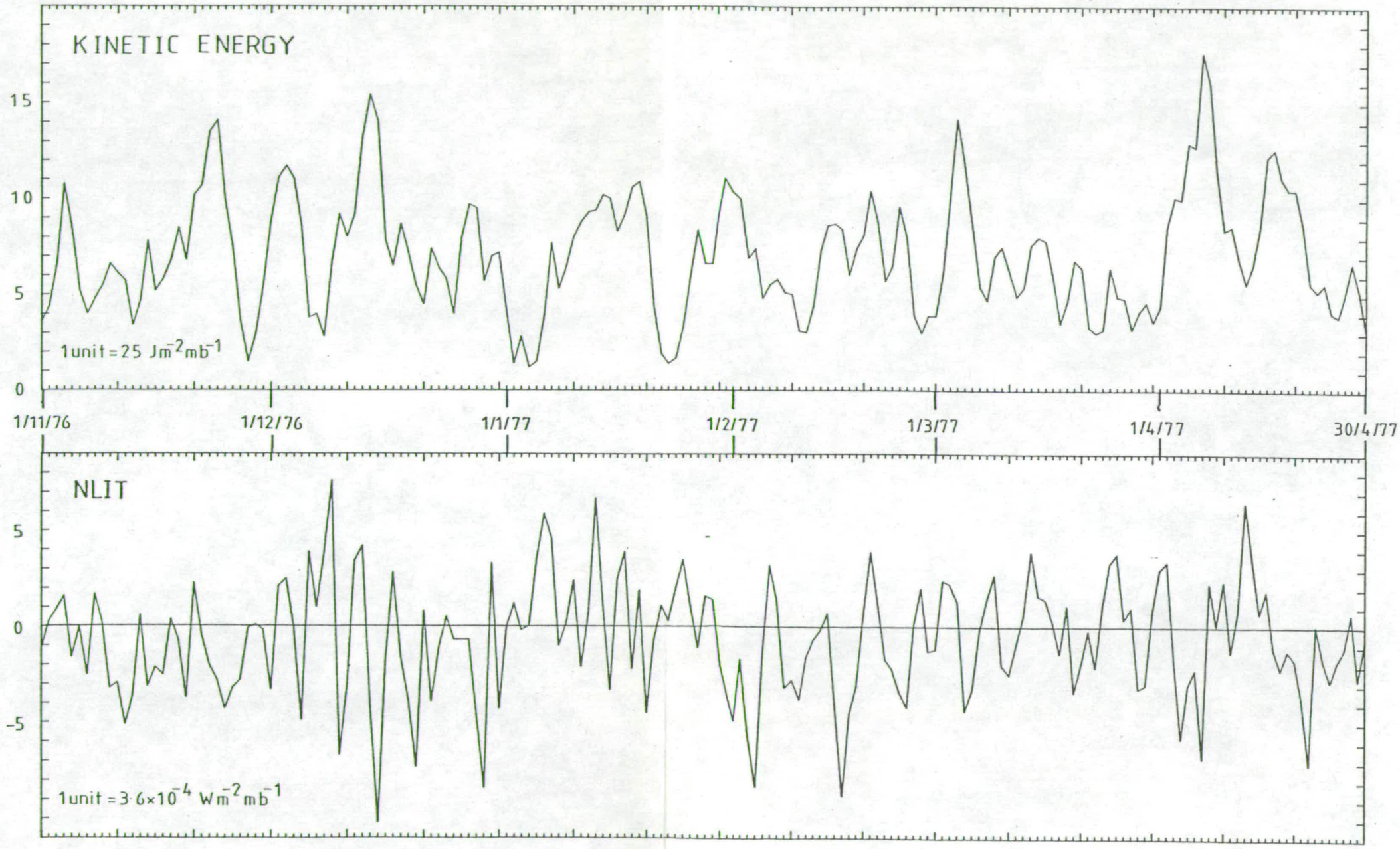
KINETIC ENERGY
15
10
5
0
1unit = 25 Jm⁻²mb⁻¹
1/11/76
1/12/76
1/1/77
1/2/77
1/3/77
1/4/77
30/4/77
NLIT
5
0
-5
1unit = 3·6×10⁻⁴ Wm⁻²mb⁻¹

WAVE 5

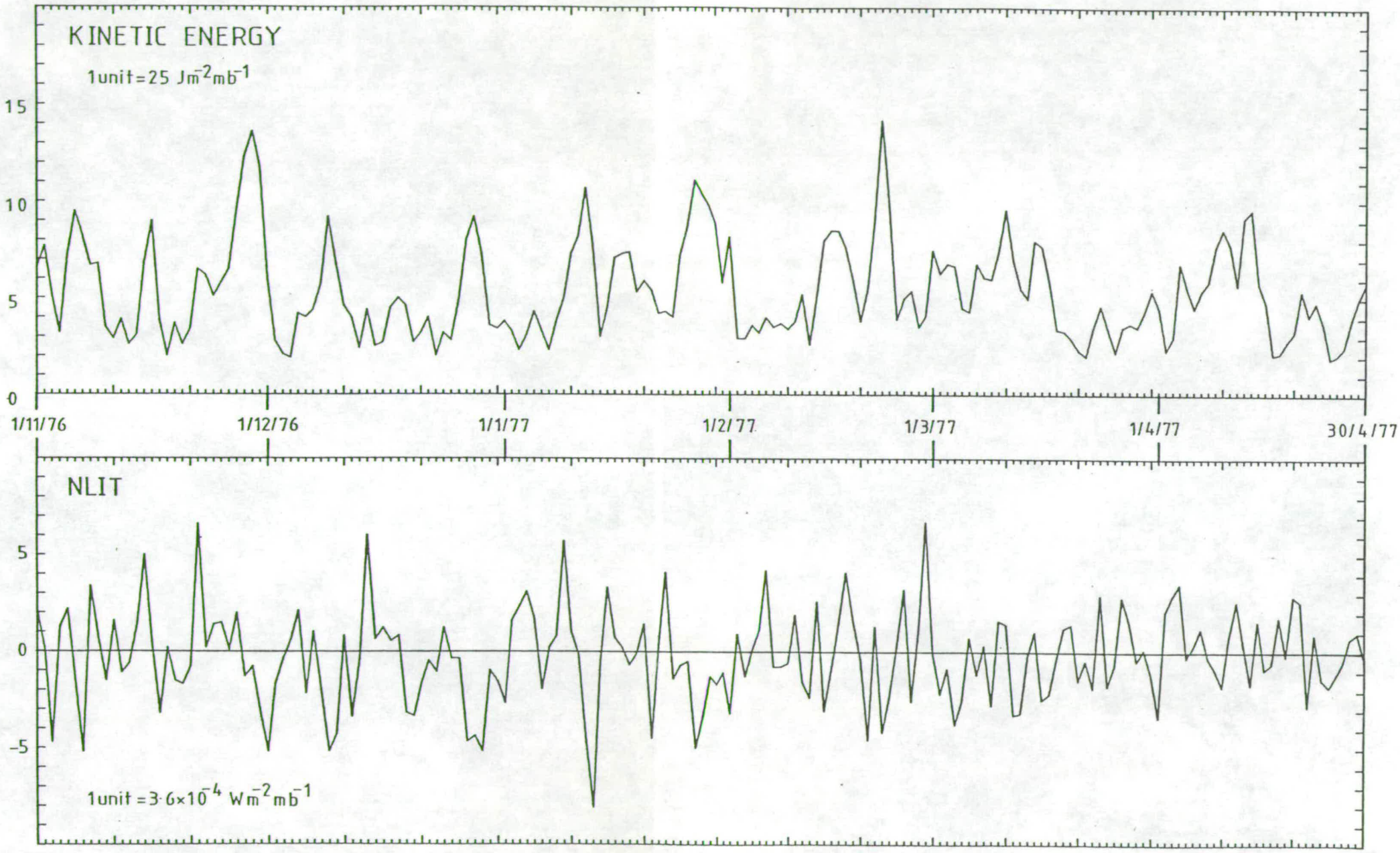
KINETIC ENERGY
1unit=25 Jm⁻²mb⁻¹
15
10
5
0
1/11/76
1/12/76
1/1/77
1/2/77
1/3/77
1/4/77
30/4/77
NLIT
5
0
-5
1unit = 3·6×10⁻⁴ Wm⁻²mb⁻¹

WAVE 6

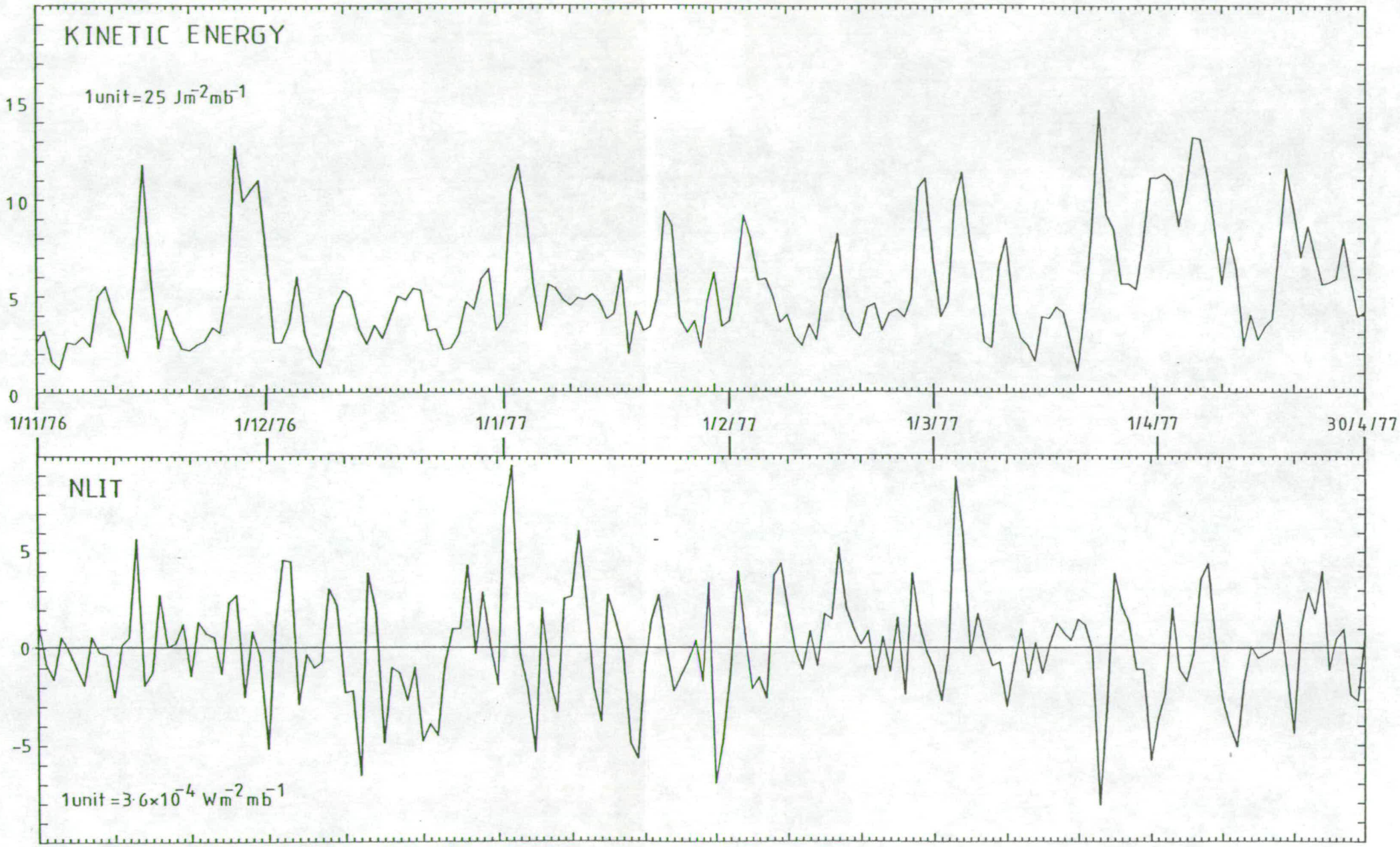
KINETIC ENERGY
1unit=25 Jm⁻²mb⁻¹
15
10
5
0
1/11/76
1/12/76
1/1/77
1/2/77
1/3/77
1/4/77
30/4/77
NLIT
5
0
-5
1unit = 3·6×10⁻⁴ Wm⁻²mb⁻¹

WAVE 7

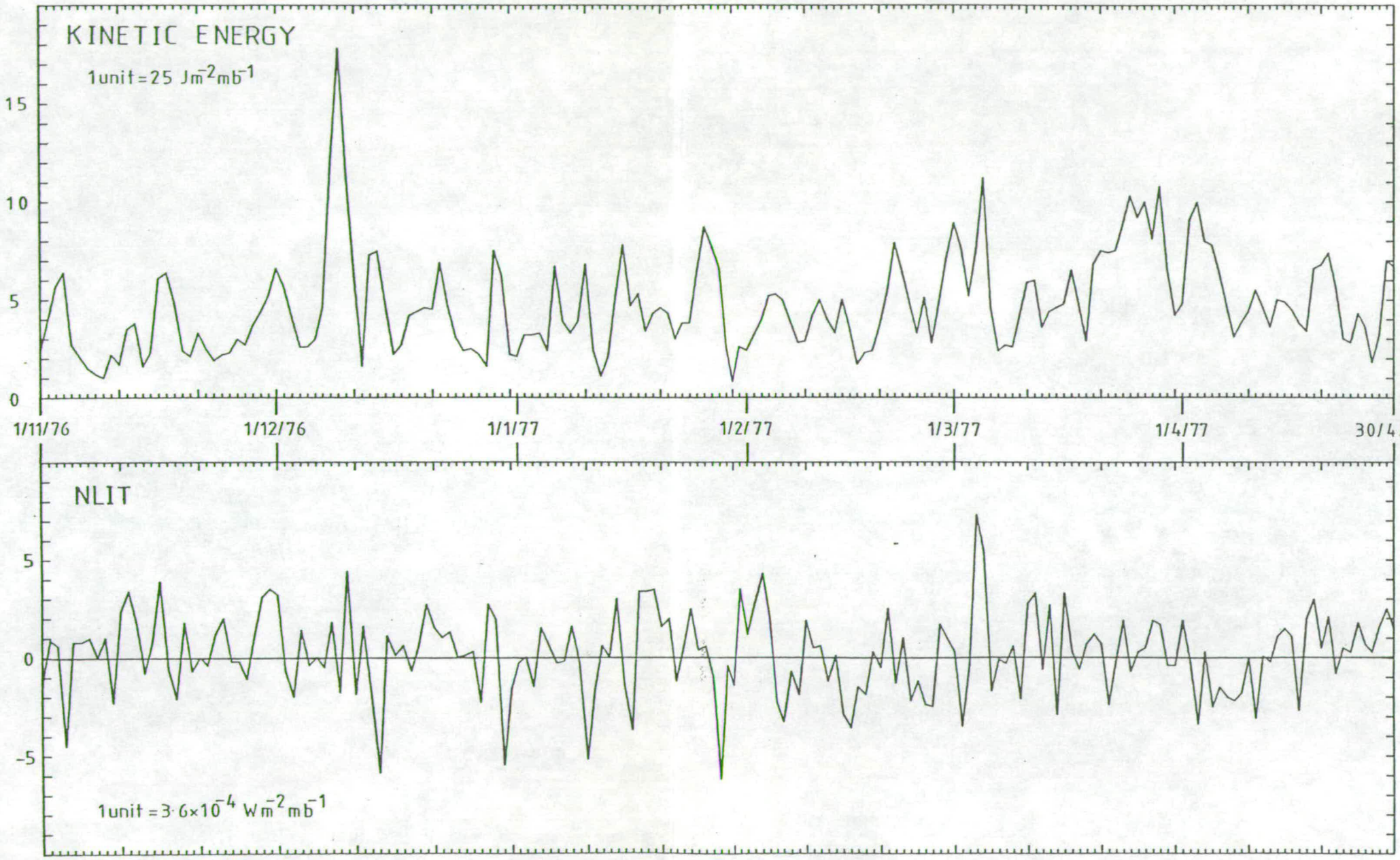
KINETIC ENERGY
1unit=25 Jm⁻²mb⁻¹
15
10
5
0
1/11/76
1/12/76
1/1/77
1/2/77
1/3/77
1/4/77
30/4/77
NLIT
5
0
-5
1unit = 3·6×10⁻⁴ Wm⁻²mb⁻¹

WAVE 8

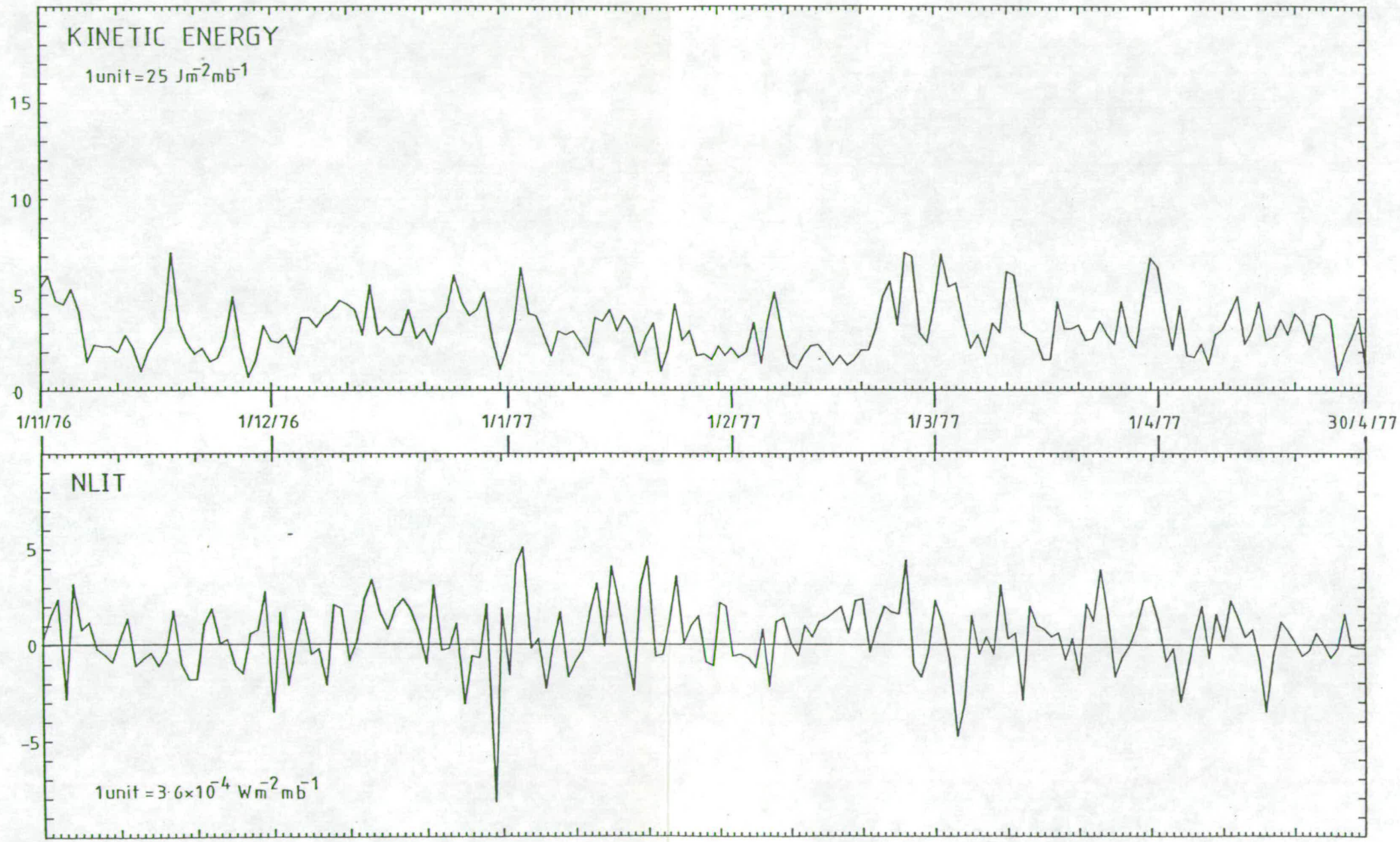
KINETIC ENERGY
1unit=25 Jm⁻²mb⁻¹
15
10
5
0
1/11/76
1/12/76
1/1/77
1/2/77
1/3/77
1/4/77
30/4/77
NLIT
5
0
-5
1unit = 3·6×10⁻⁴ Wm⁻²mb⁻¹

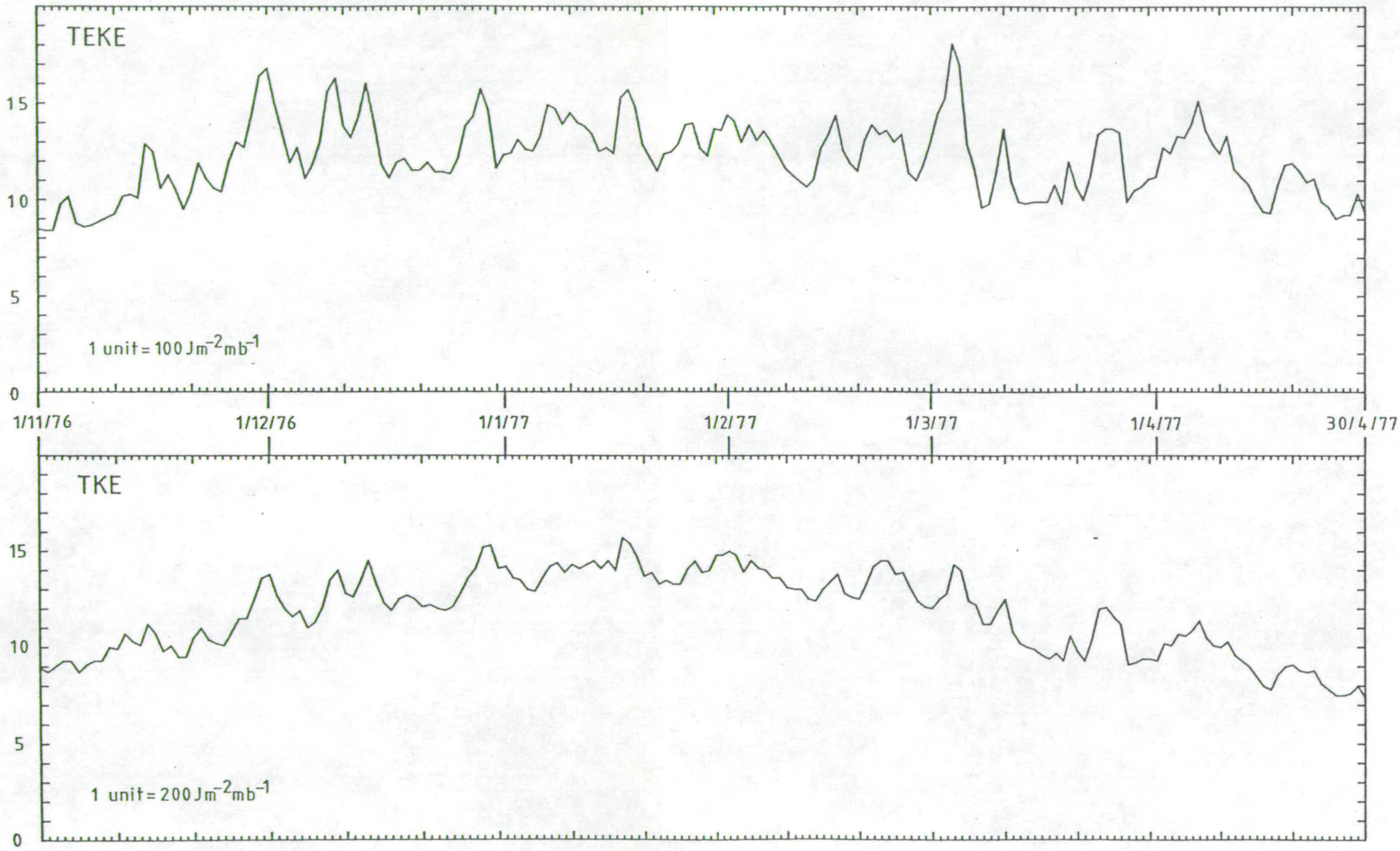
TEKE
15
10
5
0
1 unit = 100 Jm⁻²mb⁻¹
1/11/76
1/12/76
1/1/77
1/2/77
1/3/77
1/4/77
30/4/77
TKE
15
10
5
0
1 unit = 200 Jm⁻²mb⁻¹

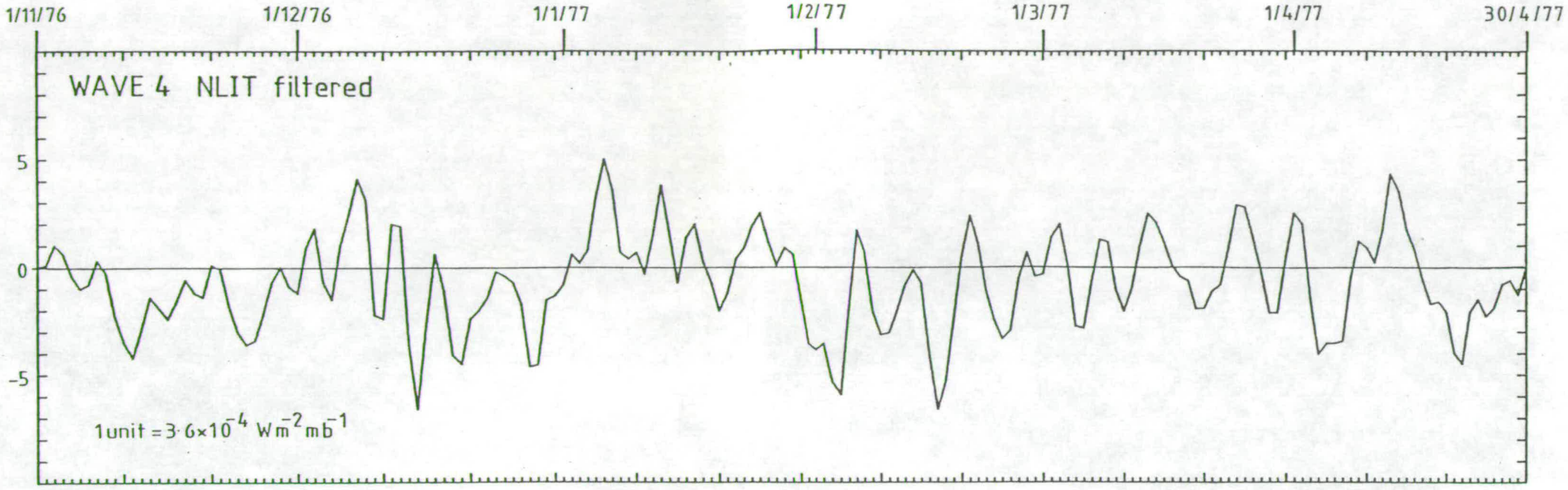

POSITIONS OF BLOCKS IN LONGITUDE AND TIME

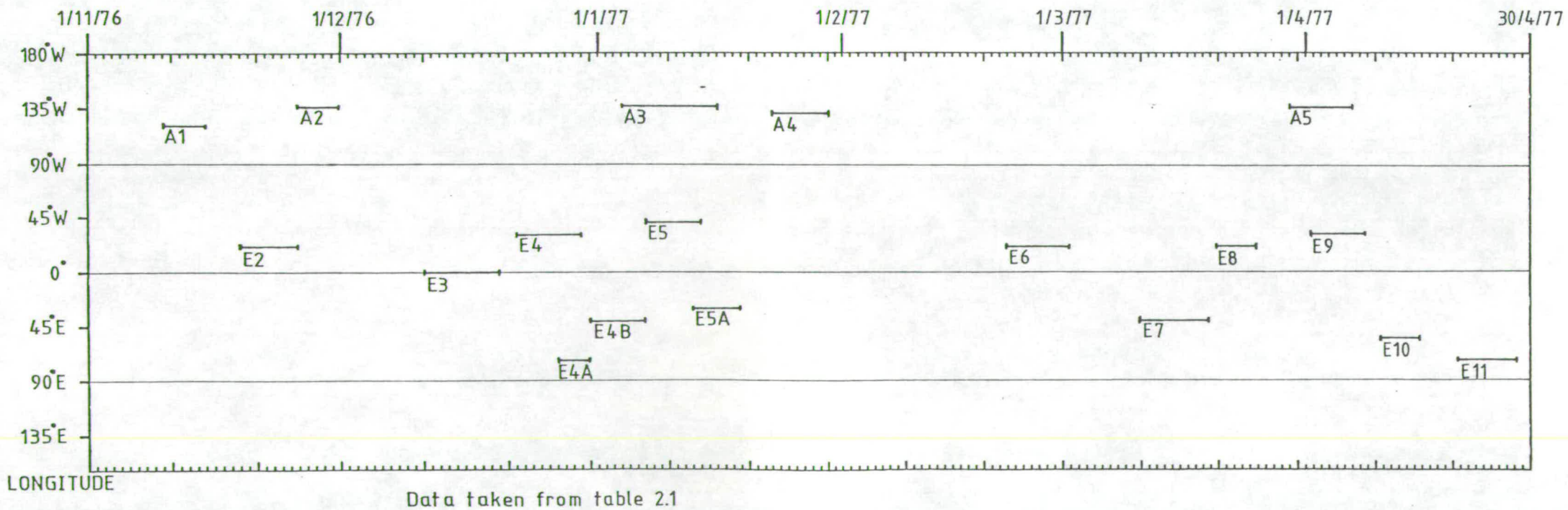

Data taken from table 2.1